Galactic gamma bays and the origin of cosmic rays

D. Dodds

GALACTIC GAMMA RAYS AND THE ORIGIN OF COSMIC RAYS

A Thesis submitted to the University of Durham for the Degree of Doctor of Philosophy.

by

D. DODDS B.Sc.

GREY COLLEGE

FEBRUARY 1977

ABSTRACT

The question of the origin of the cosmic radiation is a fundamental problem in high energy astrophysics, this thesis is concerned with one particular aspect of this question namely, whether or not the cosmic ray sources are Galactic or Extragalactic. This problem is investigated through the results of Galactic Gamma-ray astronomy.

The main mechanism for gamma ray production are discussed. The observational results of Galactic Gamma ray astronomy are described. Theories about the Galactic cosmic ray sources and the distribution of these sources are described and related to the resulting distribution of cosmic rays in various propagation models. The distribution of gas in the galaxy is described.

Calculations are presented which indicate that the role of Inverse Compton Scattering in producing the observed Galactic Gamma ray intensity is small. The reason for the disagreement of this result with earlier results is analysed.

The distribution of cosmic rays in the inner Galaxy (0-10 kpc from the Galactic Centre) is determined from a comparison of the distribution of Gamma ray emissivity and the hydrogen distribution, this is found to follow the distribution of sources between 6 - 10 kpc. The penetration of dense molecular clouds by cosmic rays is investigated. It is concluded that the uncertainties in the hydrogen distribution do not permit us to rule out an Extragalactic origin, from the inner Galaxy data .

The distribution of gamma ray intensity in the Galactic anticentre is modelled on Galactic and Extra-galactic theories and the predictions of the Galactic model are found to be in excellent agreement with observation. The cosmic ray distribution is found to be consistent with the origin in Supernovae or their remnants.

It is concluded that there is rather strong evidence for the majority of cosmic ray nuclei between 1 and 10 GeV having been produced within the Galaxy.

PREFACE

The work presented in this thesis was carried out between 1973 and 1976 while the author was a research student under the supervision of Professor A.W.Wolfendale in the Physics Department of the University of Durham.

In 1975 a visit was made to the Institute of Nuclear Research in Lodz, Poland, to work with Dr. J.Wdowczyk.

Some of the work reported here was carried out in collaboration with Drs A.W.Strong and J.Wdowczyk but most represents the work of the author.

The results obtained in this thesis have been reported in the following papers

Dodds, Strong, Wolfendale & Wdowczyk, Nature, 250, 716, (1974).

Dodds, Strong, Wolfendale & Wdowczyk, Proc. 9th ESLAB Symposium Frascati, Italy. ESRO SP 106. 221.

Dodds, Strong & Wolfendale, J.Phys. A., 8, 624, (1975).

Dodds, Strong & Wolfendale, Mon. Not. R.Astro. Soc., 171, 569, (1975).

Dodds, Strong & Wolfendale, Proc. 19th Int. Conf. Cosmic Rays, 1, 80, (1975).

Dodds, Wolfendale & Wdowczyk, Mon. Not. R.Astr. Soc., 176, 345, (1976).

Dodds & Wolfendale, GSFC Symposium on Gamma-ray Astronomy, June 1976.

CONTENTS PAGE

CHAPTER ONE

INTRODUCTION

The question of the origin of the cosmic radiation is a fundamental problem in high energy astrophysics. This thesis is concerned with the contribution to the solution of this problem which may be gained from a study of the Galactic gamma ray emission.

There are two schools of thought regarding the origin of the cosmic rays. According to the first, the cosmic rays which are observed at Earth are Galactic in origin, possibly the result of cosmic ray acceleration in supernova explosions. One of the basic arguments in favour of this hypothesis is based on the energy injection required to maintain the present density. The observed energy density of cosmic rays with energy $>$1GeV is about 0.5eV cm^{-3} (see for example, Wolfendale, 1973). If this density is constant throughout a disk confinement region of 15 kpc radius and 1 kpc thickness, then the total energy content is $\simeq 5\ 10^{54}$ ergs. If now equilibrium is assumed and the observed mean path length of 5 g cm^{-2} (Shapiro et al, 1971) is interpreted as a mean lifetime of $3\ 10^{6}$ years, this would imply an energy injection rate of $10^{40} - {}^{41}$ergs s^{-1}. A similar value is obtained if a halo confinement region is assumed (Ginzburg and Syrovatskii, 1964). For comparison a supernova rate of 1 per 26 years and a typical supernova energy release of 10^{50-51}ergs gives an energy release rate of 10^{41-42}ergs s^{-1}. However, there are some problems with this picture. There is no direct

evidence for the acceleration of cosmic rays in supernovae and there are difficulties in reconciling the observed low anisotropy of the cosmic rays with the short lifetime, (see Osborne, 1975).

According to the second school, the cosmic rays are extragalactic in origin. In this case the cosmic ray density outside the Galaxy will be equal to the density inside. While there is no doubt that there do exist powerful extragalactic cosmic ray sources capable of filling considerable volumes of intergalactic space with relativistic particles (Willis et al, 1974), the principal difficulty is one of providing enough energy. The energy requirement to populate the entire universe with a cosmic ray density of 0.5 eV cm^{-3} represents about 0.5% of the total rest mass of the visible matter. This difficulty is reduced somewhat in the modified extragalactic model of Brecher and Burbidge (1972). These authors suggest that at 1 GeV the confinement volume may be restricted to the regions of space which contain galaxy clusters. In particular they envisage confinement to the supercluster for cosmic rays with energies of 10^9 - 10^{16} eV. In this case the energy requirements are rather less severe.

There is general agreement between these schools that energy losses for electrons preclude an extragalactic origin for these particles. Similarly there is agreement that the high isotropy at 10^{17} eV requires cosmic rays of this energy to be mainly extragalactic. The area of controversy is confined to nuclei with energy between 10^9 and 10^{17} eV.

Ginzburg (1972) has proposed a test for these models which consists of searching for gamma-ray emission from the direction of the Magellanic Clouds. The argument being, that extragalactic cosmic rays interacting with the hydrogen of the Clouds will produce π^{o} mesons which decay to give gamma rays. Thus observation (or non-observation) of gamma rays will indicate the presence (or absence) of cosmic rays. However, the present observational limits are not good enough to resolve this debate.

This thesis is concerned with the problem of identifying which of the above models is the more satisfactory at the cosmic ray energies responsible for gamma ray production. Secondarily it is aimed at the related problem of investigating the cosmic ray distribution in the Galaxy using the available Gamma-ray astronomical data.

With these aims in mind Chapter 2 describes the important gamma ray production mechanisms. Chapter 3 reviews the observational results of Galactic gamma-ray astronomy. Chapter 4 describes the candidates for the Galactic cosmic ray sources, their distribution and the distribution of cosmic rays which may be expected. In Chapter 5 some of the important features of the Interstellar gas are described. In Chapter 6 a model is constructed for the distribution of gamma ray intensity due to Inverse Compton Scattering. The contribution to gamma ray production from π^{o} decay and bremsstrahlung are calculated in Chapter 7 and used to

find the Galactic distribution of cosmic rays. In Chapter 8 the gamma ray emission from the Galactic anticentre is modelled using the results from Chapter 6 and 7. Finally Chapter 9 discusses some of the conclusions reached.

REFERENCES

Brecher, K & Burbidge, G.R., 1972. Astrophys. J., 174, 253.

Ginzburg, V.L. & Syrovatski, S.I., 1964. In 'The Origin of Cosmic Rays', Pergamon.

Ginzburg, V.L., 1972. Nature Phys. Sci., 239, 8.

Osborne, J.L., 1975. In 'Origin of Cosmic Rays', eds J.L.Osborne and A.W.Wolfendale, Reidel, Dordrecht.

Shapiro, M.M., Silverberg, R. & Tsao, C.H., 1971. Proc. 12th. Int. Conf. on Cosmic Rays, University of Tasmania. 1, 221.

Willis, A.G., Strom, R.G. & Wilson, A.S., 1974. Nature, 250, 625.

Wolfendale, A.W., 1973. In 'Cosmic Rays at Ground Level', ed. A.W.Wolfendale, The Institute of Physics, London.

CHAPTER TWO

GAMMA-RAY PRODUCTION MECHANISMS

2.1 Introduction

Gamma ray production in the Galaxy is dominated by three processes; π^0 decay, bremsstrahlung and inverse Compton scattering. This chapter will describe some of the important features of these processes, their cross-sections and spectrum of gamma rays which results.

In the sections which follow and later chapters the following notation is used. $Q_x(E_\gamma, \bar{r})$ is the number of gamma rays of energy $> E_\gamma$ per cm^3 per second produced by process 'x' at $\bar{r}$ and is called the volume emissivity. $Q_x(E_\gamma)$ is the volume emissivity due to process 'x' at the solar system. In addition to these we will also use $q_x(E_\gamma, \bar{r})$ as the gamma production rate per hydrogen atom.

Thus, the intensity of gamma radiation at the Earth, $I(>E_\gamma)$ due to π^0 production is

$$I(>E_\gamma) = \int_0^\infty \frac{Q_{\pi^0}(E_\gamma, \bar{r})}{4\pi}\, dr$$

or

$$= \int_0^\infty \frac{q_{\pi^0}(E_\gamma, \bar{r})\, n_H(\bar{r})\, dr}{4\pi} \qquad 1.$$

2.2 Gamma-ray production from cosmic ray nucleus - interstellar gas nucleus collisions.

2.2.1 Collisions of protons with hydrogen

It will be seen later that the most prolific source of 100 MeV gamma rays is the decay of π^0 mesons produced

in inelastic collisions of cosmic ray protons with interstellar hydrogen. The main channels for meson production are

$$\begin{aligned} p + p &\longrightarrow p + p + a(\pi^+ + \pi^-) + b\pi^\circ \\ &\longrightarrow p + n + \pi^+ + c(\pi^+ + \pi^-) + d\pi^\circ \\ &\longrightarrow n + n + 2\pi^+ + e(\pi^+ + \pi^-) + f\pi^\circ \\ &\longrightarrow D + \pi^+ + g(\pi^+ + \pi^-) + h\pi^\circ \end{aligned} \qquad 2.$$

where in equation 2, a to h are positive constants and p, n, D are protons, neutrons and Deuterons respectively.

The minimum kinetic energy T_{min} for production of n mesons is approximately given by the relation

$$T_{min} \simeq n\,(280 + 10n) \quad \text{MeV} \qquad 3.$$

Thus, for single meson production the threshold is $\simeq$ 290 MeV. At the threshold the reactions are

$$p + p \longrightarrow p + n + \pi^+ \qquad 4.$$

$$p + p \longrightarrow p + p + \pi^\circ \qquad 5.$$

$$p + p \longrightarrow D + \pi^+ \qquad 6.$$

From the point of view of gamma ray production the reaction of equation 5 is the most important, since in almost 100% of cases the neutral pion decays to two gamma rays.

The total γ-ray yield, $Q_{\pi^\circ}(\bar{r})$, from π° decay is given by

$$Q_{\pi^\circ}(\bar{r}) = 2.4\pi \int_0^\infty n_H(\bar{r})\, I_p(T,\bar{r})\sigma_{\pi^\circ pp}(T) m_{\pi^\circ pp}(T)\,dT \qquad 7.$$

where $I_p(T,\bar{r})\,dT$ is the cosmic ray proton intensity at r with kinetic energy T, n_H is the density of interstellar hydrogen, $\sigma_{\pi^\circ pp}(T)$ is the cross-section for production of π° mesons in proton hydrogen collision and $m_{\pi^\circ pp}(T)$ is the average multiplicity of π° mesons in proton-hydrogen collisions.

Measurements of the product $\sigma_{\pi^o pp}(T) m_{\pi^o pp}(T)$ are now available from accelerator experiments up to kinetic energies of 1000 GeV. Figure 1 is a compilation of recent measurements from Stecker (1973). The product of cross-section and multiplicity, $\sigma_{\pi^o}(T)\ m_{\pi^o}(T)$ are shown in figure 2 for all three π mesons. Since the charged π mesons eventually decay to form secondary cosmic ray electrons it is obvious that regions of high gamma ray emmissivity will also be regions of copious secondary electron production.

The relative importance of different proton energies for π^o production is illustrated in figure 3 which shows the product $I_p(T)\sigma_{\pi^o pp}(T)\ m_{\pi^o pp}(T)$.

2.2.2 The contribution from interstellar Helium

The yield from this process is given by

$$Q_{\pi^o}(\bar{r}) = 8\pi \int n_{He}(\bar{r}) I_p(T,\bar{r}) \sigma_{\pi^o p\alpha}(T) m_{\pi^o p\alpha}(T) dT \qquad 8.$$

The threshold kinetic energy for the production of n pions in an enelstic collision between a cosmic ray proton and a Helium nucleus is given approximately by equation 9.

$$T_{th\ p-\alpha} \simeq 170n + 2.5n^2 \quad \text{MeV} \qquad 9.$$

Where $\dot{T}$ is the proton kinetic energy in MeV. Thus for n = 1 the threshold energy is $\simeq$ 172 MeV.

There exist few experimental measurements of the cross section $\sigma_{\pi^o p\alpha}(T)$ and multiplicity $m_{\pi^o p\alpha}(T)$ for π^o production in proton-alpha particle collisions. The cross-section plotted in figure 1 is based at low energies on an empirical model for the cross-section

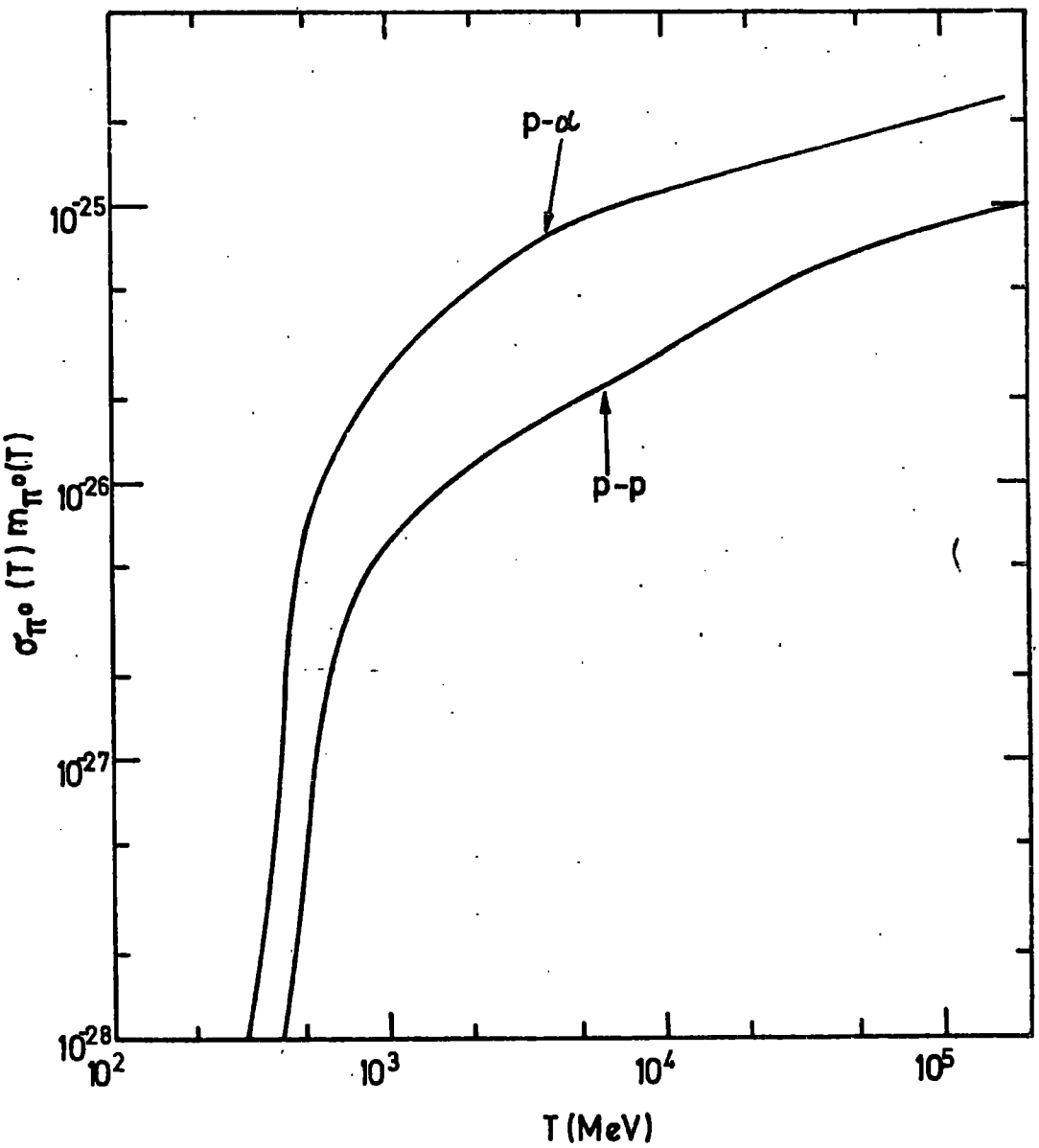

Figure 1. The product of cross-section, σ, and multiplicity, m for π^0 production in proton-proton collisions plotted against proton kinetic energy, T.

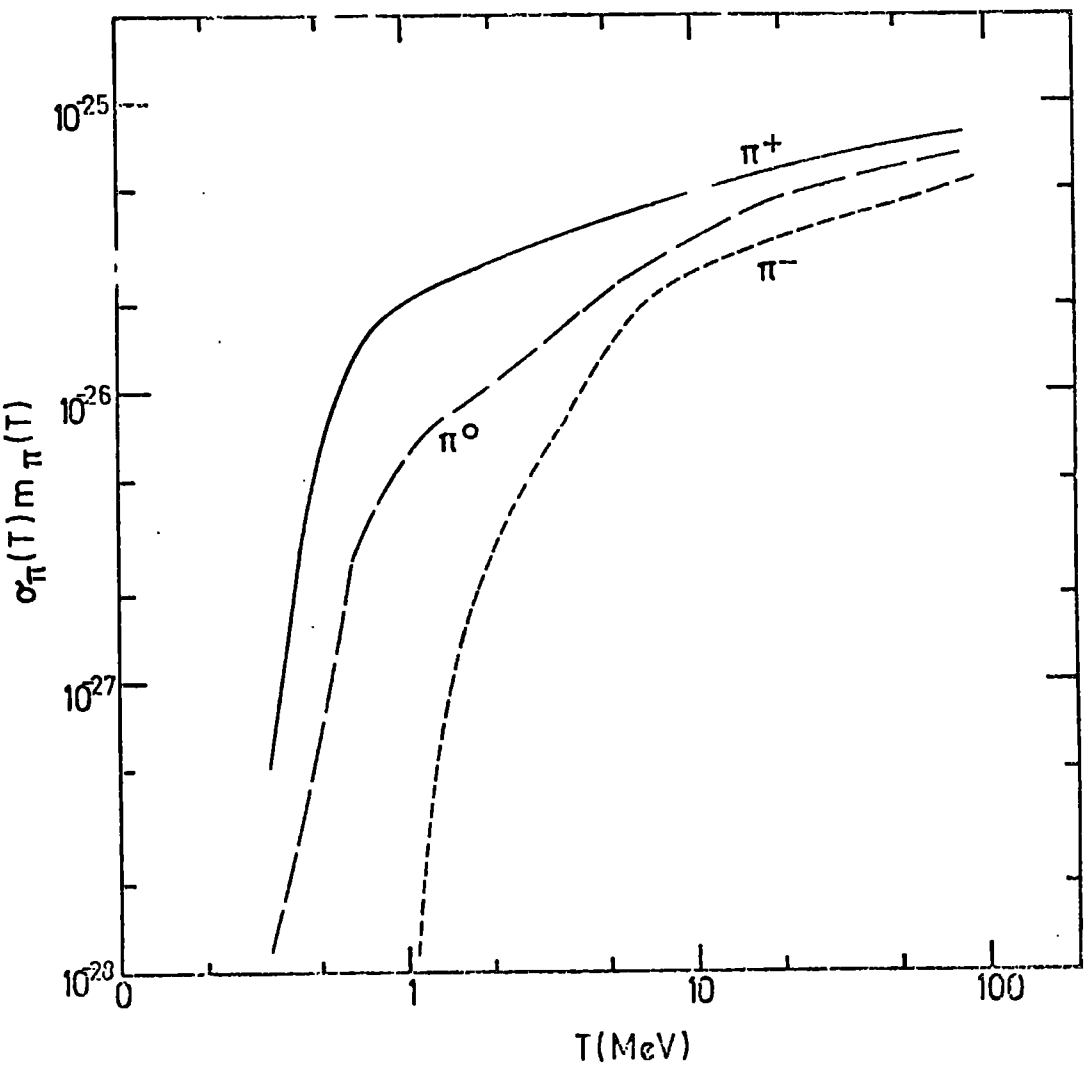

Figure 2. The product of cross-section, σ and multiplicity, m, in proton-proton collisions for all three π mesons.

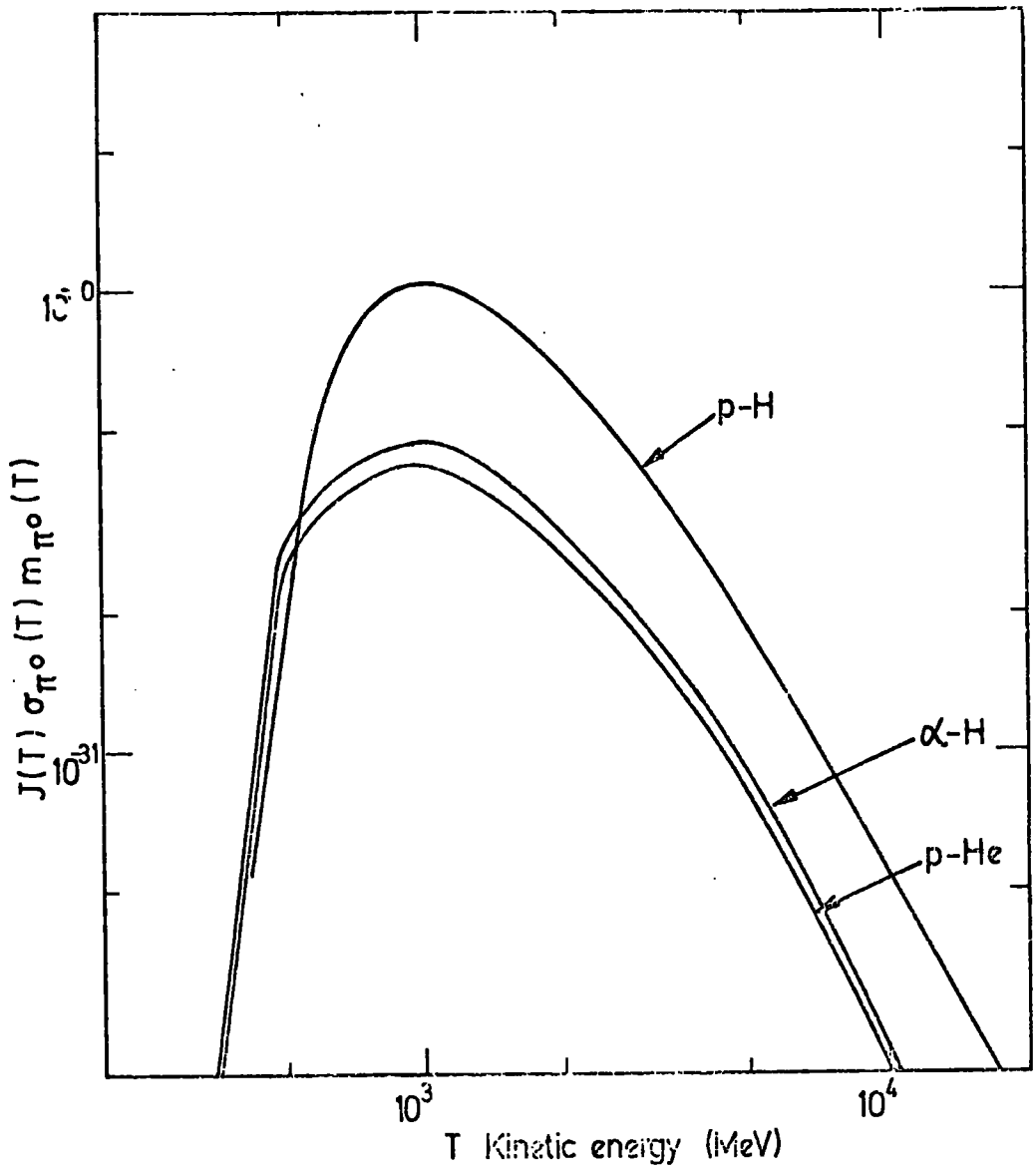

Figure 3. The product $I_{CR}(T)\,\sigma_{\pi^0}(T)\,m_{\pi^0}(T)$ versus kinetic energy, T, for π^0 production in proton-proton, proton-helium and alpha-hydrogen collisions.

for which the parameters are determined from experimental results on p - D and p - Li^6 collisions (Pollack and Fazio 1963). At high energies the cross-section is given by

$$\sigma_{pN} = s\,(Z\sigma_{pp} + Z\sigma_{pn}) \qquad 10.$$

where s is a parameter to include the effects of shadowing and is assumed to be 0.5 (Cavallo and Gould 1971). Thus, at high energies

$$\sigma_{p\alpha} \simeq 2\sigma_{pp} \qquad 11.$$

The product $(n_{He}/n_H)\ I_p(T)\sigma_{\pi^\circ p\alpha}(T)m_{\pi^\circ p\alpha}(T)$ is shown in figure 3.

2.2.3 The Contribution from cosmic ray α particle - interstellar hydrogen collisions

This process is identical with the p - He collisions discussed above. The total cross-section $\sigma_{\pi^\circ \alpha p}(T_\alpha)$ is equal to $\sigma_{\pi^\circ p\alpha}(T_p)$ at the same centre of mass (cms) energy. The relation between the laboratory kinetic energies T_p and T_α for which the cms energies are equal is given by equation 12.

$$m_\alpha T_p = m_p T_\alpha \qquad 12.$$

Since $m_\alpha \simeq 4m_p$ this gives

$$T_p \simeq \frac{T_\alpha}{4}$$

and the cross-sections $\sigma_{\pi^\circ p\alpha}$ and $\sigma_{\pi^\circ \alpha p}$ are the same for protons and alphas having the same kinetic energy per nucleon.

Figure 3 shows the product $I_\alpha(T)\sigma_{\pi^\circ \alpha p}(T)m_{\pi^\circ \alpha p}(T)$ where T is now the kinetic energy per nucleon. It can be seen from figure 3 that the total contribution from α-H and p - He collisions is approximately equal to

the contribution from p - H.

2.2.4 The Spectrum of gamma-rays from π^o decay

This problem has been thoroughly discussed by several authors, for example Stecker (1970, 1975), Cavallo and Gould (1971) and Tkaczyk (1975). The differential spectra of π^o gamma rays from these authors' work are in good agreement.

The most striking feature of the gamma ray spectrum from π^o decay is its symmetry about log $\frac{m_{\pi^o}c^2}{2}$ on a logarithmic plot. This arises because the pion decays to two identical particles. A π^o meson decaying at rest produces two gammas of identical energy $\frac{m_{\pi^o}c^2}{2}$. If the pion decays in flight then the two gamma rays will have different energies. For a pion with energy $E_{\pi o} = \gamma_{\pi^o} m_{\pi^o} c^2$ the maximum and minimum possible gamma-ray energies are

$$E_{\gamma max} = \frac{m_{\pi^o}c^2}{2} \gamma_{\pi^o} (1 + \beta_{\pi^o}) \qquad 13.$$

$$E_{\gamma min} = \frac{m_{\pi^o}c^2}{2} \gamma_{\pi^o} (1 - \beta_{\pi^o}) \qquad 14.$$

where $\beta_{\pi^o} = v_{\pi^o}/c$. The normalized distribution function for in flight decay is

$$f(E_\gamma)\, dE_\gamma = \frac{dE_\gamma}{m_{\pi^o} \gamma_{\pi^o} \beta_{\pi^o}} \qquad 15.$$

Figure 4 shows this distribution function for several different pion energies. A consequence of the symmetry seen in figure 4 is that any spectrum of pions will always give a differential spectrum of gamma rays which is symmetric about log $\frac{m_{\pi^o}c^2}{2}$ on a logarithmic plot.

Figure 5 shows the integral gamma ray spectra calculated by Stecker (1973) and Cavallo and Gould (1971).

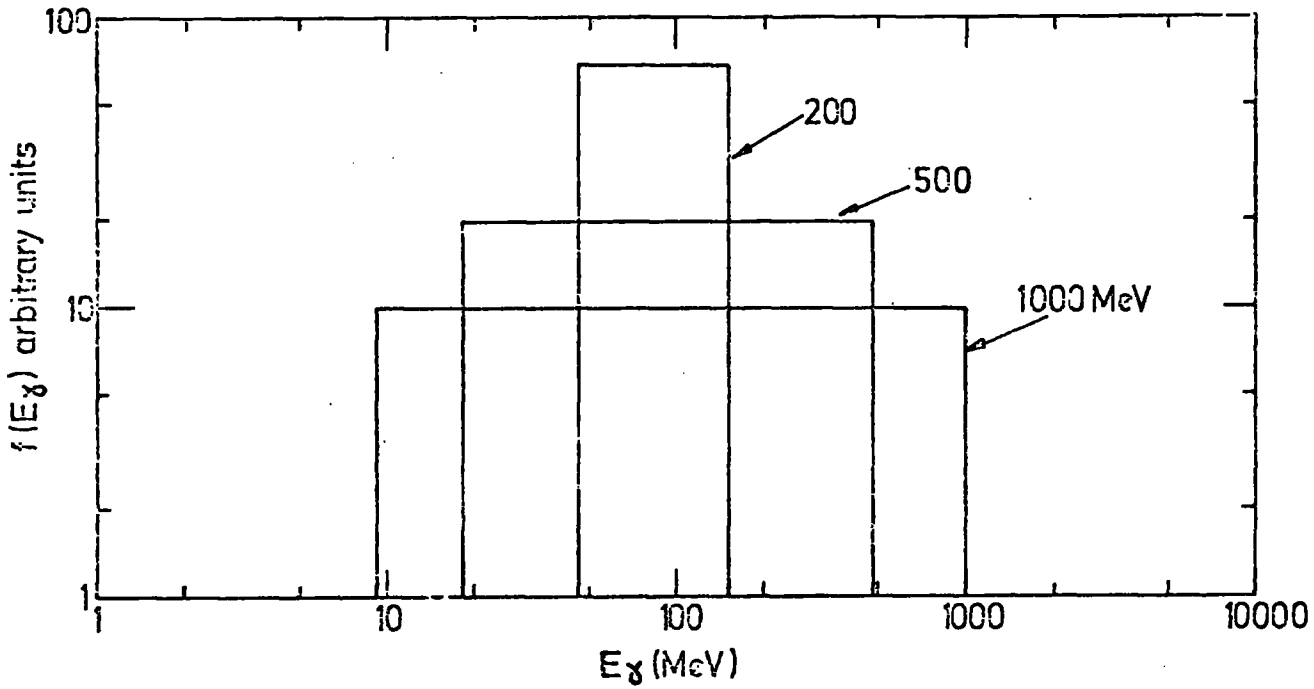

Figure 4. The distribution function of gamma rays produced by the decay of energetic π^0 mesons for three different energies.

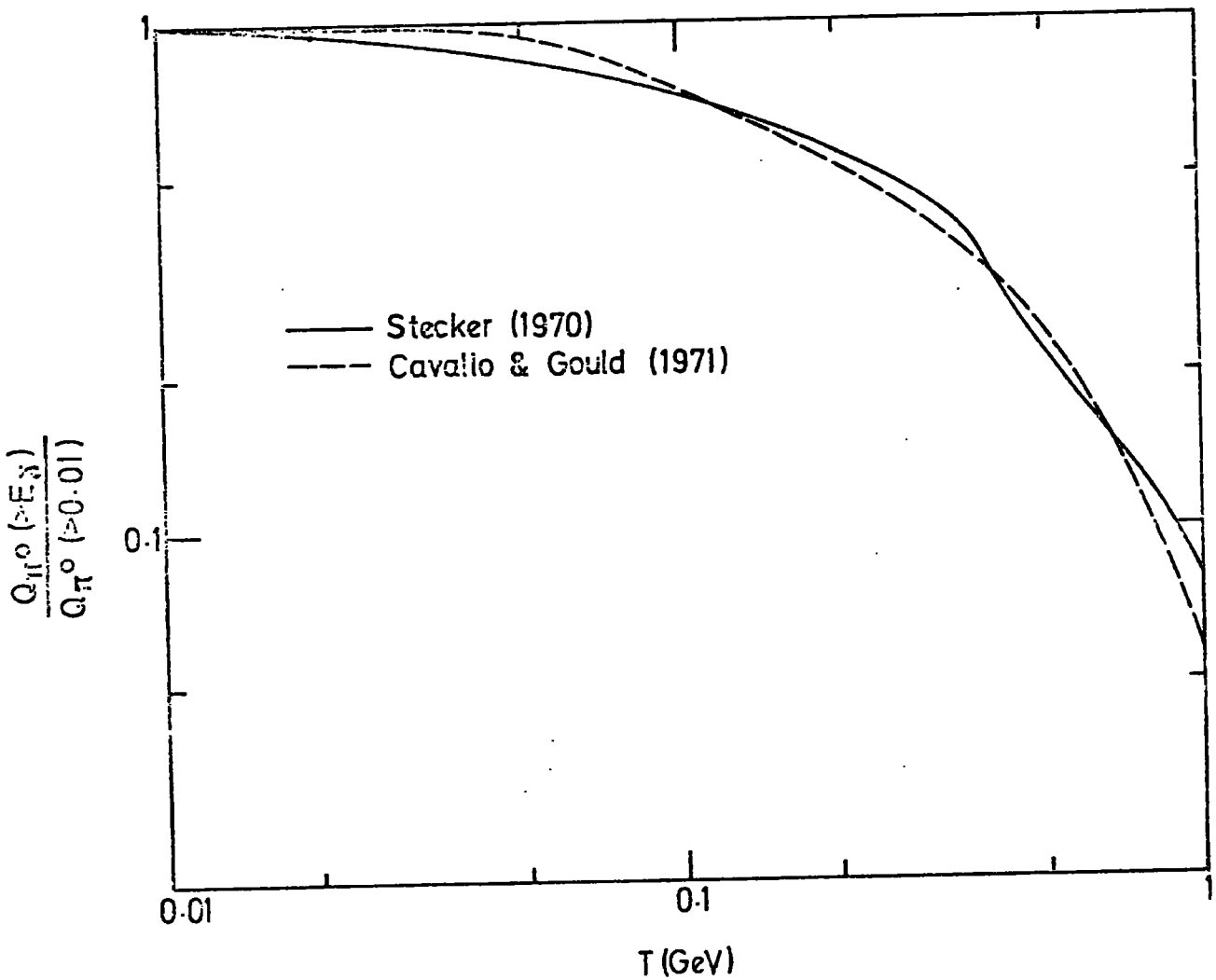

Figure 5. The integral spectra of gamma rays from π° decay as calculated by Stecker (1973) and Cavallo and Gould (1971).

The minor differences between the two spectra are artefacts of the different models used by these authors.

2.3. Gamma-ray production in electron bremsstrahlung

In this process gamma-rays are produced in collisions between cosmic ray electrons and the nuclei of interstellar gas. In the collision the electron is deccelerated and radiates a photon of energy $E_\gamma \leqslant E_e$ where E_e is the electron energy. The details of the derivation of the cross-section are given in Heitler (1954).

The cross-section $\sigma_B(E_\gamma, E_e)$ for production of a photon of energy between E_γ and $E_\gamma + dE_\gamma$ by an extremely relativistic electron in the field of a target nucleus of charge Z is

$$\sigma_B(E_\gamma, E_e)\, dE_\gamma = \qquad (E_e \gg \mu)$$

$$2\,\frac{Z^2 r_0^2}{137}\,\frac{dE_\gamma}{E_\gamma}\,\frac{E}{E_e}\left(\frac{E_e^2+E^2}{2E_eE}-\frac{2}{3}\right)\left(2\ln\left\{\frac{2E_eE}{\mu E_\gamma}\right\}-1\right) \qquad 16$$

where $E = E_e - E_\gamma$ is the energy of the electron after the collision, r_0 is the classical electron radius and μ is the electron rest mass. In the limit of low energy photons (i.e. $E_\gamma \rightarrow 0$) the intensity $E_\gamma \sigma_B$ diverges logarithmically.

The cross-section given in equation 16 corresponds to scattering by a pure Coulomb field. At the very large impact parameters which correspond to production of photons of very low energy the cross-section is calculated including the screening effects of the atomic electrons. In this case the cross-section becomes

$$\sigma_B(E_\gamma, E_e)\, dE_\gamma = \frac{2Z^2r_0^2}{137}\,\frac{dE_\gamma}{E_\gamma}\,\frac{E}{E_e}\left[\left(\frac{E_e^2+E^2}{E_eE}-\frac{2}{3}\right)2\ln(183Z^{-1/3})+\frac{2}{9}\right]$$

$$E_e \gg \mu \;\;\&\;\; \frac{E_eE}{\mu E_\gamma} \gg 137\,Z^{-1/3} \qquad 17.$$

Heitler (1954).

The differential emissivity $\frac{\partial Q_B}{\partial E_\gamma}$ is given by equation 18.

$$\frac{\partial Q_B(E_\gamma,\bar{r})}{\partial E_\gamma} = \sum_j 4\pi n_j(\bar{r}) \int_{E_\gamma}^{\infty} I_e(E_e,\bar{r})\, \sigma_{B,j}(E_\gamma,E_e)\, dE_e \qquad 18.$$

where $n_j(\bar{r})$ is the volume density of atoms of type j; $I_e(E_e, \bar{r})$ is the electron spectrum and $\sigma_{B,j}(E_\gamma,E_e)$ is the cross-section for bremsstrahlung of electrons on atoms of type j with nuclear charge z_j.

Since the screened cross-section of eq. 17 shows very little energy dependence the following approximation is often made.

$$\sigma_{B,j}(E_\gamma,E_e)\, dE_\gamma = \frac{M_j}{X_j}\,\frac{dE_\gamma}{E_\gamma} \qquad 19.$$

where M_j is the mass of the target atom in grammes and X_j is the radiation length in gm cm^{-2}. For hydrogen X_H = 62.8 gm cm^{-2} (Lang 1974).

Using the approximation given in eq. 19 in eq. 18 gives

$$\frac{\partial Q_B(E_\gamma,\bar{r})}{\partial E_\gamma} = 4\pi n_H(\bar{r})\,\frac{I_e(>E_\gamma,\bar{r})}{E_\gamma}\,\frac{M_H}{X_H} \qquad 20.$$

A power-law differential electron spectrum $I_e(E_e\bar{r}) = A_e(\bar{r})\, E_e^{-\Gamma}$, $(\Gamma > 2)$ yields

$$\frac{\partial Q_B(E_\gamma,\bar{r})}{\partial E_\gamma} = A_\gamma(\bar{r})\, E_\gamma^{-\Gamma} \qquad 21.$$

Thus a differential electron spectrum of slope, Γ, gives a bremsstrahlung spectrum with the same slope.

The contribution of this process to the Galactic emission and the energy spectrum are considered in more detail in a later chapter.

2.4. Gamma Ray production in Inverse Compton Scattering

This is one of the most important energy loss mechanisms for relativistic electrons in the interstellar medium and was originally discussed from this point of view by Feenberg and Primakoff (1948). Since then the Inverse Compton (IC) process has been extensively discussed as a mechanism for creating high energy gamma rays (see, for example Felten and Morrison, 1966).

Essentially the process involves a low energy photon scattering off a relativistic electron and carrying off some of the electron's energy. Figure 6a illustrates this scattering process, for the case of an electron of energy, $E_e = \gamma M_e c^2$ moving to the right and scattering a photon of energy ϵ, creating a gamma ray of energy E_γ.

Figure 6b shows the geometry of the same process when viewed from the electron rest frame. (In this figure and below quantities measured in the rest frame frame will be denoted by a prime, thus E'). Equation 22 gives the relationship between the lab. and rest frame energies.

$$\begin{aligned} \epsilon &= \gamma \epsilon' (1 - \beta \cos\alpha') \\ E_\gamma &= \gamma E_\gamma (1 + \beta \cos\alpha_1') \\ \epsilon' &= \gamma \epsilon (1 + \beta \cos\alpha) \\ E_\gamma' &= \gamma E_\gamma (1 - \beta \cos\alpha_1) \end{aligned} \qquad 22.$$

In the electron rest frame the scattering process becomes simply the ordinary Compton effect and hence the well known relation between the initial and final energies of the photons may be used. Thus

$$E_\gamma' = \frac{\epsilon'}{1 + \frac{\epsilon'}{m_e}(1 - \cos\theta')} \qquad 23.$$

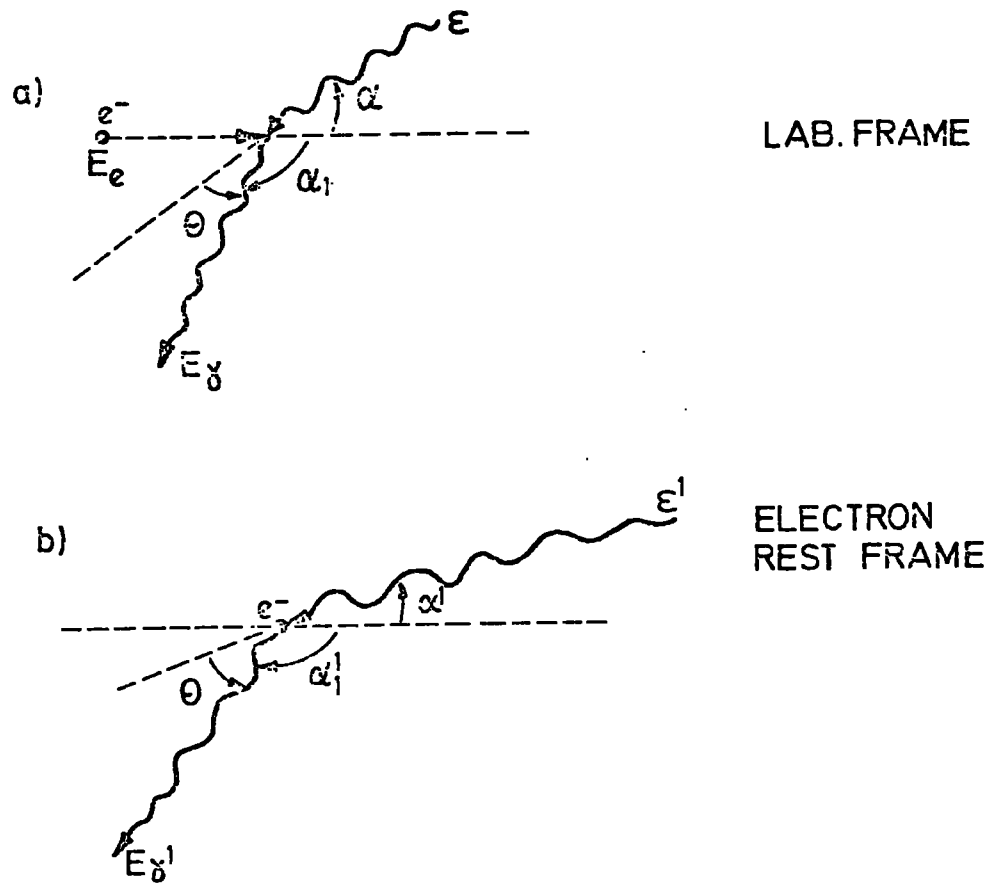

Figure 6a and 6b. The inverse Compton scattering process, showing the notation used above.

Substituting for E_γ and ϵ' in equation 23 using the relations in equation 22 gives

$$\frac{E_\gamma}{E_e} = \frac{\frac{\gamma\epsilon}{m_e}(1+\beta\cos\alpha')(1+\beta\cos\alpha)}{1+\frac{\gamma\epsilon}{m}(1+\beta\cos\alpha)(1-\cos\theta')} \qquad 24.$$

Examination of equation 24 shows that there are two interesting extreme cases; firstly for $\gamma\epsilon \ll M_e c^2$ then $E_\gamma \simeq \gamma^2\epsilon$ and secondly that for $\gamma\epsilon \gg M_e c^2$ then $E_\gamma \simeq E_e$ In fact the former is simply equivalent to $\epsilon' \ll M_e c^2$ and in this limit the process in the rest frame becomes 'classical' Thomson scattering.

Now, in the interstellar medium the important photon energies lie between leV for starlight and 5 10^{-4} eV for the 2.7° blackbody radiation. For these photons to produce 100 MeV gamma rays by this process requires electrons with)'s such that the first condition ($\gamma\epsilon \ll M_e c^2$) is satisfied. Clearly, describing this process as Inverse Compton Scattering is incorrect since strictly the process is Inverse Thomson Scattering.

The differential emissivity $\partial Q_{IC}/\partial E_\gamma$ is given by equation 25.

$$\frac{\partial Q_{IC}(E_\gamma,\bar{r})}{\partial E_\gamma} = 4\pi \int_{E_e}^{\infty} I_e(E_e,\bar{r}) \int_0^{\infty} n_{ph}(\epsilon,\bar{r})\, \sigma_{IC}(E_\gamma,\epsilon,E_e)\, d\epsilon\, dE_e \qquad 25.$$

Where $I_e(E_e,\bar{r})$ is the spectrum of relavistic electrons, $n_{ph}(E,\bar{r})$ is the number density of photons with energy between ϵ and $\epsilon + d\epsilon$ and $\sigma_{IC}(E_\gamma, \epsilon, E_e)$ is the cross-section for gamma ray production by an electron of energy E_e scattering off the photon of energy ϵ.

The derivation of the cross-section $\sigma_{IC}(E_\gamma, \epsilon, E_e)$

from the Klein-Nishina cross-section is fairly simple and is given by Ginzburg and Syrovatskii(1964). The resulting expression for the cross-section is

$$\sigma_{IC}(E_\gamma, \epsilon, E_e) =$$

$$2\pi r_o^2 \left[\frac{m_e^2}{\epsilon E_e^2} + \frac{m_e^4 E_\gamma}{4\epsilon^2 E_e^4} - \frac{m_e^6 E_\gamma}{8\epsilon^3 E_e^5} + \frac{m_e^4 E_\gamma}{2\epsilon^2 E_e^4} \ln\left(\frac{m_e^2 E_\gamma}{4\epsilon E_e^2}\right) \right] \quad 26.$$

The cross-section may also be used to find $\langle E_\gamma \rangle$ the mean gamma ray energy which results from the collision. This is given by

$$\langle E_\gamma \rangle = \frac{1}{\sigma_T} \int_0^{4\gamma^2\epsilon} E_\gamma \sigma_{IC}(E_\gamma, \epsilon, E_e) dE_\gamma \quad 27.$$

where $$\sigma_T = \int_0^{4\gamma^2\epsilon} \sigma_{IC}(E_\gamma, \epsilon, E_e) dE_\gamma$$

= Thomson cross-section

Upon integration equation 27 gives

$$\langle E_\gamma \rangle = \frac{4}{3} \gamma^2 \epsilon \quad 28.$$

A frequently used approximation for the cross-section uses 28 thus

$$\sigma_{IC}(E_\gamma, \epsilon, E_e) = \sigma_T \delta\left(E_\gamma - \frac{4}{3}\left(\frac{E_e}{m_e}\right)^2 \epsilon\right) \quad 29.$$

For a power law electron spectrum of the type $A_e E_e^{-\Gamma}$ the spectrum of gamma rays which results from solving equation 25 by using either 26 or the approximation 29 is also a power law, but of exponent $-(\Gamma + 1)/2$. Thus the solution to 25 has the form

$$\frac{\partial Q}{\partial E_\gamma} = A_\gamma E_\gamma^{-\left(\frac{\Gamma + 1}{2}\right)} \quad 30.$$

The spectrum of gamma rays from this process will be considered in detail in Chapter 6.

REFERENCES

Cavallo, G. & Gould, R.J., 1971. Nuovo Cim., 2B, 77.

Feenberg, E. & Primakoff, H., 1948. Phys. Rev., 73, 449.

Felten, J.E., & Morrison, P., 1966. Astrophys, J. 146, 686

Ginzburg, V.L., & Syrovatskii, V.I., 1964. In 'The Origin of Cosmic Rays', Pergamon.

Heitler, W., 1954. In 'The Quantum Theory of Radiation', Oxford.

Lang, K.R., 1974. In 'Astrophysical Formulae', Springer - Verlag, Berlin.

Pollack, J.B., & Fazio, G.G., 1963. Phys. Rev., 131,2684.

Stecker, F.W., 1970. Astrophys. and Sp. Sci.,6, 377.

Stecker, F.W., 1973. Astrophys. J., 185, 499.

Stecker, F.W., 1975. In 'Origin of Cosmic Rays', ed. J.L. Osborne & A.W.Wolfendale, Reidel, Dordrecht.

Tkaczyk, W., 1975. Ph.D. Thesis, University of Lodz, Poland.

CHAPTER THREE

THE GALACTIC GAMMA-RAY OBSERVATIONS

3.1. Introduction

Gamma ray astronomy began with the moon-probe Ranger III which carried a scintillator sensitive to photons of about 1 MeV. Since that first experiment many other instruments have been flown to detect cosmic gamma rays. However, the majority of these instruments were, like the first, omnidirectional detectors designed to detect the diffuse gamma ray background; only a few have been specifically designed to have the angular resolution and sensitivity necessary to be able to observe gamma rays specifically from the Galaxy. In the sections which follow, the main observational results of these experiments are described. Attention will be confined to observations of gamma rays with energies > 1MeV.

3.2. Low Energy Gamma Rays from the Galactic Plane ($1 \leqslant E_\gamma \leqslant 10$MeV)

The detection of gamma rays which arise in the Galaxy requires instruments with quite a high degree of directionality. Unfortunately of the many experiments operated in this energy interval few have had sufficiently good directional sensitivity to investigate the flux from the Galactic plane.

A most important result was obtained by Schonfelder and Lichti (1974) using a double Compton telescope with an angular resolution of 30°. This telescope was used in drift scans across the Galactic plane and hence observed both the Galactic and diffuse gamma ray compon-

ents. These authors deduce from the angular distribution of the gamma ray intensity that at least 80% of the flux they observed between 1 - 10 MeV belongs to the isotropic component and hence that upper limits only may be set for the Galactic plane.

Thus it appears that at about 10 MeV the emission from the Galactic plane begins to disappear into the gamma ray background. Figure 1 shows a summary of the background from Strong et al.(1976).

3.3 High Energy Gamma rays from the Galactic Centre ($E_\gamma > 10$ MeV)

The first experiment to demonstrate the existence of a galactic component was the telescope flown on the satellite OSO III in 1967 - 68 (Kraushaar et al. 1972). This experiment measured a finite flux of gammas (with energy $E > 100$ MeV) from the Galactic plane and despite having only moderate ($\sim 15^{\circ}$) angular resolution the telescope was able to map out most of the main features of the Galactic plane.

This experiment was followed by a series of balloon-borne experiments (for example, Fichtel et al. 1972, Helmken and Hoffman 1973, Frye et al. 1974, Share et al. 1974, Sood et al. 1974). These experiments were designed to observe the gamma ray emission from the Galactic Centre, subsequently, a second satellite experiment was launched (on SAS II, Fichtel et al 1975) and this also has provided a map and spectrum of the Galactic Plane.

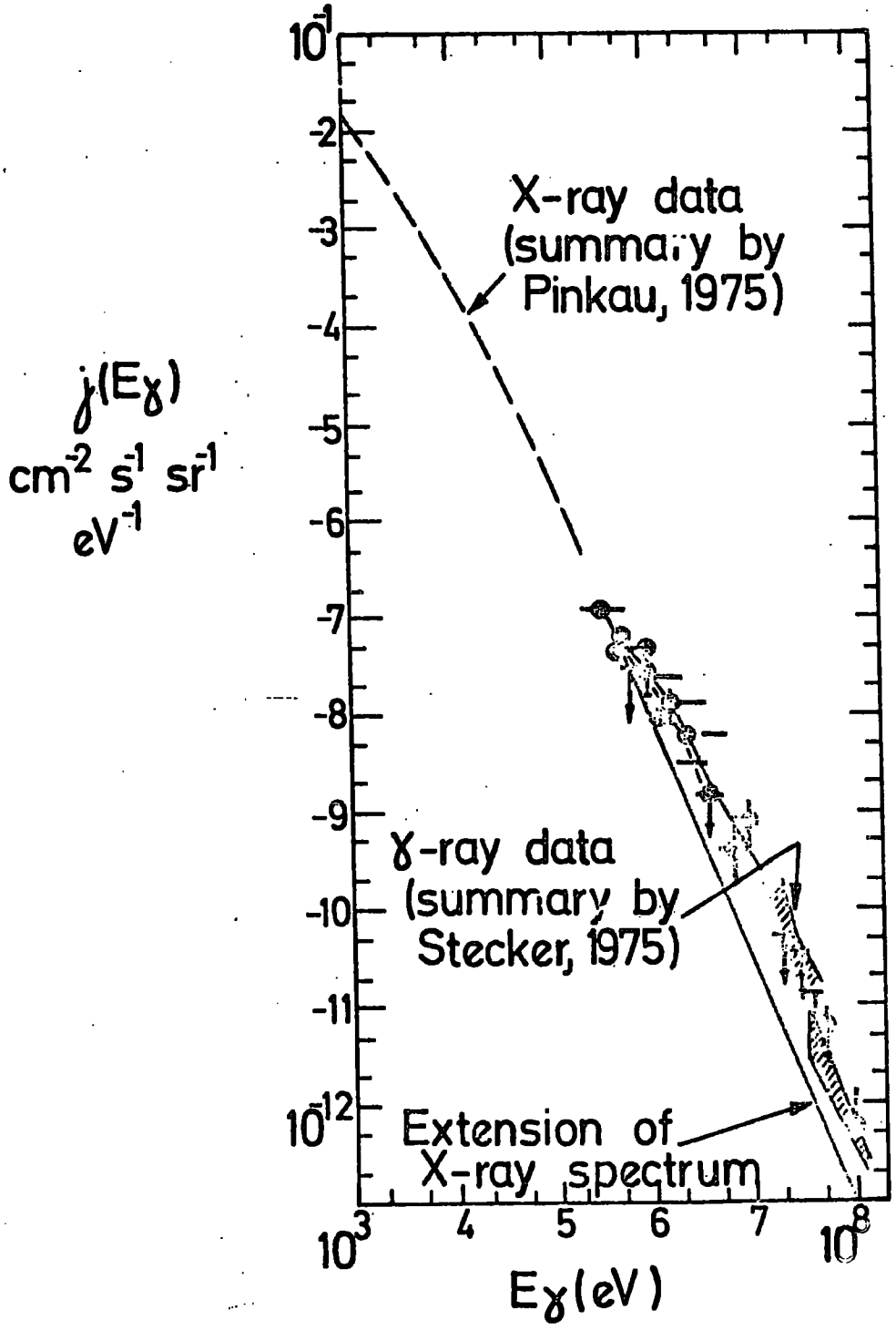

Figure 1. The diffuse gamma-ray background. A summary of data from Strong et al (1976).

Figure 2 shows a summary of the results from these experiments for the Galactic Centre spectrum in the region between $l = 330^{\circ}$ and $l = 30^{\circ}$.

It should be noted that although in general these experiments measure the integral flux at some energy, the published results of Helmken and Hoffman and Share et al. actually refer to the differential spectrum. For this reason the integral flux calculated for these experiments and shown in figure 2 are dependent on the spectral shape assumed at higher energies. The upper and lower values shown for the Share et al. point correspond to the extreme assumptions of an entirely π^{o} decay spectrum or an E^{-2} power law respectively. The evidence of the higher energy observations in figure 2 suggests that a hard spectrum such as the π^{o} spectrum dominates.

The Share et al. observations have provided evidence for a soft component of the Galactic Centre flux which may become dominant at low energies. Figure 3 shows the differential spectra for both the Galactic Centre and atmospheric albedo gamma ray fluxes. Comparison of the Galactic centre spectrum with the π^{o} decay spectrum of Stecker (1973) indicates the presence of a steep component at low energies. Such an interpretation is supported by comparison with the differential spectrum of atmospheric gamma rays which shows similar structure and is known to have such a two component origin.

3.4 The Galactic Intensity Vs Longitude distribution

As commented above this was first determined by the gamma ray telescope on OSO III (Kraushaar et al 1972) and

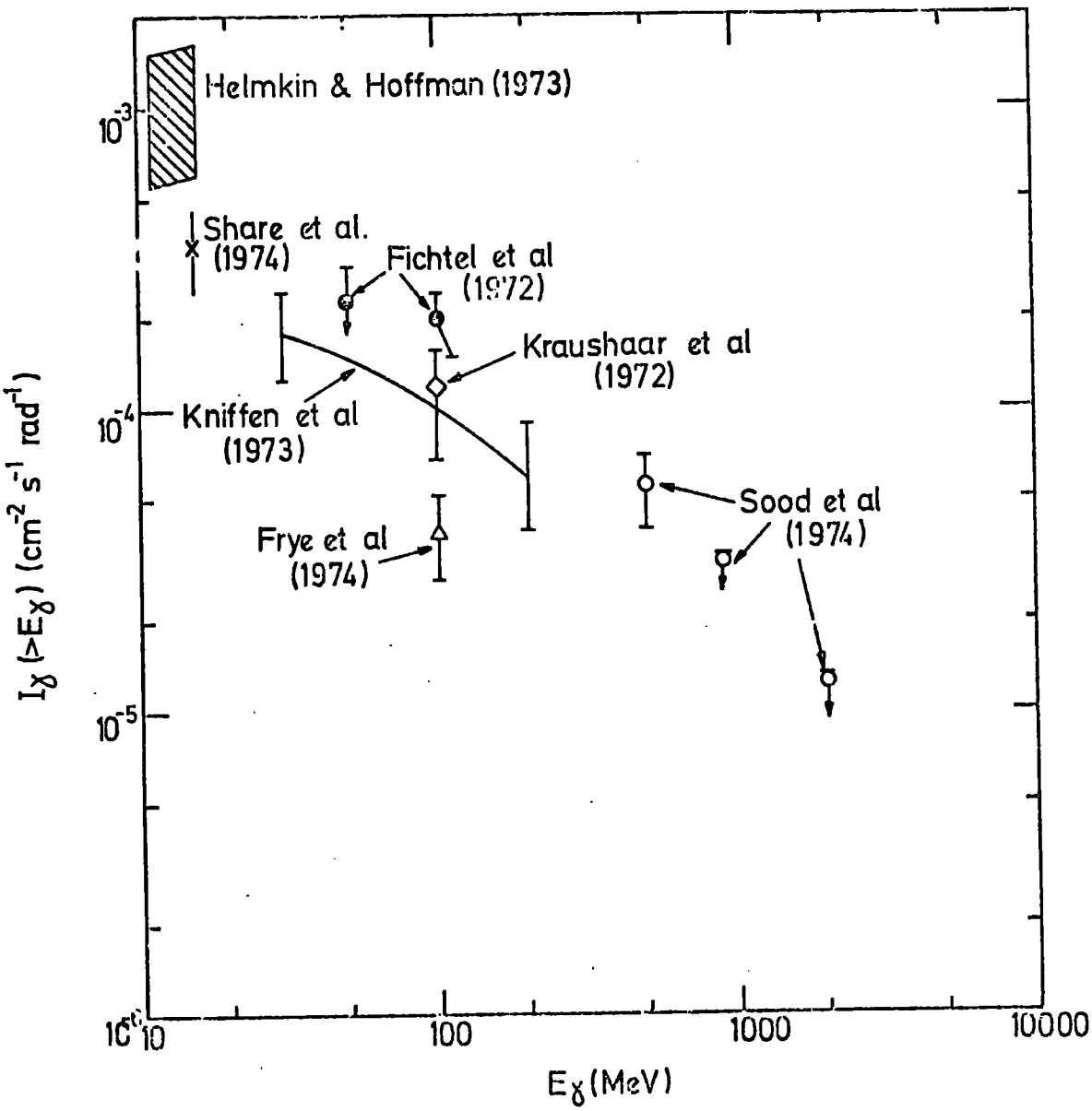

Figure 2. The spectrum of gamma-rays from the Galactic centre. Most points represent averages over a broad region around the Galactic Centre.

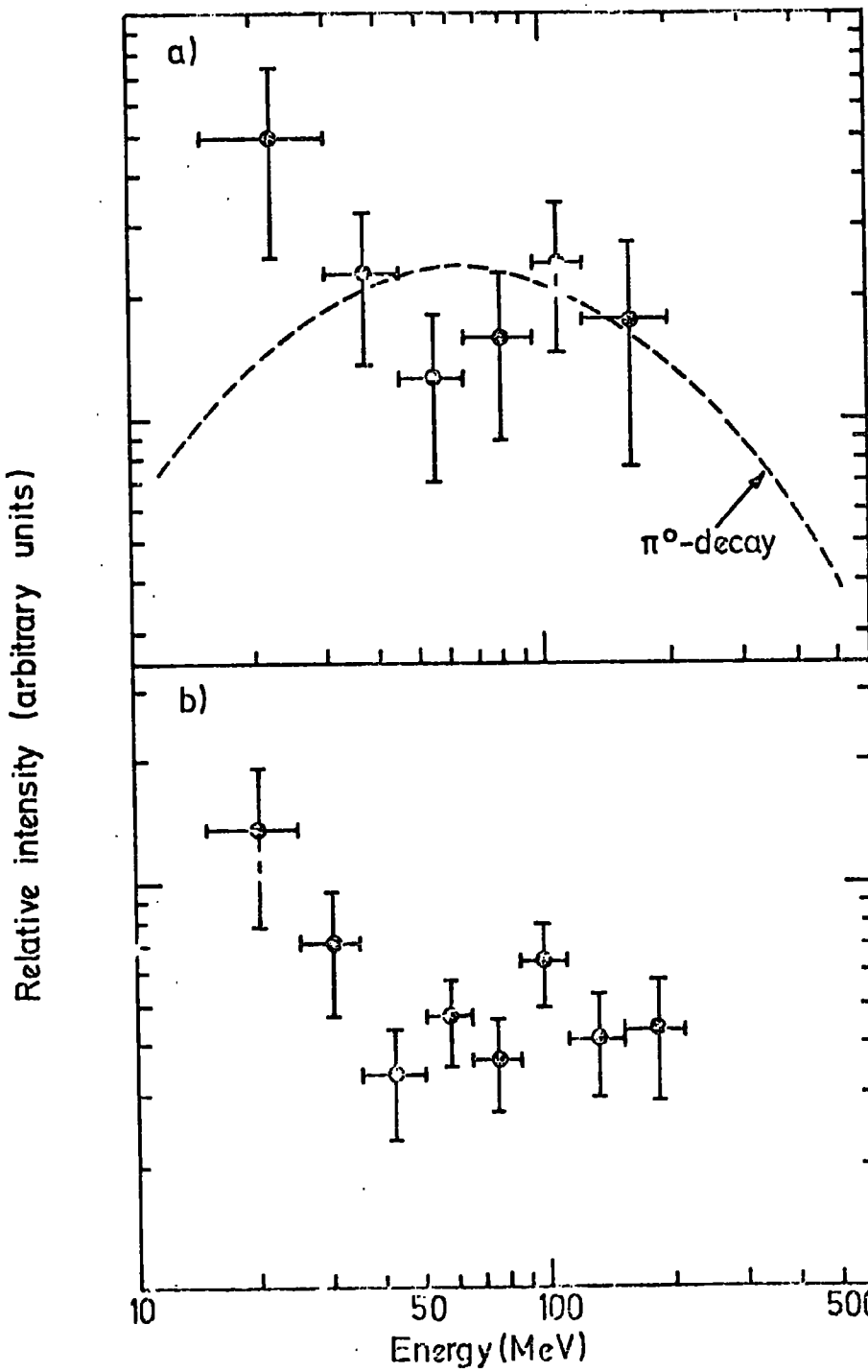

Figure 3. The differential gamma-ray spectra measured by Share et al (1974) for a) the Galactic centre and b) the atmospheric albedo gamma rays. Also included is the π^0 decay spectrum of Stecker (1973).

later studied with greater sensitivity and angular resolution by SAS II. Their results are shown in figures 4 and 5.

There are two main reasons for the differences between figures 4 and 5. Firstly, the 15° angular resolution of the OSO III telescope was very much wider than the 3° angular resolution of the SAS II instrument. Secondly, the sensitivity of the latter was such that about three times the number of photons were detected by the SAS II experiment than were detected by OSO III.

There is however, good general agreement between the results from the two satellite. In particular, SAS II confirms the existence of a broad region of enhanced intensity near the Galactic centre. Away from the Galactic centre a recent balloon telescope experiment (McKechnie et al, 1976) has measured a line strength from the Cygnus region in good agreement with SAS II results.

Four point sources have been identified by SAS II group, three associated with the pulsars, 0833 - 45, 0531 + 21, 1747 - 46 (Thompson et al 1974b,1975, 1976) and a fourth unidentified source at $l = 193^{\circ}$ $b = +3^{\circ}$. (Kniffen et al 1975). Browning et al (1972) previously detected a number of point sources in the Galactic centre with a balloon-borne telescope and suggested that the excess from this region arises from the superposition of a number of faint sources. However, Thompson et al (1974a) reports that the SAS II data does not indicate any point sources in this region and

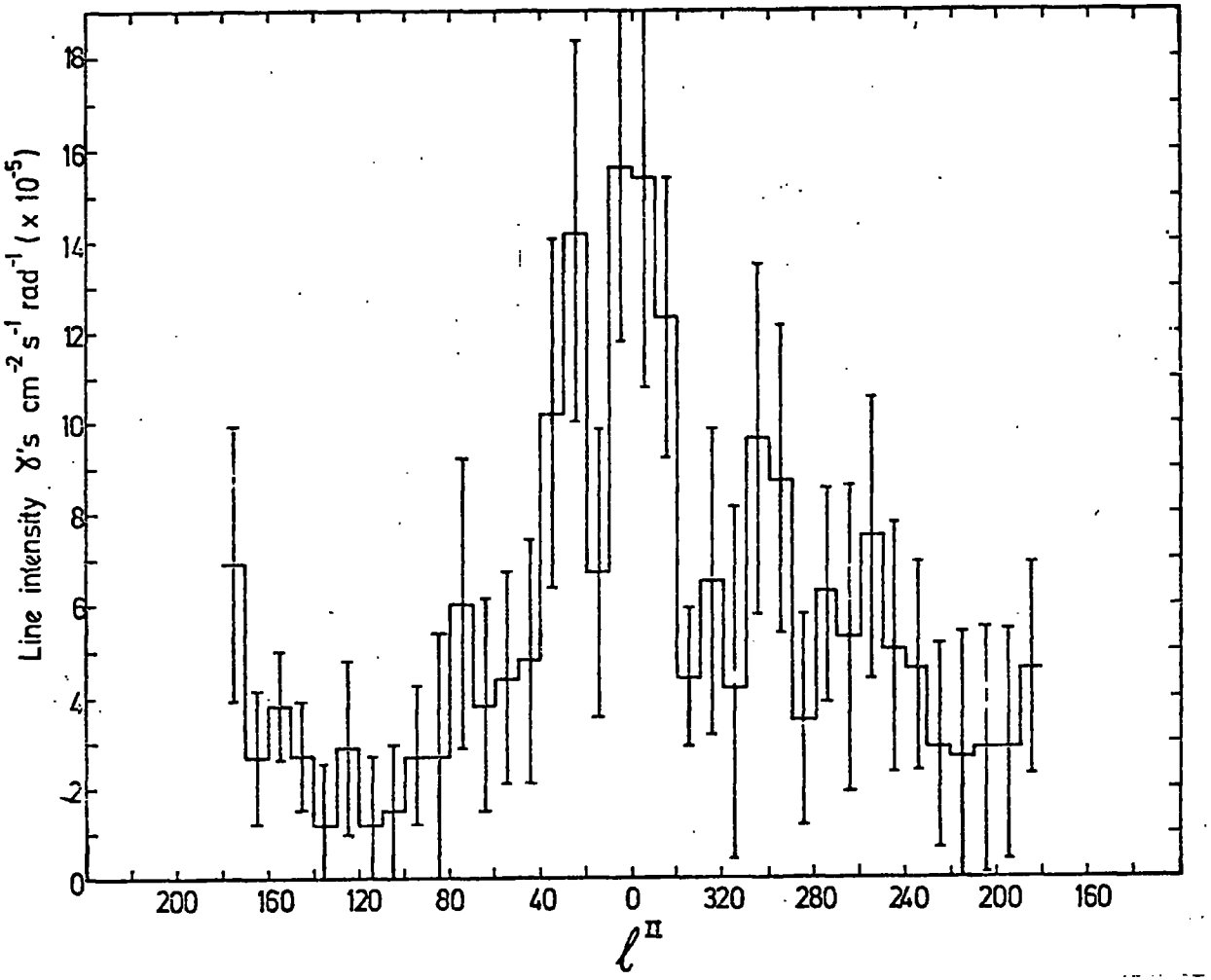

Figure 4. The distribution of gamma-ray intensity with Galactic longitude as measured by Kraushaaur et al (1972) using the OSO III satellite.

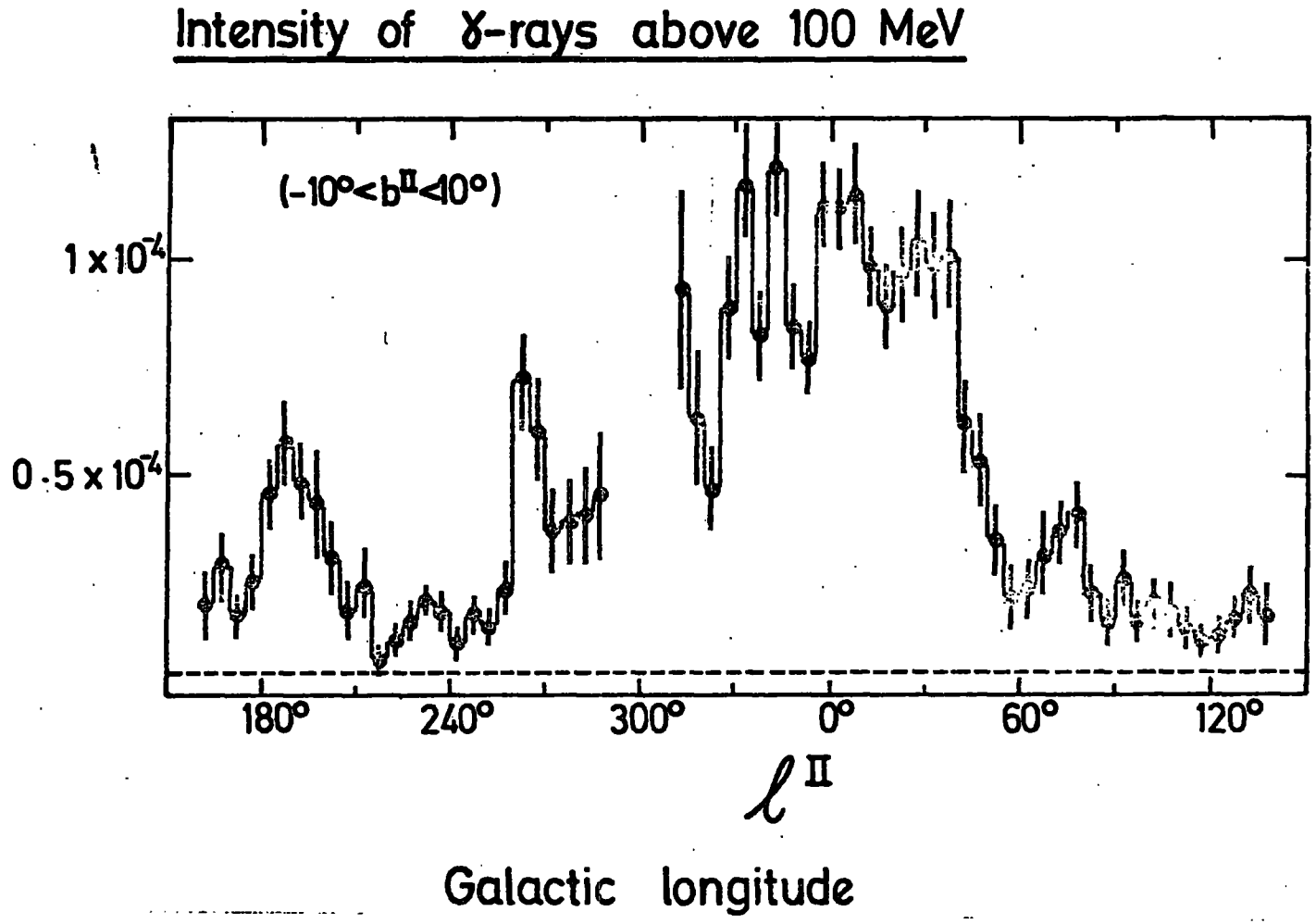

Figure 5. The distribution of gamma ray intensity with Galactic Longitude as measured by Fichtel et al using the SAS II satellite.

that there is no change in the spectral shape with position in the Galactic plane. This is very suggestive of a single process responsible for gamma ray production at all longitudes.

3.5. The Distribution of Gamma-ray Intensity with Latitude

The intensity vs latitude distribution obtained by the OSO III telescope had an angular width of about 15°; however, as this was the angular resolution of the telescope the true width was obviously considerably less than this value.

This result was considerably improved upon by the balloon-borne telescope of Share et al. (1974). Their telescope had an angular resolution of $1\frac{1}{2}^{\circ}$ at 15 MeV and recorded a width of 3° in latitude for the Galactic plane towards the Galactic centre. This result highlights one distinct advantage that balloon borne telescopes possess over satellites, namely that the telescope is recoverable. As a result nuclear emulsions may be used and this gives a very remarkable improvement in the angular resolution over the resolution of, say, a spark chamber at the same energy.

The angular width of the Galactic centre source may be used to give a mean distance to the emitting region, when the width of the emitting layer is known. If the main process is π^{o} decay, then the width of the emitting layer will be the width of the gas layer which is ~200pc. Using this value, then the Share et al. result implies a distance to the source region of 3 to 4 kpc.

The more comprehensive data from the SAS II telescope confirms the existence of a narrow emitting region. Their results are shown in figure 6. In this figure the distributions are shown for two regions; the Galactic centre (from $l = 330^{\circ}$ to $l = 30^{\circ}$) and for a broad region around the Galactic anticentre comprising $l = 90^{\circ} - 150^{\circ}$, $160^{\circ} - 170^{\circ}$ and $200^{\circ} - 260^{\circ}$.

In figure 6 the width in latitude of the Galactic Centre emission is very close to that expected for pure instrumental broadening. At these energies (> 100 MeV) the SAS II telescope angular resolution is $\lesssim 2^{\circ}$.

At higher latitudes, the slight enhancement at $+20^{\circ}$ towards the Galactic Centre and -20° towards the anti-centre has been tentatively identified (Fichtel et al 1975) as being due to the local hydrogen feature associated with Gould's belt (Davies 1960).

The broadness of the anticentre distribution is particularly interesting, it reflects the rapid increase of the gas layer thickness which occurs at the edge of the Galaxy. However, this will be discussed in more detail in chapter 9.

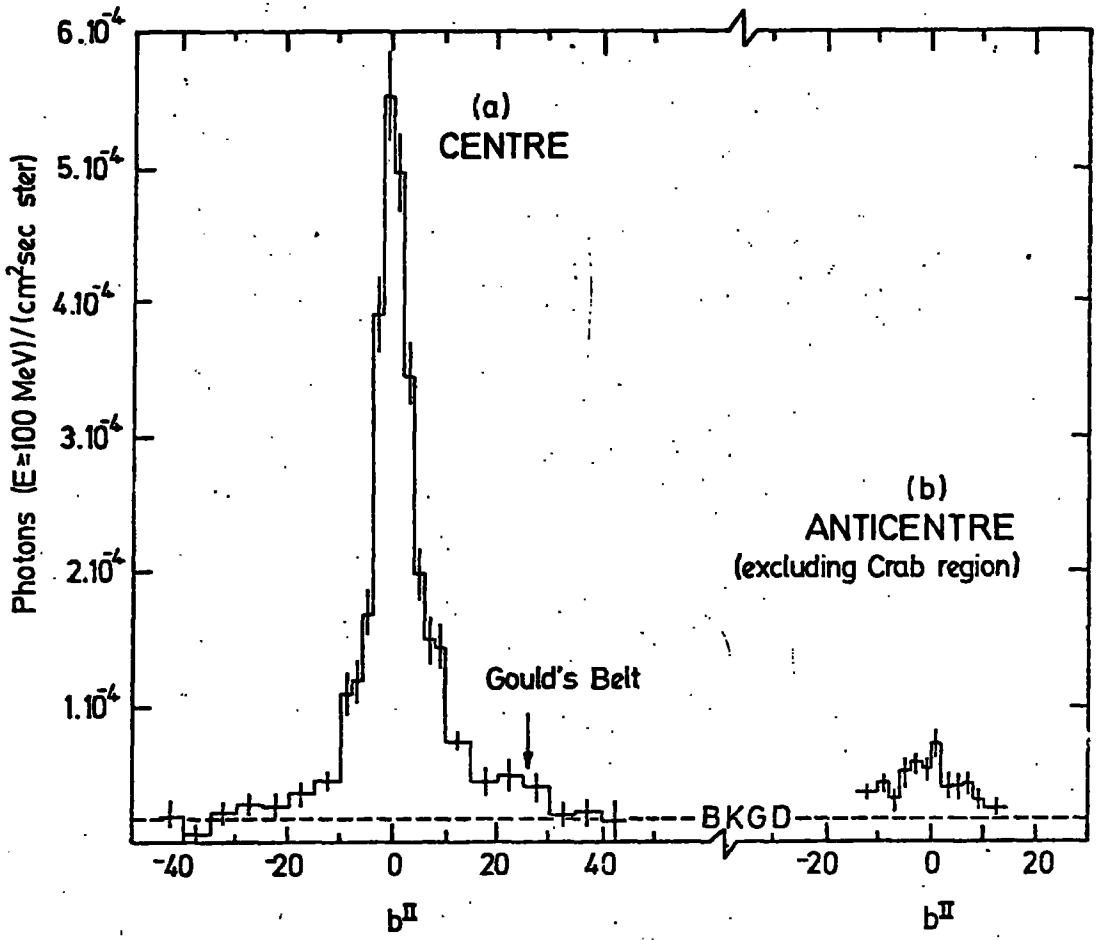

Figure 6. The distribution of gamma ray intensity with Galactic latitude, within $\pm$ 30° of the Galactic centre and for a broad region around the anticentre comprising l = 90° to 150°, 160° to 170° and 200° to 260°.

REFERENCES

Browning, R., Ramsden, D. & Wright, P.J., 1972. Nature, 238, 138.

Davies, R.D., 1960. Mon. Not. R. astr. Soc., 120, 483.

Fichtel, C.E., Hartman, R.C., Kniffen, D.A., & Sommer, M., 1972. Astrophys. J., 171, 31.

Fichtel, C.E., Hartman, R.C., Kniffen, D.A., Thompson, D.J., Bignamie, G.F., Ogelman, H., Ozel, M.F., Tumer, T., 1975. Astrophys. J., 198, 163.

Frye, G.M., Albats, P., Thomson, G.B., Hopper, V.D., Mace, O.B., Thomas, J.A., & Staib, J.A., 1974. Proc. Ninth ESLAB Symposium, ESRO SP - 106, p. 265.

Helmken, H. & Hoffman, J., 1973. Nature Phys. Sci., 243, 6.

Kniffen, D.A., Bignami, G.F., Fichtel, C.E., Hartman, R.C., Ogelman, H., Thompson, D.J., Ozel, M.F. & Tumer, T., 1975. Proc. 14th Int. Conf. on Cosmic Rays, Munich, 1, 100.

Krauschaar, W.L., Clark, G.W., Garmire, G.P., Borken, R., Higbie, P., Leong, C. & Thorsos, T., 1972. Astrophys J. 177, 341.

McKechnie, S.P., Mount, K.E. & Ramsden. D., 1976. Astrophys J. 207, L157.

Schonfelder, V. & Lichti, G., 1974. Astrophys J. 192, L1.

Share, G.H., Kinzer, R.L. & Seeman, N., 1974. Astrophys. J. 187, 45.

Sood, R.K., Bennett, K., Clayton, P.G., & Rochester, G.K., 1974. Proc. Ninth ESLAB Synposium, ESRO SP- 106, p. 217.

Stecker, F.W., 1973. Astrophys. & Sp. Sci., 20, 47.

Strong, A.W. , Wolfendale. A.W., & Worrall, D.M., 1976. J.Phys. A. In the press.

Thompson, D.J., Bignami, G.F., Fichtel, C E., Hartman, R.C., & Kniffen, D.A., 1974a. Proc Ninth ESLAB Symposium, ESRO SP- 106, p. 201.

Thompson, D.J., Fichtel, C.E., Kniffen D.A. & Ogelman, H., 1975. Astrophys. J., 200, L.79.

Thompson. D.J., Fichtel, C.E., Kniffen, D.A., Lamb, R.C. & Ogelman, H. 1976. GSFC preprint X-662 - 76 - 94.

CHAPTER FOUR

ON THE ORIGINS AND DISTRIBUTION OF COSMIC RAYS IN THE GALAXY

4.1. Introduction

If the main source of cosmic rays do in fact lie within our galaxy there are three important questions which naturally arise:-

1. What are these sources?
2. How are they distributed?
3. What is the distribution of cosmic rays which results?

In this chapter the aim is to describe the main candidates for the sources of cosmic rays and their distribution in the Galaxy. Having thus answered (1) and (2) above, the answer to (3) is approached through a discussion of present ideas on cosmic ray propagation.

4.2. The nature of the CR sources

The total energy injection rate to maintain the present energy density in cosmic rays severely limits the possible candidates. If the local cosmic ray energy density of 0.5 eV/cm^3 is assumed constant over the whole galaxy, then for a disk of radius 15 kpc and thickness 1 kpc the total energy content in cosmic rays is 5 10^{54} ergs. There is evidence (Lal 1974) that the cosmic ray flux has remained constant for at least the last 10^9 yr. Equilibrium between the energy input from the sources and the energy loss by escape

must therefore have been achieved and this enables an estimate of the total power of the sources to be made. The measured escape time of $3\ 10^6$ yr implies a total power for the sources of 10^{40-41} ergs. sec^{-1}.

The observation of synchrotron radiation from cosmic ray electrons in the shells of supernova remnants make supernovae strong candidates. An often quoted figure for the mean rate of supernovae in our galaxy is 1 per 26 yr. In order to supply all the cosmic rays in the Galaxy each supernova must therefore release $3\ 10^{50}$ ergs in cosmic rays out of a total energy release of 10^{50} to 10^{52} ergs. Thus the energy available in SNe explosions is quite adequate to provide the whole of the cosmic ray flux observed.

The mechanism by which the energy release of a supernova may be channelled into cosmic rays remains uncertain. The acceleration may occur during the supernova explosion itself, or at some later stage, either in the shell of ejecta and swept up interstellar matter, or near the surface of a pulsar which forms from the supernova.

The first of these alternatives, namely that cosmic rays are accelerated hydrodynamically during the supernova explosion has been described in detail by Colgate (1975). In this model the cosmic rays are accelerated by a shock wave which in propagating through the outer layers of the star becomes relativistic as it reaches the atmosphere of the star. For a 1.4 $M_\odot$ star Colgate calculates that $\sim 10^{-6}\ M_\odot$ of relativistic ejecta will be produced taking $3\ 10^{50}$ ergs out of a total available

energy of 7 10^{51} ergs. The spectrum of relativistic particles produced is in good agreement with the observed cosmic ray spectrum. However, the Galactic cosmic ray composition does not appear to be consistent with the expected composition of supernovae ejecta. Reeves (1975) has summarized recent work on the cosmic ray source composition and concludes that there is strong evidence for an acceleration mechanism which becomes operative after the ejected matter has mixed with a few times its own mass in interstellar matter and hence by implication that acceleration occurs some time after the supernova.

Mechanisms for the acceleration of cosmic rays in supernova remnants have been discussed by Gull (1973) and Scott and Chevalier (1975). The first author envisages the acceleration taking place at the boundary between the ejecta and the interstellar matter when the amount of interstellar gas swept up becomes equal to the ejected mass. In this situation a Rayleigh-Taylor instability occurs and the dense matter of the shell penetrates the interstellar gas, the resulting turbulence generated amplifies the magnetic field and thereby accelerates the cosmic rays. Scott and Chevalier propose a similar mechanism in their model of cosmic ray acceleration in the Supernova remnant Cas A. These authors suggest that the fast moving knots in Cas A are responsible for generating magnetic turbulence with a typical scale size like that of the knots themselves. Acceleration is due to the Fermi

process, the particles gain energy as they are reflected from the fast moving turbulent eddies. Both models easily satisfy the restrictions on the source composition imposed by observations.

An alternative source of cosmic ray particles and yet another possible way of transferring the energy release of a supernova explosion could be pulsars. In the Crab nebula the observed Xray spectrum is radiated by electrons whose lifetime is much less than the known age of the remnant, implying that within the nebula particle acceleration still takes place. The Crab nebula pulsar could well be the source of these electrons but the mechanism is uncertain. Gunn and Ostriker (1969) have proposed a model in which the acceleration is due to the low frequency electromagnetic waves produced by a magnetized neutron star with the axis of rotation and magnetic axis non parallel. They have investigated the history of a charged test particle in these waves and showed that energies up to 10^{21} eV were possible by this mechanism. In this model the composition of the cosmic rays which result will depend on where the particle originates. If the nuclei come from the surface of the neutron star mainly iron nuclei are to be expected, alternatively, if the pulsar accelerates material in a supernova remnant shell it is quite easy to obtain the composition required by experiment, provided acceleration takes place after the ejecta has thoroughly mixed with matter from the ISM.

4.3 The Galactic Distribution of Supernovae and Pulsars

4.3.1 The distribution of supernovae

The low rate of occurence of supernovae and the presence of obscuring dust in the Galactic disk makes the task of determining the time averaged distribution of supernovae in our own Galaxy impossible. Studies of extra-galactic supernovae in spiral galaxies have been used to give the general features of the supernovae distribution. Barbon et al. (1975) have recently published a study of the radial distribution of supernovae within their parent galaxies. These authors derive the surface density distribution shown in figure 1. In figure 1, $\theta = r/R$ where r is the distance of the supernova from the centre of the galaxy and R is the galactic radius. The straight line represents an exponential fitted to the data and, adopting a mean Galactic radius of 8 kpc as suggested by Barbon et al. gives a radial surface density distribution of the form $\rho/\rho_o = \exp(-\alpha r)$ where $\alpha^{-1} = 3.66$ kpc. This distribution is very similar to the distribution of surface brightness in spiral galaxies for which $\alpha^{-1} = 1$ to 5kpc (Freeman 1970). If the average Mass to luminosity ratio is assumed constant over the galaxies, then in the absence of significant amounts of absorption the distribution of surface brightness is also the distribution of stellar surface mass density. Figure 1 must therefore imply a proportionality between the supernova rate and mass density and hence that in our Galaxy the distribution of the stellar mass density will give

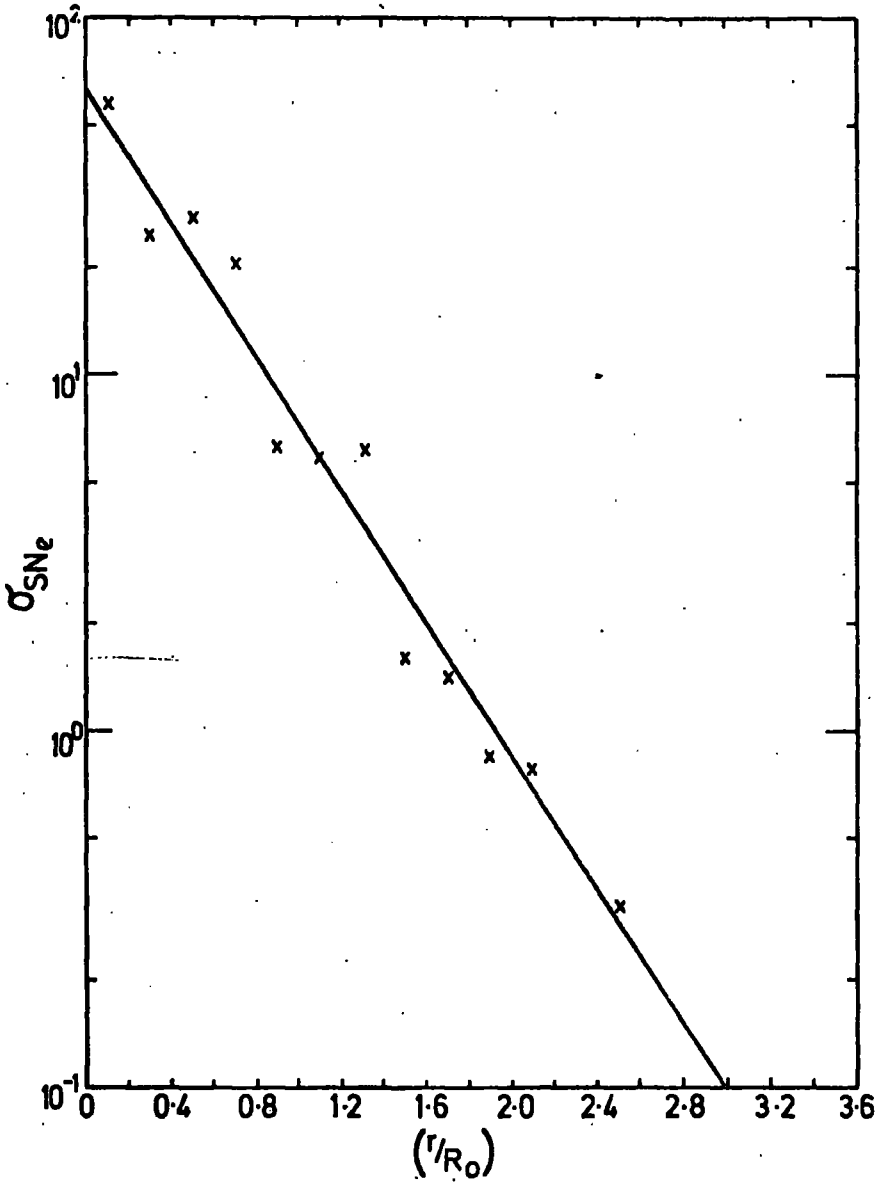

Figure 1. The surface density distribution of supernovae as a function of galactic radius as deduced by Barbon et al (1975) from extragalactic supernovae.

the time averaged radial distribution of supernovae.

The problem of the Galactic supernova rate has been examined by Tammann (1973) using the statistics of extra-galactic supernovae. He has analysed the data for the various galaxy types and deduces a rate for supernovae in our galaxy of 1 per 31^{+40}_{-11} yr. if the Galaxy is a type Sb.

4.3.2 The Distribution of Galactic Supernova Remnants

The remnant of a supernova expands into the surrounding interstellar gas at a rate which depends on the total energy released and the density of interstellar gas (see for example Shklovsky, 1968). It remains intact for up to 10^5 years after the original explosion. Since every known supernova remnant radiates a non-thermal radio spectrum these remnants are observable by radio telescopes over the whole of the Galaxy. A number of catalogues of supernova remnants have been compiled which give the positions of these objects (for example Ilovaisky and Lequeux, 1972, Downes 1971).

However, there are various selection effects which limit the number of detectable supernova remnants and this means that the Galactic distribution of remnants cannot be derived from the catalogues in any simple manner, (see Ilovaisky and Lequeux 1972). A number of authors have attacked this problem and deduced the radial distribution of supernova remnants from the catalogues after corrections for the various selection effects have been included. Figure 2 shows the

radial distribution of supernova remnants from Kodaira (1974) and Pimley (1975) and, for comparison, the surface density of stars is included. It is interesting to compare the distribution of supernova remnants with the time averaged supernova distribution which is predicted in 4.3.1a to follow the stellar mass density. Good agreement is obtained except in the innermost regions of the Galaxy where there is a deficit of SNR's and it is possible that remnants are being missed in radio surveys due to the high background flux. Vettolani and Zamorani (1976) have investigated the apparent distribution of SNR's which would result from a time-averaged supernova distribution which follows the stellar mass denisty. They find a distribution of remnants in good agreement with the observed distribution of remnants and argue that the distribution of supernovae in the Galaxy has the same form as is deduced for other galaxies. Ilovaisky and Lequeux (1972) have deduced the SNe rate for our galaxy based on the statistics of supernova remnants. They deduce a rate 1 per 50 $\pm$ 25 yr which agrees well with the estimate above.

4.3.3 The Galactic Distribution of Pulsars

As with supernova remnants the deduction of the pulsar distribution from the catalogues of known pulsars requires inclusion of various corrections to cancel out the selection effects. In this particular case this is best achieved by using the results of a pulsar search made by a single instrument to provide a complete sample.

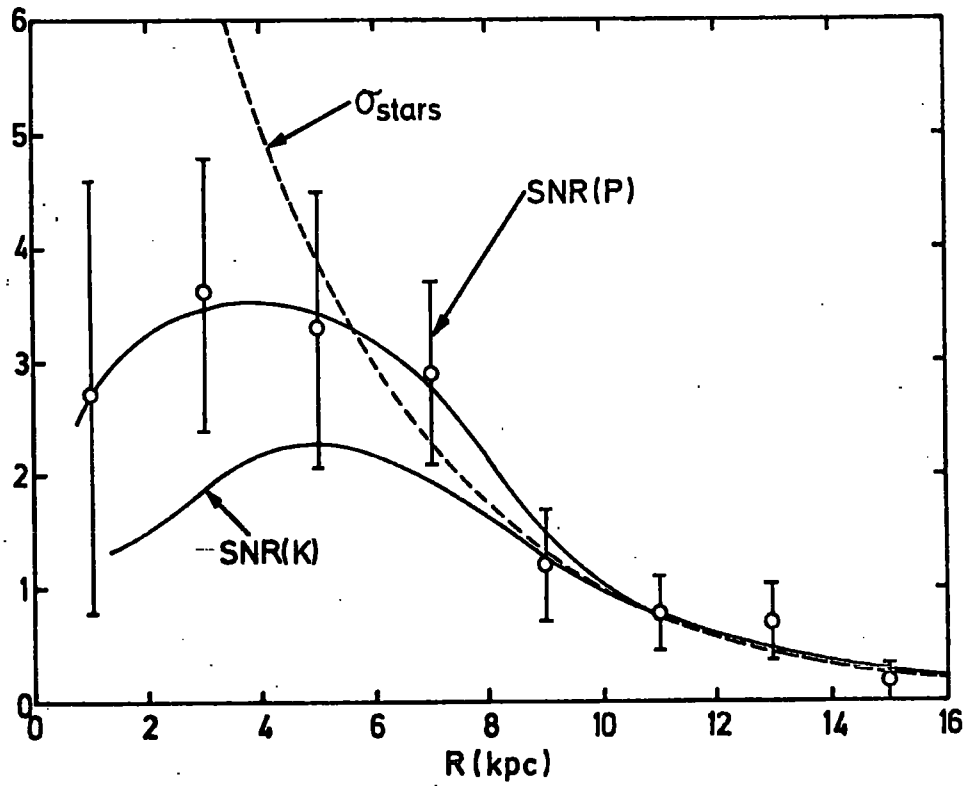

Figure 2. The radial distribution of supernova remnants in the Galaxy as deduced by Kodaira (1974) and Pimley (1975).

Two sky surveys have now been carried out, by the Jodrell Bank (Lyne, 1974) and the Arecibo groups (Hulse and Taylor 1975). Figure 3 shows the radial distribution obtained using the Jodrell Bank data (Lyne, Private Communication). Comparison with the SNR distribution of Kodaira indicates that the pulsars are peaked somewhat higher at 6 kpc than the SNR's. Once again there is a suggestion of a deficit of pulsars near the Galactic centre although the uncertainty becomes large. Hulse and Taylor find evidence for a cut off in the radial distribution of pulsars at radii 10 kpc, a result which is in general agreement with the radial distribution of figure 3.

The pulsar birth rate has been estimated using the data of figure 3 Seiradakis (1976) gives a rate of 1 per 25 years which is in good agreement with the SNe rate deduced by Ilovaisky and Lequeux and is therefore quite consistent with the hypothesis of a supernova birth for all pulsars.

4.4 Cosmic ray Propagation

The propagation of cosmic rays in the Galaxy is a very difficult problem. The aim of a propagation model is to reconcile the observational properties of the cosmic rays with the hypothesis of origin in discrete sources. In the section which follows some of the important features of the cosmic ray propagation models will be outlined with the object of predicting the distribution of Cosmic rays which may result from a source distribution such as those described above.

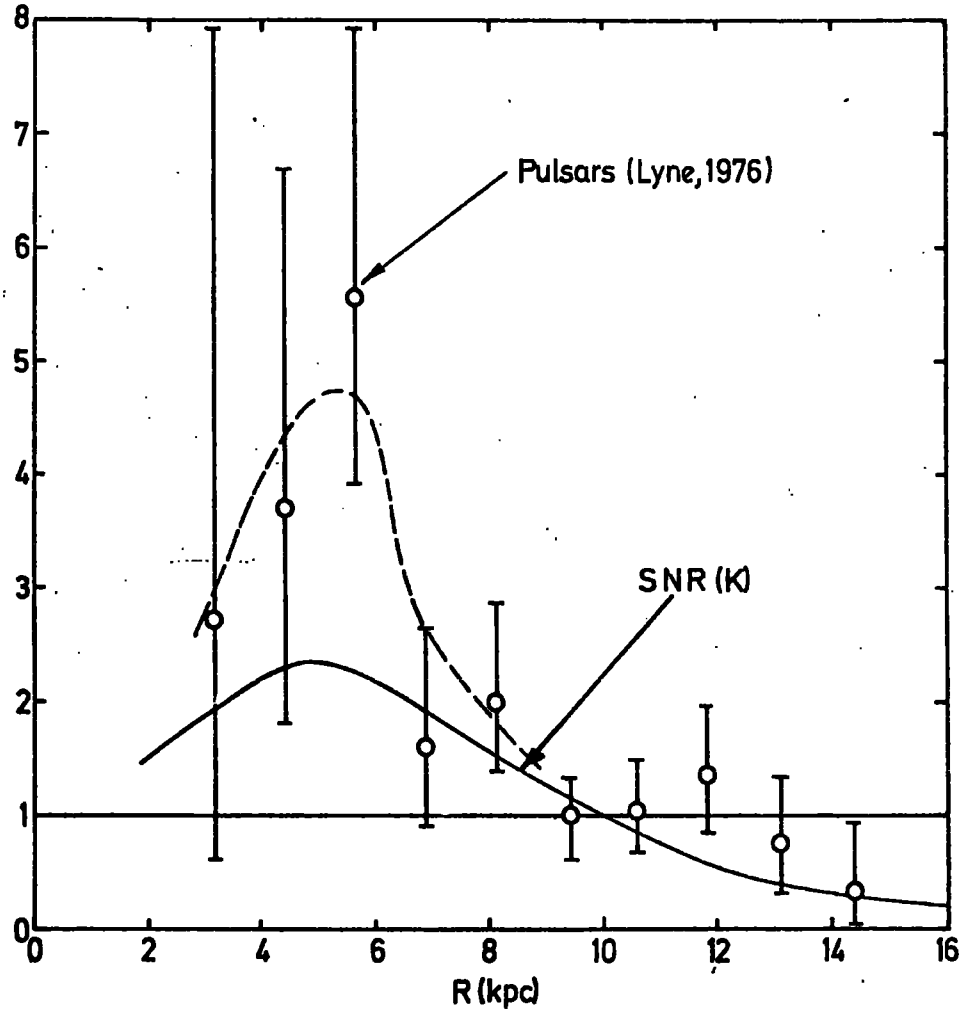

Figure 3. The radial distribution of pulsars in the Galaxy derived from the Jodrell Bank survey.

4.4.1 Diffusion Models

The simplest approach is to assume that the cosmic ray motion is random and that the density satisfies a diffusion equation. For the case of 3 dimensional diffusion one obtains a general equation for the density of cosmic rays $N(\bar{r},t,E)$ as a function of space time and energy of the form

$$\frac{\partial N}{\partial t} - \nabla.(D\nabla N) + \frac{\partial}{\partial E}\left(\frac{\partial E}{\partial t}N\right) + \frac{N}{T_c} = Q(\bar{r},t,E) \qquad 1$$

where D is the diffusion coefficient, $\frac{\partial E}{\partial t}$ is the energy loss rate, T_c is the life time of the particles due to catastrophic processes and $Q(\bar{r},t,E)$ is the source per unit time and per unit energy at $\bar{r}$ and t. The diffusion coefficient for isotropic diffusion is $D = \lambda c/3$ where λ is the mean free path and may be a function of energy. For protons the energy loss term is ignored but for electrons this is important. The catastrophic life-time T_c is ∞ for both electrons and protons and is important only for nuclei.

Consider the case of a disk confinement region 280 pc thick and 15 kpc in radius with a source function $Q(\bar{r}, E)$. Since the escape time of the particles is $\ll$ the loss time by collisions, the equilibrium density of cosmic rays is governed only by the local value of the source function and the escape time. Thus by assuming an escape time T_e independent of position the equilibrium density $N(\bar{r}, E)$ is given by

$$N(\bar{r}, E) = Q(\bar{r}, E)\, T_e$$

This equilibrium solution may be derived from equation 1 by setting $\frac{\partial N}{\partial t}$, $\frac{\partial}{\partial E}\left(\frac{\partial E}{\partial t}N\right)$ and $\frac{N}{T_c} = 0$

and by replaing the diffusion term by N/T_e which corresponds to postulating an energy independent escape probability (Ramaty 1974).

The general solution to equation 1 has been discussed in detail by Ginzburg and Syrovatskii(1964). In the solution the choice of parameters are governed by the observables of the cosmic radiation i.e. the anisotropy, mean age and constancy.

The natural choice for the diffusion mean free path, λ is the observed scale length of irregularities in the magnetic field which is 10 to 30 pc. Unfortunately, however, for the disk confinement region described above the choice of λ = 10 pc leads to an escape time in clear disagreement with observation. Even more severe difficulties are encountered with the anisotropy. The probability of obtaining an anisotropy in the observed range for a supernova rate such as that discussed above is extremely low for this choice of λ.

The assumption of isotropic 3-dimensional diffusion may not be valid. The protons in the cosmic radiation with $E < 10^{14}$ eV the gyroradius is <10pc. Hence the cosmic rays will behave as though bound to the field lines and experiments at the Earth sample only those cosmic rays bound to field lines passing within one gyroradius of the Earth. The problem thus becomes one-dimensional diffusion and even greater difficulties are encountered in trying to reconcile the observed anisotropy with a set of discrete sources randomly distributed in space and time (Dickinson and Osborne 1974).

4.4.2 Self Confinement of Cosmic Rays

One type of model frequently discussed can achieve consistency with observation. This is the 'leaky-box' model, in which cosmic rays are pictured as propagating almost freely inside a box with partially reflecting walls. A version of this model has been proposed by Skilling (1971) and Holmes (1974) in which the partially reflecting boundaries are formed by the scattering of cosmic rays on Alfven waves.

Resonant scattering of cosmic rays by Alfven waves occurs when the wavelength is a few times the gyroradius (Wentzel 1974). In this process the mean free path for reversing the cosmic ray direction is approximately the gyroradius multiplied by the ratio of the energy densities in the galactic magnetic field and the Alfven waves. These waves are set up whenever cosmic rays stream down a density gradient with a streaming velocity $V_s > V_A$, where V_A is the Alfven velocity. Such a situation would arise at, say, the surface of a disk confinement region or near a cosmic ray producing supernova. Thus on this model the cosmic rays are self-confined i.e. the Alfven waves which scatter the cosmic rays are generated by the cosmic rays themselves.

In passing it is interesting to note that when this model is applied to the propagation of cosmic rays away from a source such as a supernova the predicted adiabatic energy losses for the cosmic rays become prohibitively large. (Kulsrud 1975). The problem then becomes one of understanding how a source

can inject enough energy to overcome this problem.

In the Skilling-Holmes model the region close to the Galactic plane is labelled the 'free' zone and the region of strong scattering by Alfven waves is the 'wave' zone. The boundary between these zones is the z height from the Galactic plane at which the growth rate Γ_G and damping rate Γ_D of the Alfven waves are equal and for any particular energy and spectrum of cosmic ray particles is specified by the z distributions of the ionized and neutral gas. Thus, for a 3GeV particle and a cosmic ray spectrum of exponent 2.5 the boundary occurs at 286 pc.

The basic version of this model pictures cosmic rays propagating at almost the velocity of light within the free zone being frequently reflected in collisions with the wave zone.

Dickinson (1975) has modified this basic model to include a realistic model of the propagation of the particles in the free zone and examines in detail the consequences for the Galactic distribution of cosmic rays. His models E and F are of particular interest here since he uses a source distribution proportional to the stellar mass density which is the same source distribution as is implied by the observations of extragalactic supernovae. His results are surprising. Despite having a source distribution which peaks at the Galactic centre at 60x the local value he finds variations in cosmic ray concentration across the Galactic disk which are very much smaller than this. At 1GeV he finds in model E an increase of only 30% at

the Galactic Centre and in model F, which includes the effects of propagation in spiral arms, he finds an increase of 15% at 5 kpc and a decrease of 15% at 14 kpc relative to the concentration at 10 kpc. For source distributions which are constant in R he finds variations in concentration between 0 and 10 kpc of $<$ 1%.

REFERENCES

Barbon, R., Capaccioli, M. and Ciatti, F., 1975. Astron.Astrophys., 44, 267.

Caswell, J.L., Clark, D.H., Crawford, D.F. and Green, A.J., 1975. Aust. J. Phys. Astrophysical Supplement No. 37.

Colgate, S.A., 1975. Origin of Cosmic Rays, Ed. J.L. Osborne and A.W.Wolfendale. D.Reidel, Dordrecht.

Dickinson, G.J. and Osborne,J.L., 1974. J.Phys. A., 7, 728.

Dickinson, G.J., 1975. Ph.D. Thesis, University of Durham.

Freeman, K.C., 1970. Astrophys. J., 160, 811.

Ginzburg, V.L. and Syrovatskii, S.I., 1964. The Origin of Cosmic Rays, Pergamon, Oxford.

Gull, S.F., 1973. Mon. Not. R.A.S., 161, 47.

Gunn, J.E. and Ostriker, J.P., 1969. Phys. Rev. Lett., 22, 728.

Holmes, J.A., 1974, Mon. Not. R. Astr. Soc., 166, 155.

Hulse, R.A. and Taylor, J.H., 1975. Astrophys. J. Lett, 201, L55.

Ilovaisky, S.A. and Lequeux, J., 1972. Ast. Astrophys., 20, 347.

Kodaira, K., 1974. Publ. Astron. Soc. Japan, 26, 255.

Kulsrud, R, & Zweibel, E., 1975. Proc. 14th Int. Conf. Cosmic Rays, Munich. 2, 465.

Lal, D., 1974, Phil Trans. Roy. Soc., 277, 395.

Lyne, A.G., 1974. Galactic Radio Astronomy, IAU Symposium 60, D.Reidel, Dordrecht.

Pimley, K., 1975. M.Sc. Thesis, University of Durham.

Ramaty, R., 1974. High Energy Particles and Quanta in Astrophysics. Eds. F.B.McDonald and C.E.Fichtel, MIT Press.

Reeves, H., 1975. Origin of Cosmic Rays. Ed. J.L. Osborne and A.W.Wolfendale. D.Reidel, Dordrecht.

Scott, J.S. and Chevalier, R.A., 1975. Astrophys. J., 197, L5.

Seiradakis, J., 1976. Goddard Space Flight Centre Symposium on Gamma Ray Astronomy, to be published.

Shklovsky, I.S., 1968. Supernovae, Wiley-Interscience.

Skilling, J., 1971 Astrophys. J. 170, 265.

Tammann, G.A., 1974. Supernovae and Supernova Remnants. Ed. C.B. Cosmovici, D.Reidel, Dordrecht.

Vettolani. G. and Zamorani, G., 1976. Reprint.

Wentzel, D., 1974. Ann. Rev. Astron. and Strophys. Vol.12.

CHAPTER FIVE

THE INTERSTELLAR GAS

5.1 Introduction

This chapter reviews the main observational results on the interstellar medium (ISM) which are relevant to the problem discussed later. In particular interest is concentrated on the observed distribution of the interstellar gas on a galactic scale. Since the dominant component of the ISM is hydrogen, studies of this atom are obviously of paramount importance.

5.2 The Galactic Distribution of Neutral Atomic Hydrogen

5.2.1 21cm Observations

The hyperfine transition of neutral hydrogen produces a spectral line of wavelength 21 cm which has been observed in emission in every direction on the sky. As a result, emission studies in this line have become one of the major tools in the study of the large scale structure of our Galaxy. This importance is enhanced by the fact that the 21 cm emission regions are completely resolvable in both velocity structure and angle by the typical radio telescope.

A typical profile in this line gives the intensity as a function of frequency, I_ν, Doppler shifted from the line's natural frequency of 1420.406 MHz. In radio astronomy it is common practice to express intensity in terms of a brightness temperature, T_b, where

$$T_b = \frac{c^2}{2\nu^2 k} I_\nu \quad \text{(Rayleigh-Jeans approximation)}$$

The condition for this approximation is that $h\nu/kT \ll 1$. Since for the 21 cm line $h\nu/k = 0.07K$, this condition is always satisfied in 21 cm studies.

In studies of the Galactic plane the measured frequencies are converted to radial velocities relative to the local standard of rest which has been determined from the motions of the nearby stars. The Galactic rotation curve may then be obtained from profiles in the Galactic longitude interval $270 < l < 90$. This involves the measurement of the terminal velocities contributed by material on the locus of subcentral points for which the Galactocentric radius is $R = R_o |\sin l|$. The rotation curve so determined for $R < R_o$ can be extended to R = 13 kpc by observations of Cepheid variables and is extrapolated beyond this distance by using a model of the Galactic mass distribution which is constructed to fit the galactic rotation curve for $R < R_o$. Figure 1 shows the rotation curve and surface density of matter on the Mass model which is derived from the rotation curve (Innanen 1973).

The primary goal of 21 cm astronomy has always been the transformation of the observed intensity-velocity profiles into a map of the spatial distribution of hydrogen. In particular it was hoped that the spiral structure would become evident in the HI maps. Burton (1976) has discussed in detail the major problems encountered in achieving this goal. He stresses that a grand design of a spiral structure in the overall HI distribution is not established and there is little

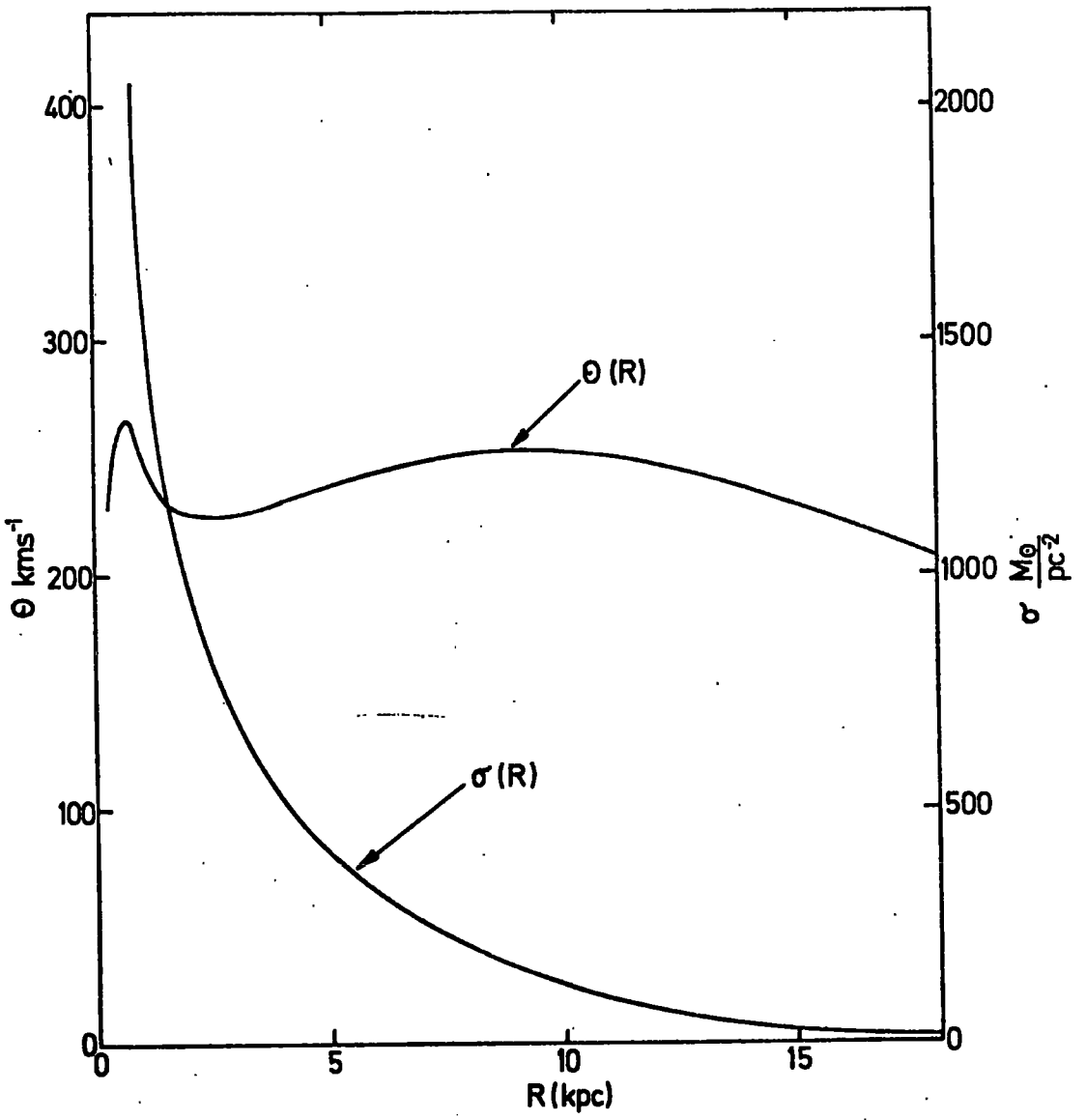

Figure 1. The Galactic rotation curve and surface mass density distribution from the mass-model of Innanen (1973).

evidence at all for spiral structure features in the radial distribution of atomic neutral hydrogen from these studies.

5.2.2.1 The R and Z distributions of atomic hydrogen

The column density of atomic hydrogen in a particular direction is given by

$$N_{HI} \text{ cm}^{-2} = 1.823 \times 10^{18} \int T_k \tau(v)\, dv$$

v is the velocity

where T_k is the excitation temperature of the line, and τ is the optical depth. As mentioned above, the observations give $T_B(v)$ where

$$T_B(v) = T_k \left[1 - \exp(-\tau(v))\right]$$

If the line is optically thin i.e. $\tau \ll 1$ then $T_B(v) = T_k\, \tau(v)$ and the column density is given by

$$N_{HI} = 1.823\ 10^{18} \int T_B(v)\, dv$$

which is easily obtained by integration of the observed profile.

In the galactic plane $T_k \simeq 120$ K and the line is usually optically thick; if the line is completely saturated, $T_B(v) = T_k$.

Figure 2 shows the radial variation of atomic hydrogen density in the galactic plane from Gordon and Burton (1976). The average hydrogen density along a line of length Δr is calculated from

$$n_H = \int_{v(r)}^{v(r+\Delta r)} \frac{T_b(v)\,dv}{\Delta r}$$

when the line is optically thin. Figure 2 includes corrections for the partial saturation of the line.

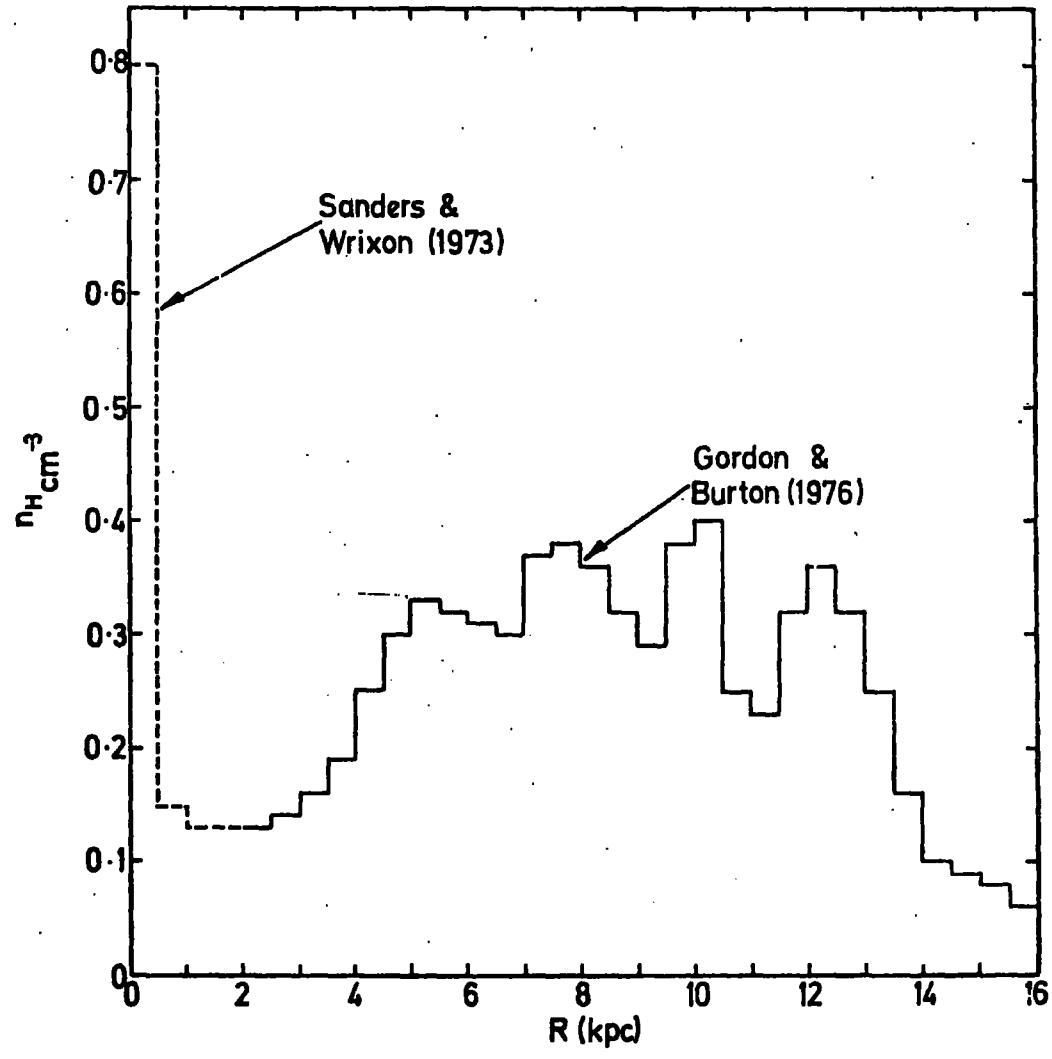

Figure 2. The radial variation of atomic hydrogen density in the Galactic plane. The densities for $R > 2$ kpc come from Gordon and Burton (1976), for $R < 2$ kpc the model of Sanders and Wrixon has been used.

The densities near the galactic centre were taken from the model of Sanders and Wrixon (1973).

A further important observation in 21 cm astronomy is the thickness of the atomic hydrogen layer. This has been determined for a range of positions in the Galaxy by Jackson and Kellman (1974) from the portions of profiles corresponding to the locus of subcentral points, where the distance is unambiguous. Figure 3 shows that their results for the variation of $Z_{\frac{1}{2}}$ with R.Burton (1976)has also determined the variation of $Z_{\frac{1}{2}}$ with R, he gives the expressions

$$Z_{\frac{1}{2}} = 200 \text{ pc} \quad , \quad R < 9.5 \text{ kpc}$$

$$Z_{\frac{1}{2}} = 200 + 38\ (R - 9.5) \text{ pc}; \quad R > 9.5 \text{ kpc}$$

This is plotted in figure 3 for comparison with the results of Jackson and Kellman.

Gordon and Burton (1976) utilize these data on the scale height to calculate the surface density of atomic hydrogen which is shown in figure 4. Once again the model of Sanders and Wrixon is used to calculate the surface density of gas in the nucleus.

5.2.2.2 The fine scale structure of the atomic hydrogen

Although 21 cm emission in the galactic plane can provide an accurate description of the large scale distribution of atomic hydrogen in the Galaxy, for details of the fine scale structure observations of the emission profiles at high latitude are used. An alternative technique in this kind of study is to observe the absorption profile of the 21 cm line in front of bright radio continuum sources. Comparison with a nearby emission profile enables

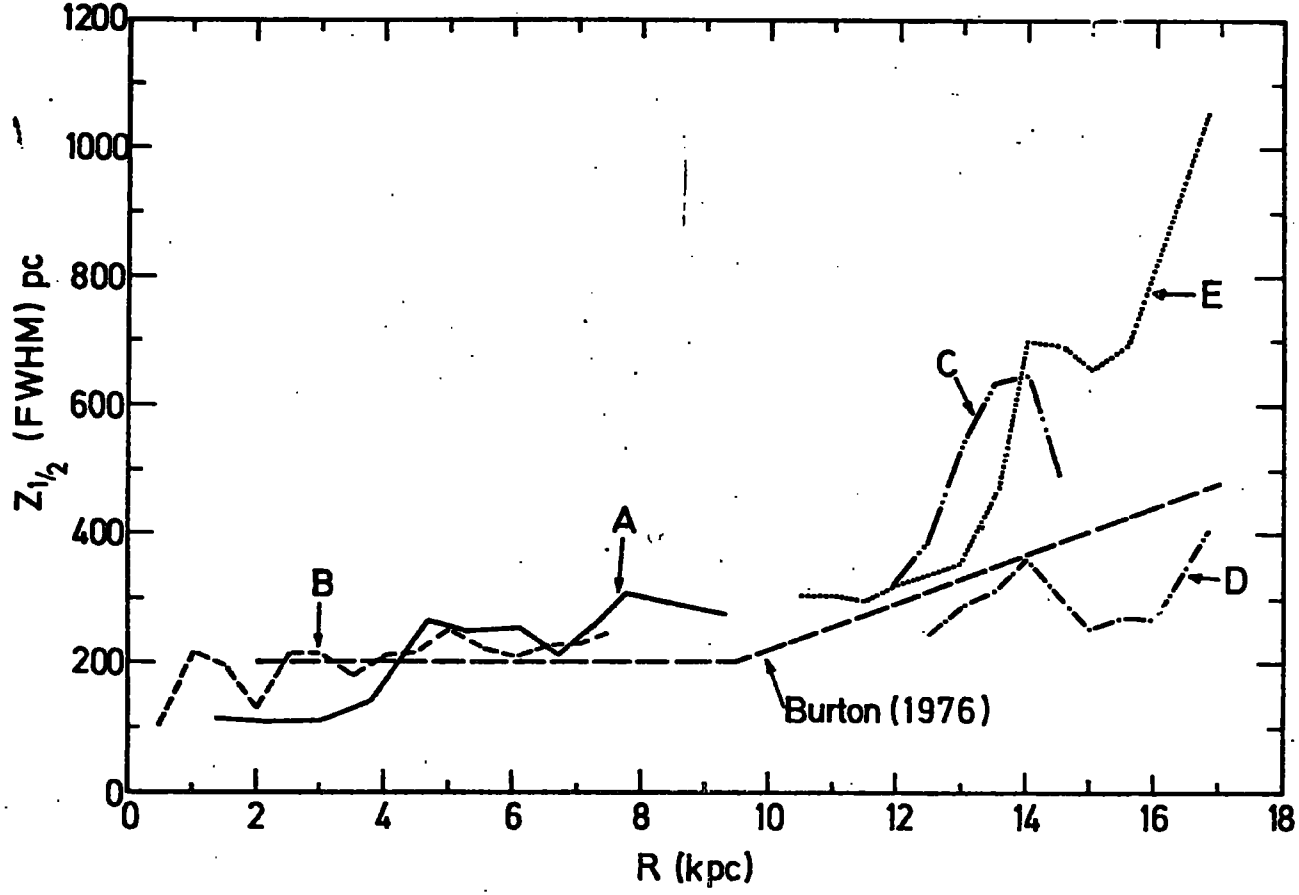

Figure 3. The variation of $Z_{\frac{1}{2}}$ with Galactocentric radius R. Curves A-E are from Jackson and Kellman (1974) and refer to the longitude intervals; A, $0 < l < 90$; B, $270 < l < 360$; C, $160 < l < 205$; D, $110 < l < 160$; E, $200 < l < 300$. For comparison the results of Burton (1976) are also shown.

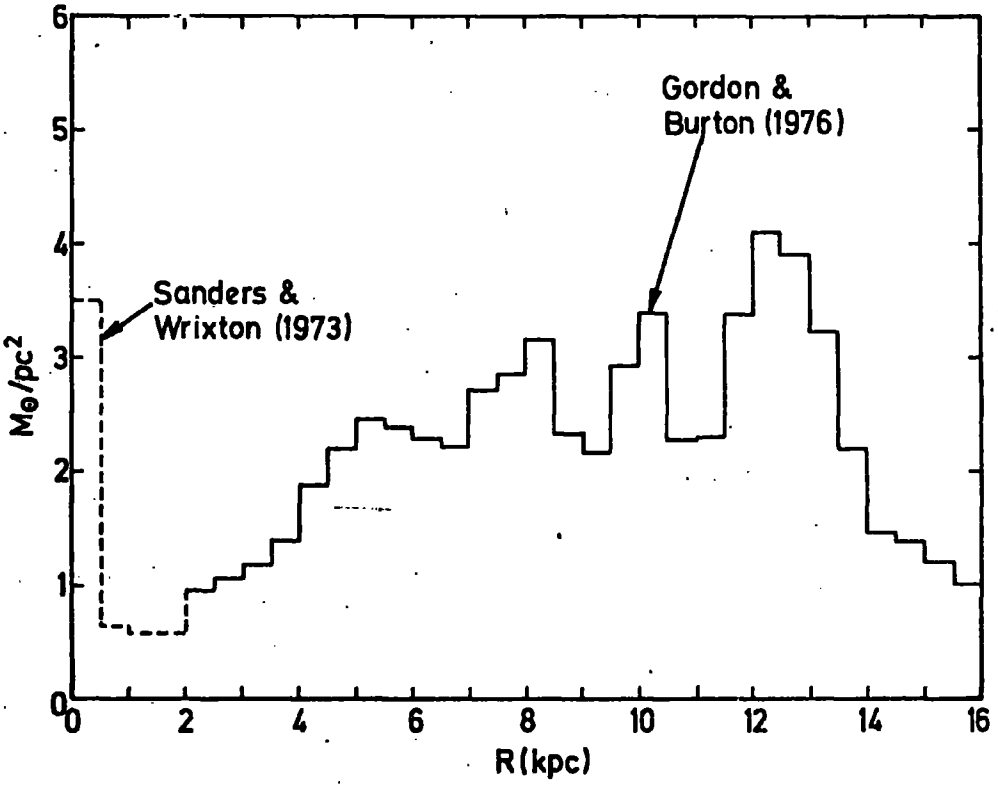

Figure 4. The Distribution of the surface density of atomic hydrogen with Galactocentric Radius, R.

the column density, spin temperature and velocity structure of the emitting gas to be determined unambiguously.

A general picture which emerges from these studies is of a 'raisin pudding' interstellar medium consisting of cold, dense clouds in a hot tenuous intercloud medium. The properties of the cold clouds have been investigated in absorption studies (Radhakrishnan and Goss 1972, Hughes et al. 1971) and an average HI cloud is found to have a column density of $3\ 10^{20}$ cm^{-2} and a temperature of 60 K, which is significantly less than the 120 K quoted above. If this lower temperature is correct the use of 120 K would lead to the under-estimation of column densities. This may be important for the work of section 9 where the γ-ray flux in the anticentre is calculated from the measured hydrogen column densities in this region.

5.2.3 Far UV Observations

This involves the observation of the resonance absorption lines (e.g. Lyman α at 1216Å) in the line of sight to hot stars which are used to provide continuum background light sources.

Since the technique relies upon rocket or satellite borne instruments this is an even younger branch of astronomy than 21 cm radio astronomy. It is, however, a very powerful method of investigating the spatial distribution of atomic hydrogen out to 1 kpc from the Sun.

Jenkins and Savage (1974) use data from rocket flights and OAO-2 observations to determine the local distribution of gas. They find an average density of 0.6 atoms cm^{-3} with a large range in the observations (from < 0.1 to > 1.0 atoms

cm^{-3}). Near to the sun they suggest a density of n_H = 0.25 atoms cm^{-3} may be representative. More recently Bohlin (1975) has reanalysed the available data on Ly - α absorption and attempts to correct for the observational bias. This author finds a mean atomic hydrogen density near the sun of 0.9 atoms cm^{-3}. In addition these authors find a correlation between the hydrogen column density to a star and the stellar colour excess E(B-V), yielding

$$\frac{N_H}{E(B-V)} = 5 \quad 10^{21} \text{ atoms cm}^{-2} \text{ mag}^{-1}$$

This correlation has important implications for gamma ray astronomy. Adopting an $A_V/E(B-V)$ ratio of 3 it is found that in dense dust clouds for which A_V may be > 6 this suggests column densities $> 10^{22}$ atoms cm^{-2}. However, 21 cm studies of dark clouds give much lower column densities (Heiles, 1969). The implication of this result, which is that the atoms have been converted to molecules is examined in the next section.

5.3 The Galactic Distribution of Molecular Hydrogen

In the last section it was mentioned that the correlation of hydrogen column density with interstellar extinction appears to break down when applied to regions in which the interstellar absorption is large, such as in large dust clouds. The interpretation of this result is that in the centre of these clouds the atomic hydrogen is converted to molecular hydrogen with almost 100% efficiency. In the general

interstellar medium hydrogen molecules are rapidly dissociated by UV photons in starlight; however, in dust clouds molecular hydrogen is shielded from UV photons and hydrogen atoms rapidly combine to form molecules. The next two subsections will describe the distribution of molecular hydrogen as deduced from observations.

5.3.1 Direct Observations

Unfortunately, molecular hydrogen has no observable transition in the optical and radio wavebands. In fact, under interstellar conditions it is observable only via the absorption lines in the far ultraviolet and is thus accessible to direct observation only from rockets and satellites.

The richest source of data came from the studies using the Copernicus satellite (Spitzer et al. 1973) which has been used to measure the column density of molecular hydrogen in the line of sight to nearby hot stars. They find that for stars for which the line of sight intersects an interstellar gas cloud (i.e. those for which $E(B-V) > 0.1$) the fraction of hydrogen in molecular form exceeds 0.1. On the other hand, for stars with $E(B-V) < 0.05$ there is no trace of the absorption implying $< 10^{-7}$ of the hydrogen in molecular form. Thus, they confirm the hypothesis that H_2 will form at the centre of clouds for which the extinction is large enough to shield the molecules. Their results imply that some 50% of the local interstellar hydrogen is in

molecular form.

In a recent review paper Jenkins (1976) gives an average molecular hydrogen density near to the solar syste of 0.2 atoms cm^{-3} which together with the atomic hydrogen density gives a total density of 1.1 atoms cm^{-3}.

Unfortunately these techniques are limited to the space within 1 kpc of the sun. The unravelling of the Galactic distribution of molecular hydrogen requires recourse to indirect methods.

5.3.2 Indirect Observations of the distribution of Galactic H_2.

After molecular hydrogen, carbon monoxide is expected to be the most abundant molecule in the interstellar medium. This is due, not only to the relative abundance of its constituents and the ease by which it can form, but mainly to the fact that it is the most stable diatomic molecule known, with a dissociation energy of >11 eV. The far UV observations by Jenkins et al. (1973) have confirmed its abundance especially in the spectra of reddened stars which also show H_2 lines. Jenkins et al. find a $N(CO)/N(H_2)$ ratio of $\sim 10^{-8}$ for the four stars they observed.

Large column densities of CO have also been detected in dense dust clouds by observing the $J(1 \rightarrow 0)$ rotational transitiion of ^{12}CO at 2.6 mm, (Penzias et al 1972). Since it is the same dust clouds which have a dense core of molecular hydrogen the 2.6 line presents

itself as a powerful tool for the examination of the Galactic Distribution of molecular clouds.

The actual brightness temperature-velocity profiles in this line have provided further confirmation of the existence of high densities of neutral molecules alongside the CO. The typical excitation temperature in this line is 20 K, it can be shown, (Robinson 1973), that to achieve this sort of temperature excitation must be due to collisions with neutrals and that the density of neutrals must be of order 10^3 - 10^4 cm^{-3}. Thus implying the existence of molecular hydrogen in high densities.

Several surveys of the galactic plane have now been made in this line (Scoville and Soloman 1975, Burton et al. 1975, Gordon and Burton 1976) and there is now some concensus on the general features of the Galactic distribution of CO and hence by inference the distribution of molecular Hydrogen. Figure 5 shows the distribution of CO in R as determined by Gordon and Burton. In obtaining figure 5 the average density of CO molecules along a line of sight distance Δr is calculated from

$$n(CO) = \frac{N(CO)}{r} = 3.43 \; 10^{14} \frac{[^{12}C]}{[^{13}C]} \int \frac{T_B(^{12}CO)dv}{\Delta r}$$

(Gordon and Burton 1976). In this expression $[^{12}C] / [^{13}C]$ is the relative abundance of the ^{12}C and ^{13}C isotopes. In calculating N(CO) Gordon and Burton assume a $[^{12}C] / [^{13}C]$ ratio of 40 for the ISM compared to a terrestial abundance ratio of 89.

Figure 5 also shows the surface density of CO

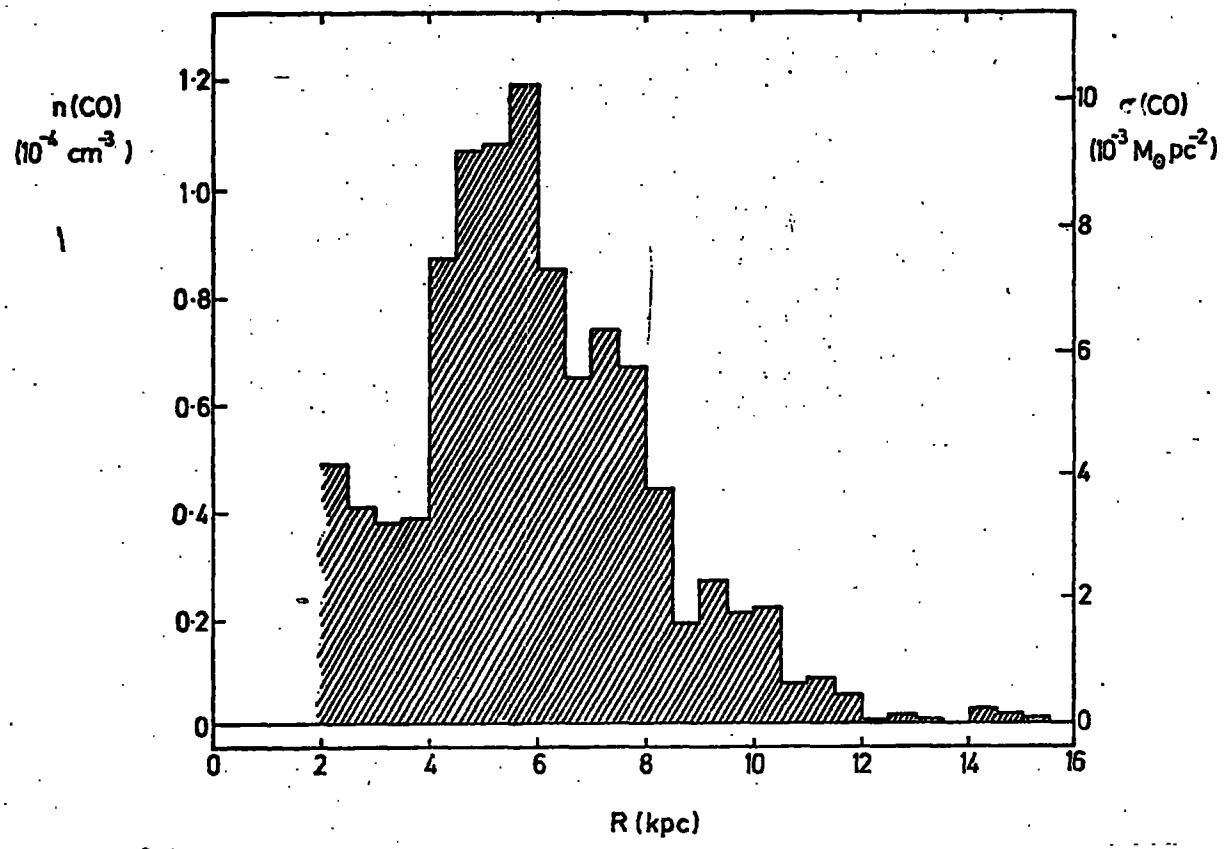

Figure 5. The distribution of the carbon-monoxide density n(CO), and surface density, N(CO), with Galactocentric radius, R. The data is from Gordon and Burton (1976).

which is calculated from n(CO) and the total layer thickness, which was measured by Burton and Gordon (1976) at $l = 21^{\circ}$ and found to be 117pc. Scoville and Solomon also quote a layer thickness, which at 100pc is in quite good agreement with the Burton and Gordon figure.

The volume and surface density of molecular hydrogen can be calculated using the data in figure 5 from the relative abundance of carbon and hydrogen in the ISM if the fraction of carbon in CO is known. Gordon and Burton quote a figure of 10% for the latter quantity leading to an $n(CO)/n(H_2)$ ratio of $6\ 10^{-5}$. Figure 6 shows the distribution of molecular hydrogen in the galactic plane calculated from the data in figure 5 and using this ratio. In addition, to the molecular hydrogen $n(H_2)$ figure 6 also shows the distribution of atomic hydrogen, n(HI) and the total hydrogen density $2n(H_2) + n(HI)$. Essentially the same distribution was found by Scoville and Solomon except that these authors quote a density of 5.0 molecules cm^{-3} at the peak near 5.5 kpc., compared to Gordon and Burton's peak value of 1.9 molecules/cm^3.

Figure 7 shows the surface density of molecules, atoms and the total hydrogen. The molecular surface density is calculated from the data in figure 6 using the layer thickness quoted above. The data presented in figure 7 strongly implies that the picture of the inner galaxy derived from 21 cm astronomy greatly underestimates the total gas content.

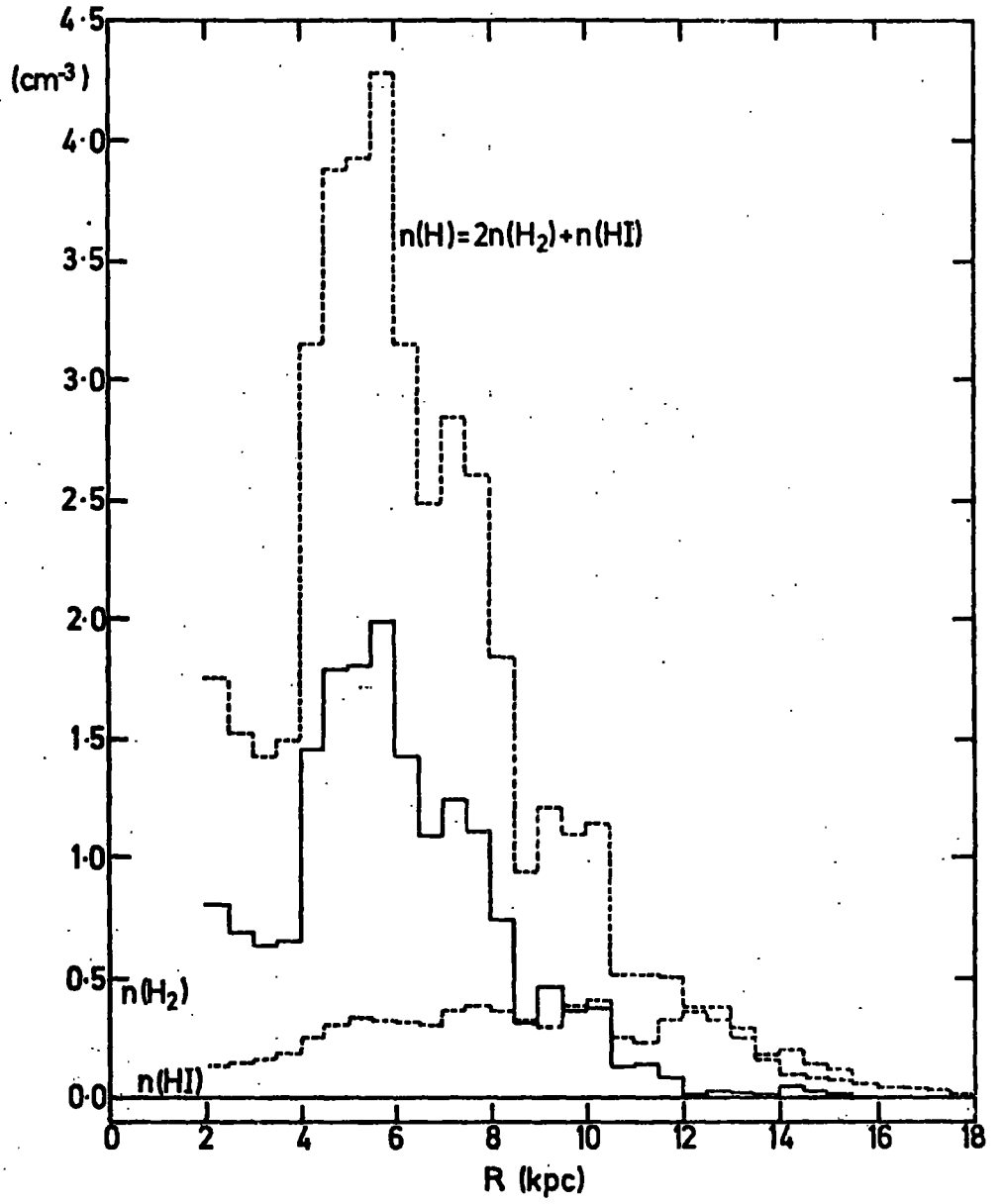

Figure 6. The radial distribution of the total hydrogen density, $n(H) = 2n(H_2) + n(HI)$.

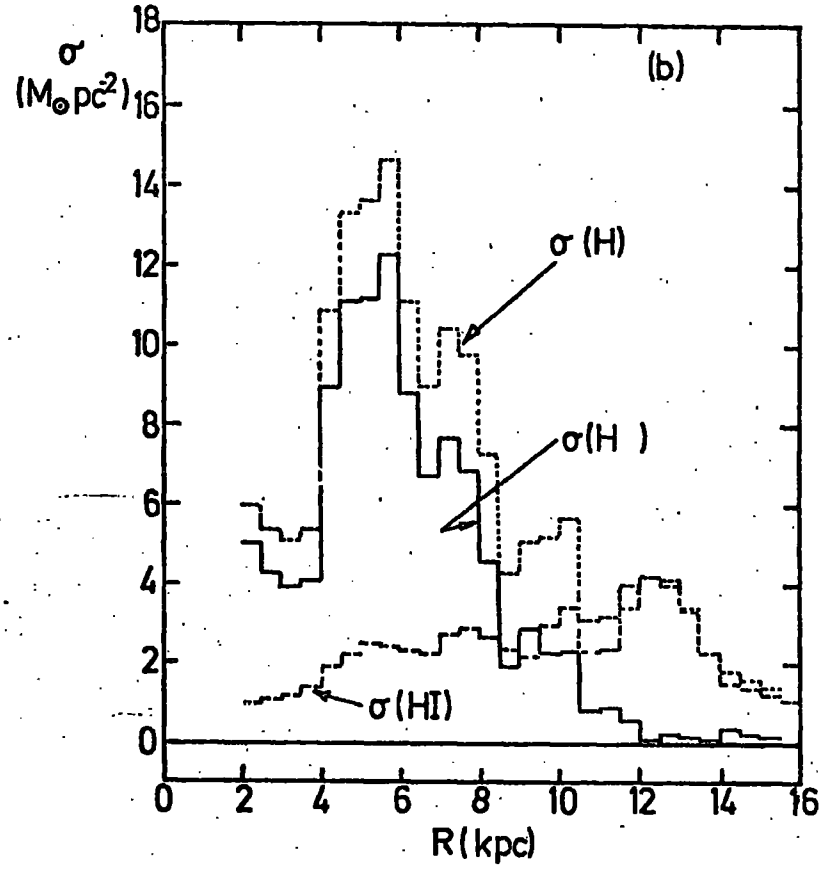

Figure 7. The radial distribution of the surface density of hydrogen according to Gordon and Burton (1976).

In fact Burton (1976) estimates that as much as 93% of the hydrogen gas in the inner galaxy may be in molecular form. However, the difficulties in calculating the molecular hydrogen density from the CO observations mean that there must remain considerable uncertainty in this estimate. In addition there remains an uncertainty in the density of molecular hydrogen in lower density clouds. The Gordon and Burton results pertain only to the distribution of dense clouds, the large fraction of H_2 discovered by Spitzer et al. 1973 is simply not included in their results. Clearly, the possible uncertainty in the published figures is large.

5.4 The Density and Distribution of other Atoms

In later chapters the interstellar gas will be regarded mainly as a target material for interactions of the interstellar cosmic ray flux. Thus, in addition to the hydrogen it is important to include the material in the interstellar medium with atomic number above 1. This is best achieved through a multiplying factor $\overline{M}$ such that

$$\overline{M} = \sum_A \frac{M_A f(M_A)}{M_H}$$

where M_A is the mass of the atom of atomic number A and $f(M_A)$ is the relative abundance of this atom compared to hydrogen.

Trimble (1975) in a recent survey gives abundances for three regions: the solar atmosphere, the Orion nebula and for planetary nebulae. Using these abundances $\overline{M}$ is found to be 1.34, 1.46 and 1.71. Allen (1973) quotes 1.36 but both

Pagel (private communication 1976) and Trimble (private communication 1976) propose higher values, 1.42 and 1.46 respectively. Therefore for the best estimate for $\overline{M}$ pertaining to the locality of the sun a value $\overline{M} = 1.42$ is adopted.

However, it is likely that the composition of the interstellar gas will vary with position in the galaxy. Measurements on other galaxies support this view and there is evidence from our own galaxy too (see D'Odorico et al. 1976). Peimbert (Private Communication 1976) considers that $\overline{M}$ may increase from 1.42 near the sun to 1.8 or 1.9 near the Galactic centre.

In the region near 5-6 kpc where the peak of the hydrogen density occurs $\overline{M}$ might only be larger by 10% than the solar value. A 10% variation in the C/H ratio between 10 and 5 kpc might have to be taken into account in deriving the molecular hydrogen densities when better data are available.

REFERENCES

Allen, C.W., Astrophysical Quantities, Athlone Press, London.

Bohlin, R.C., 1975. Astrophys. J., 200, 402.

Burton, W.B., Gordon, M.A., Bania, T.M. and Lockman, F.J., 1975. Astrophys. J., 202, 30.

Burton, W.B., 1976. Ann. Rev. Astron and Astophys vol. 14.

Burton, W.B. and Gordon, M.A., 1976. Preprint.

D'Odorico, S., Peimbert, M. and Sabbadin, F., 1976. Astron. Astophys., 47, 341.

Gordon, M.A. and Burton, W.B., 1976. Preprint.

Heiles, C., 1969. Astrophys. J., 186, 493.

Hughes, M.P., Thompson, A.R. and Colvin, R.S., 1971. Astrophys. J.Suppl. 200., 23, 323.

Innanen, K.A., 1973. Astrophys and Space Sci.,22, 393.

Jackson, P.D. and Kellman, S.A., 1974. Astrophys. J., 190, 53.

Jenkins, E.B. and Savage, B.D., 1974. Astrophys. J., 187, 243.

Jenkins, E.B., 1976. Goddard Space Flight Centre Symposium on Gamma ray Astronomy; to be published.

Penzias, A.A., Solomon, P.M., Jefferts, K.B. and Wilson R.W., 1972. Astrophys. J., 174, L43.

Radhakrishnan, V. and Goss, V.M., 1972. Astrophys. J.Suppl. 203.

Robinson,B.J.,1974. The Interstellar Medium, Ed. K.Pinkau, D.Reidel, Dordrecht.

Sanders, R.H. and Wrixon, G.T., 1973. Astron Astrophys, 26, 365.

Scoville, N.Z. and Solomon, P.M., 1975. Astrophys. J., 199, L105.

Spitzer, L., Drake, J.F., Jenkins, E.B., Morton, D.C., Rogerson, J.B. and York, D.G., 1973. Astrophys. J., 181, L116.

Trimble, V., 1975. Rev. Mod. Phys., 47, 877.

CHAPTER SIX

THE CONTRIBUTION TO GALACTIC GAMMA-RAYS FROM INTERACTIONS BETWEEN COSMIC RAYS AND THE INTERSTELLAR RADIATION

6.1. Introduction

The aim of this chapter is to calculate the contribution to the gamma radiation which arises from the Inverse Compton Effect (ICE) and to investigate the longitude distribution of gamma radiation which arise from this process.

This problem has received the attention of several authors (Cowsik and Hutcheon 1971, Dodds et al. 1974, Beuermann 1974) but the actual fraction of the observable gamma flux which is produced in this process remains the subject of debate. Cowsik and Voges (1975) argue that the contribution from the Galactic centre is at least 60% ICE, whereas in earlier work we obtained a maximum of 10%. (Dodds et al. 1974). Needless to say it is important for our understanding of the origin and distribution of CRs that narrower limits be set.

6.2 A Model for the Gamma-ray emission due to ICE.

6.2.1 The ICE Mechanism and Cross-section

The kinematics of this process were described in chapter 2. In the calculation the cross-section used is that given in equation 1

$$\sigma(E_\gamma, \epsilon, E_e)dE = 2\pi r_o^2\left[\frac{m_e^2}{\epsilon E_e^2} + \frac{m_e^4 E_\gamma}{4\epsilon^2 E_e^4} - \frac{m_e^6 E_\gamma^2}{8\epsilon^3 E_e^6} + \frac{m_e^4 E_\gamma}{2\epsilon^2 E_e^4}\ln\left(\frac{m_e^2 E_\gamma}{4\epsilon E_e^2}\right)\right] dE_\gamma \quad 1.$$

6.2.2 The Intensity of the interstellar radiation field.

This is an important problem for several areas of Astrophysics and as a result has received the attention of a number of authors (Zimmermann 1964, Witt and Johnson 1975, Habing 1968, Gondhalekar and Wilson 1976) In particular interest has been focussed on the wavelength region between 912 and 3000 Å which is of importance in understanding the ionization equilibrium of the interstellar medium. Figure 1 shows the radiation intensity as a function of frequency from the results of several different calculations.

It is immediately obvious from an examination of the luminosity function of stars as a function of their spectral type that the intensity of starlight is dominated by the radiation from G-type stars with surface temperature of 6000 K (for example see Mihalas 1968). To a good approximation the interstellar radiation can be represented by a 'greybody' spectrum (i.e. a diluted black-body spectrum) with temperature 6000 K. Figure 1 shows the spectrum adopted here, the dilution factor was obtained by adopting a total energy density for starlight of 0.45 eV cm^{-3}(Allen 1973). This spectrum is in good agreement with results of the other calculations.

In addition to the local energy density and spectrum of starlight the spatial variation of energy density with position is required. In these calculations it is assumed that the energy density of starlight follows the total mass density in the galaxy and the Innanen

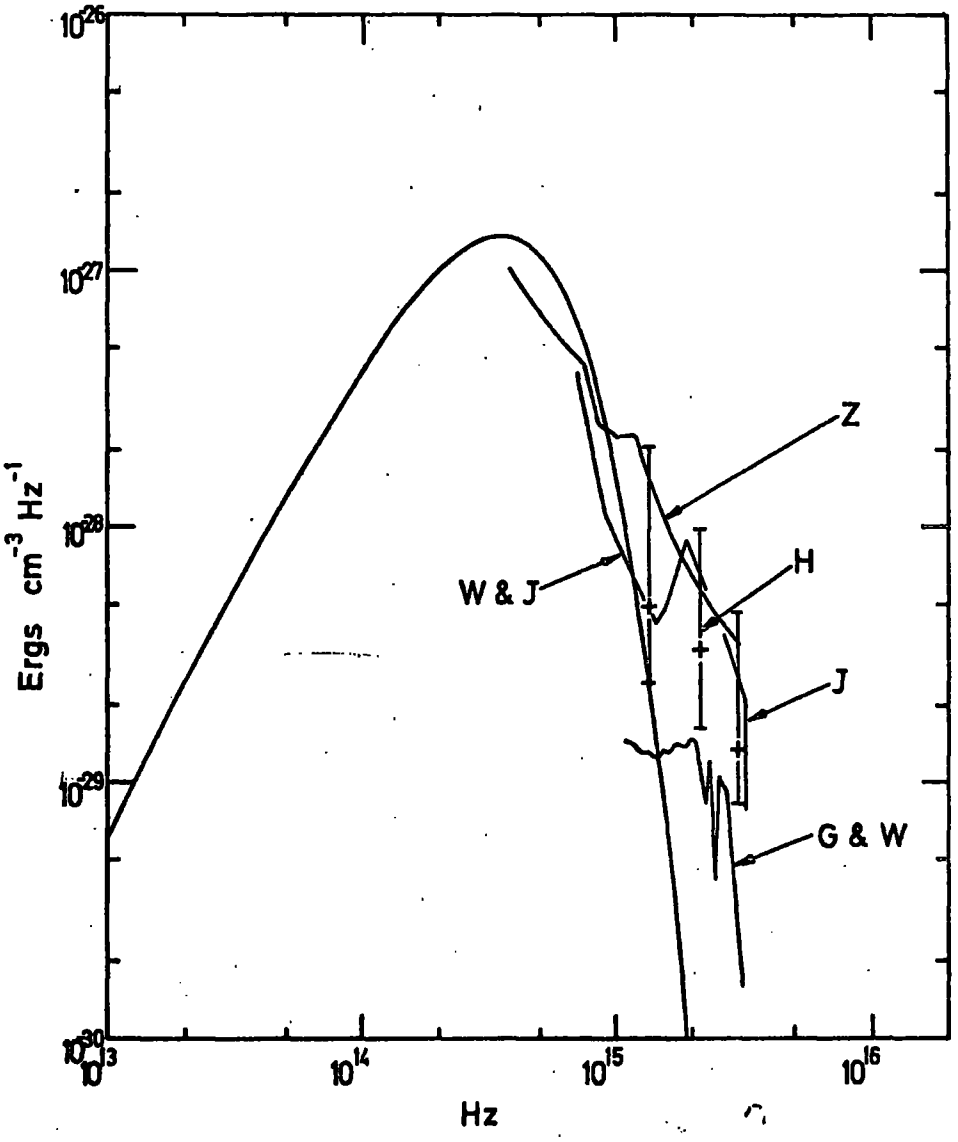

Figure 1. The distribution of starlight energy density with frequency for a 6000 K diluted black body spectrum with total energy density 0.45 eV cm^{-3}. Also included for comparison are the results of the calculations mentioned in the text;

Z - Zimmerman (1964)
H - Habing (1968)
W&J - Witt and Johnson (1973)
J - Jura (1975)
G&W - Gondhalekar and Wilson (1976).

(1973) mass model has been adopted. Confirmation of the validity of this approach comes from studies of other spiral galaxies (de Vaucouleur 1959, Freeman 1970, Simkin 1975) which show that the surface brightness distribution of spiral galaxies have the general form $I(R) = I_o \exp(-\alpha R)$. This is also the form of the distribution of the surface density of matter as obtained by Innanen. Furthermore it is assumed that there is no change in the spectral distribution of the light as a function of position, in agreement with the recent observations by Simkin (1975).

The other component of the interstellar radiation field which is included in the calculations is the universal blackbody radiation. The thermal nature and (near perfect) isotropy of this radiation is well established, in these calculations a temperature of 2.7 K is adopted.

6.2.3 The Electron Spectrum

Figure 2 shows a compilation of observations of the cosmic ray electron spectrum from Meyer (1975). Above 10GeV the experimental points probably represent accurately the local interstellar electron spectrum, however, below this energy the spectrum is modulated by interaction with the solar wind and the correct interstellar spectrum is somewhat uncertain.

The energies of the electrons required to produce Compton gamma rays may be estimated from equation 28 of chapter 2. The mean photon energies of the two

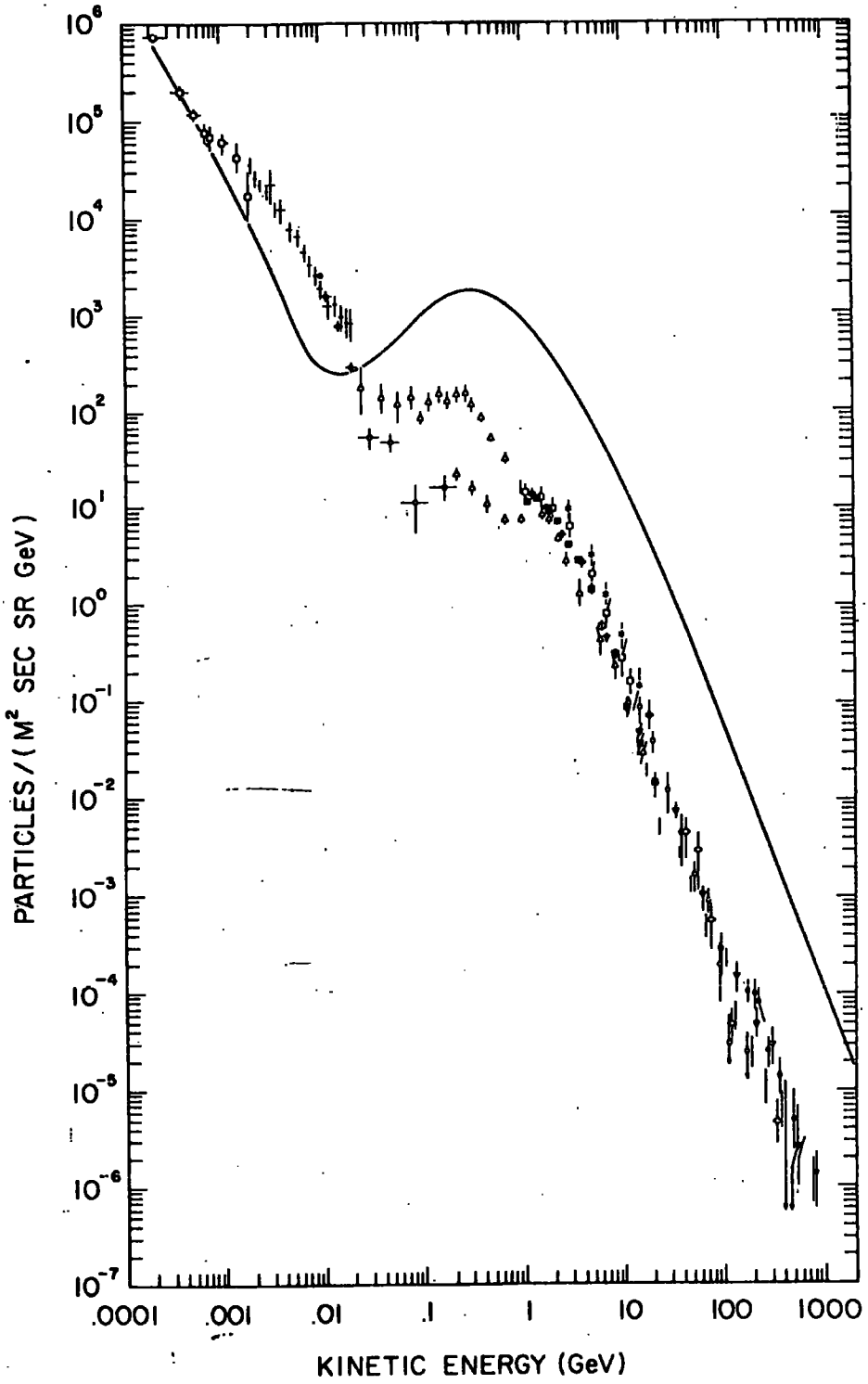

Figure 2. A compilation of measurements of the interstellar electron spectrum from Meyer (1975). The continuous line gives the proton spectrum for comparison.

radiation fields described above are 1.39 and $6.3\ 10^{-4}$ eV respectively. Upon using equation 28 it is found that the electron energies required to produce γ-rays with a mean energy of 100 MeV are $3.5\ 10^{9}$ eV and $1.8\ 10^{11}$ eV respectively. Referring again to figure 2 it is noted that the former energy lies in the region where the spectrum is modulated by the solar wind. In addition it is to be noted that this implies that for

$\epsilon = 1.4$ eV and $E_\gamma =$ 100 MeV the minimum electron energy required is $2\ 10^{9}$ eV.

Although the interstellar electron spectrum in this energy region is not directly observable because of solar modulation the main features of the spectrum can be identified from an examination of the galactic non-thermal radio emission; for example, Cummings et al. (1973) have used the available observations of the galactic radio spectrum to derive an interstellar electron spectrum under the assumption that the radiation process is synchroton radiation in an interstellar magnetic field. Figure 3 shows the derived electron spectra which are compatible with the radio observations. The large range in the spectra which they deduce is due to the uncertainty in the important astrophysical parameters; nevertheless, the medial spectrum is in very good agreement with the demodulated spectrum of Bedijn et al. (1973).

The most important point about the electrum spectrum to emerge from studies of the radio emission is that the radio spectrum requires an electron spectrum which is flatter below about 2 GeV than the high energy electron

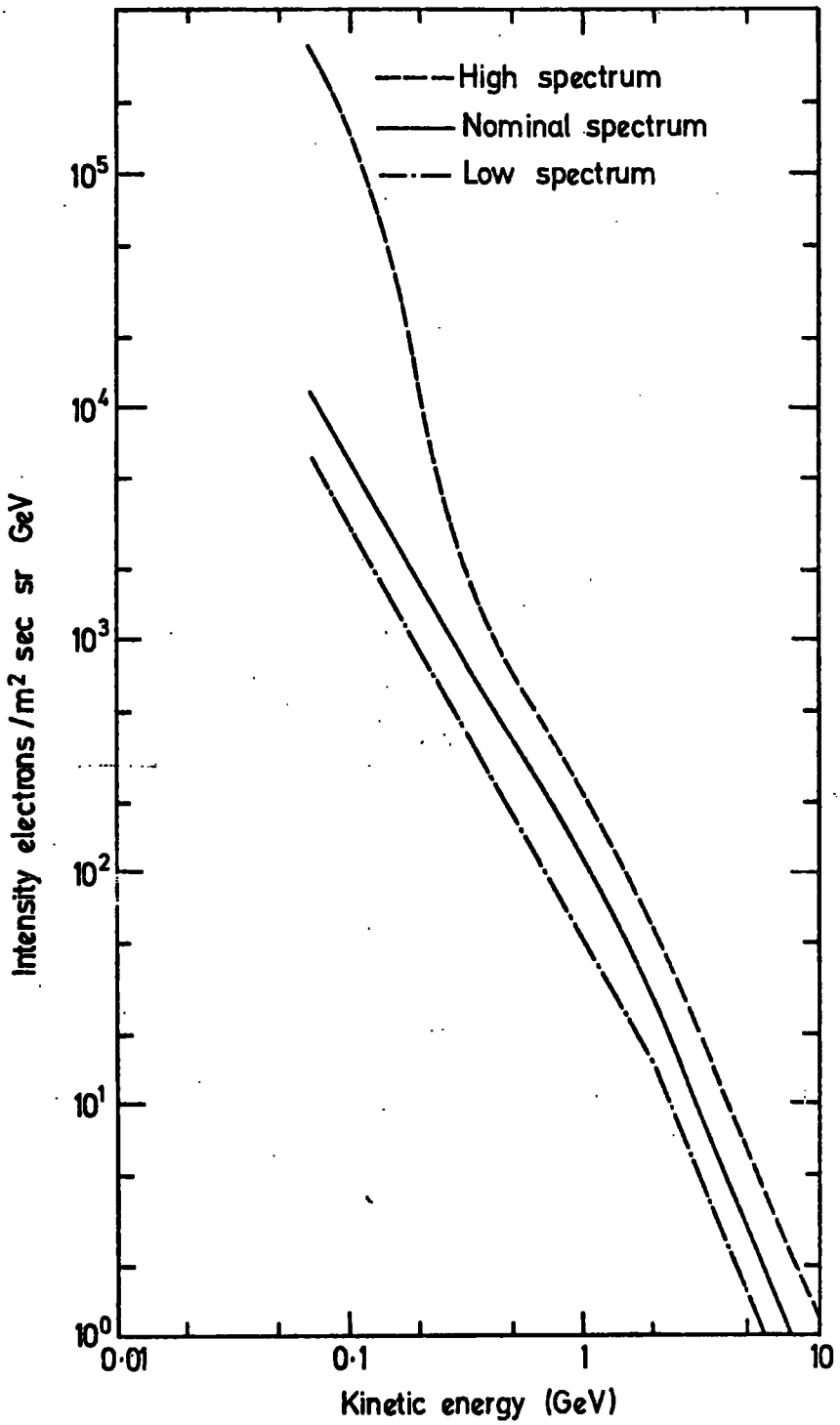

Figure 3. The interstellar electron spectrum at low energies as derived by Cummings et al (1973) from the observed Galactic non-thermal radio emission.

spectrum. Meyer (1975) points out that this flattening is confirmed by the measurements of the electron positron ratio. This increaseswith decreasing energy belcw about 1 GeV, implying that the slope of the spectrum of positrons is steeper than that of the electrons. The former can be calculated from the kinematics of π^+ decay and turns out to be of order 2.0. Therefore the slope of the low energy ($\lesssim 2$ GeV) electron spectrum must be considerably less than the slope of the high energy spectrum which is $\simeq 3.0$.

The nominal spectrum of figure 3 adopted in the calculations is:-

$$I_1(E_e) = 1.34\ 10^5\ E_e^{-1.8} \qquad 7.0\ 10^7 \leq E_e \leq 2\ 10^9 \text{ eV}$$

$$\text{cm}^{-2}\ \text{s}^{-1}\ \text{sr}^{-1}\ \text{eV}^{-1} \qquad 2.$$

$$I_2(E_e) = 4.35\ 10^{11}\ E_e^{-2.5} \qquad 2\ \ 10^9 \leq E_e$$

At high energies the spectrum adopted is that proposed by Webber (1973) as the best fit to the measurements above 10 GeV; $I(E) = 2\ 10^{16}\ E_e^{-3}$.

6.2.4 The Spatial Variation of the Electrons

In the calculation the spectral shape and composition of the cosmic ray electrons are assumed constant over the whole galaxy. These simplifying assumptions are in agreement with the results of a study of the Galactic non-thermal radio spectrum by Stephens (1969) who found that the spectrum of radio emission was independent of position. However, these assumptions are probably not true for the high energy electrons which interact with the microwave radiation. The reason is straightforward

It is well known that at the very highest energies the equilibrium electron spectrum is steeper than the injection spectrum by one power, due to the electrons losing energy by synchroton radiation and Inverse Compton Scattering. Approximately, the energy at which the steepening begins is the energy at which the escape and energy loss lifetimes are equal. Thus:

$$E_{cr} = \frac{1}{b\, T_e\, (\Gamma - 1)} \qquad 3$$

where T_e is the escape lifetime, Γ is the exponent of the injected energy spectrum and b is defined by the energy loss rate $\frac{dE}{dt}$:-

$$\frac{dE}{dt} = - bE^2 = - (4 \times 10^{-6} B^2 + 10^{-16} w_{ph}) E^2 \qquad 4.$$

Near the sun the break energy, E_{cr} is expected to be 200 GeV. If the escape lifetime is constant over the whole galaxy then in the Galactic Centre where the starlight energy density is some 60x higher, the value of E_{cr} becomes 6 - 10 GeV. Clearly the assumption of the same high energy spectrum over the whole galaxy is not valid. However, it will be seen later that the emission from the Galactic Centre is so completely dominated by the scattering off starlight that the effects of this assumption will be minor.

For the spatial variation of the cosmic ray density the two most extreme cases are the most interesting. These are a) the cosmic ray density constant over the whole galaxy, and b) the cosmic ray density varying as the stellar mass distribution. In chapter 4 some of the current ideas on cosmic ray propagation were

discussed and the cosmic ray density distribution which would result were described. Thus case a) would be the result of the cosmic ray propagation model of Holmes (1975) were correct and case b) would be the result, if the cosmic ray escape time, T_e, were constant over the galactic disk and the cosmic ray sources were distributed as the stars. Case b probably represents the most extreme large scale variation of the cosmic ray density which is consistent with the radio observations of the synchroton radiation. French and Osborne (1976) have modelled the observed longitude distribution of brightness temperature at 150 MHz in terms of emission by electrons in the random and ordered magnetic fields of the Galactic spiral arms. These authors find the ratio of emissivities between 5 kpc and 10 kpc to be about 3:1.

The z distribution of cosmic ray electrons is also studied via their radio emission. Figure 4 shows the observed brightness temperature versus latitude distribution at 150 MHz at a galactic longitude of 60 . The data for figure 4 were taken from the compilation of Landecker and Weilebinski (1970). Ilovaisky and Lequeux (1972) used this same data with the observed longitude distribution to derive the z distribution of the radio emission which is shown in figure 5. Baldwin (1976) has used a similar approach with the 400 MHz observations and obtains a z distribution in good agreement with that of figure 5. In both cases the z distribution implies the existence of cosmic rays and magnetic fields at

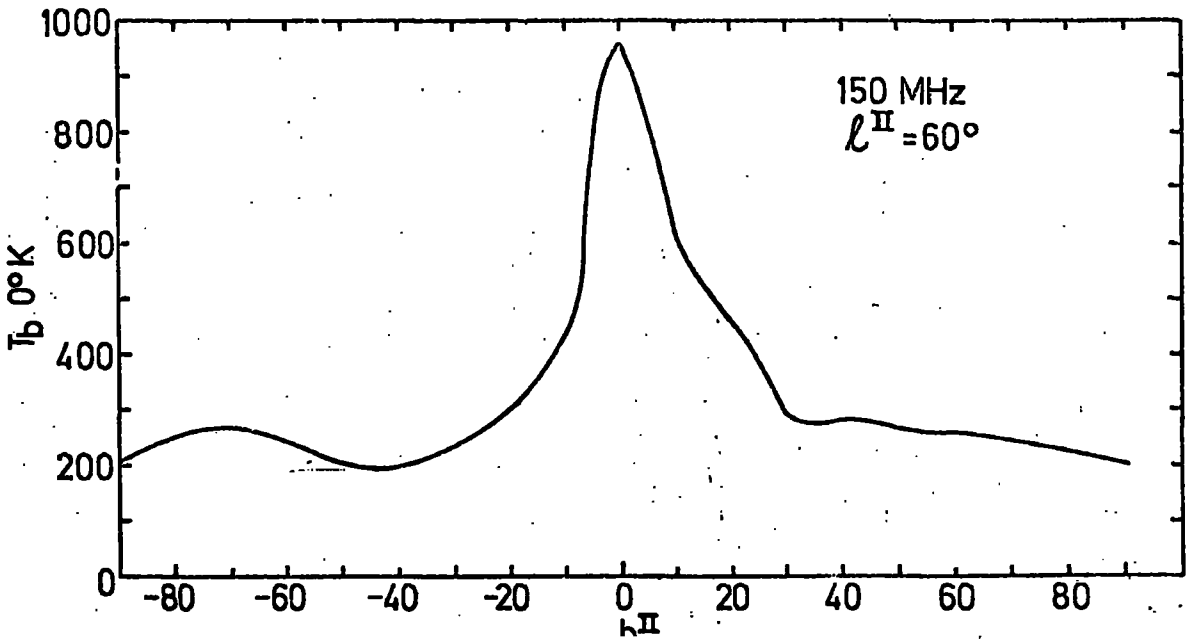

Figure 4. The distribution of the radio brightness temperature with Galactic latitude at a longitude of 60°. The data for this figure comes from the compilation of Landecker and Wielebinski (1970).

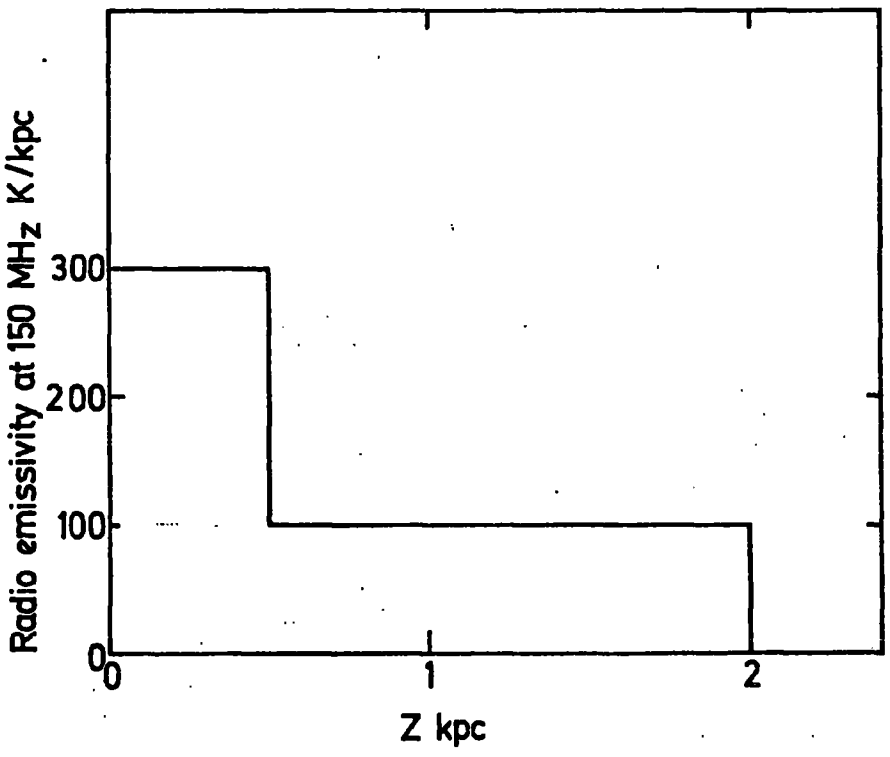

Figure 5. The distribution of radio emissivity with height, z, above the Galactic plane as derived by Ilovaisky and Lequeux (1972).

large distances from the Galactic plane.

In the calculations the z distribution of figure 5 was used to represent the electrons. The results are not sensitive to the form of the z-distribution but to the equivalent width which is 1 kpc. For comparison calculations were performed using a Gaussion with the same equivalent width. These gave results in good agreement with those described above.

The starlight density has a very broad distribution in z (Shukla and Paul 1976) since the scale height of the most important stellar component, the G stars, is 700 pc. Here the starlight density is assumed to be constant in z at least over the region occupied by the electrons. Thus the z-distribution used for the electrons is used to represent that of the gamma-ray emissivity.

As described in chapter 3 the intensity versus longitude data of Fichtel et al. (1975) is presented as the strength of a line source i.e. as γ's $cm^{-2}s^{-1}rad^{-1}$. In the calculation, the flux, $F_\gamma(l)$, from a bin of width 5° in l extending to $\pm 10^\circ$ in b is first calculated, where

$$F_\gamma(l) = \int_{l-2.5}^{l+2.5} \int_{-10}^{+10} \int_{0}^{\infty} q^{IC}(r,z)\, dr\, db\, dl \qquad 5$$

and the line strength $I_\gamma(l)$ averaged over 5° in l is given by

$$I_\gamma(l) = \frac{36}{\pi} F_\gamma(l) \qquad 6$$

The integrations in equation 5 were performed numerically using the R, and z dependences of the gamma ray emission function which were described above. The

resulting intensity vs longitude plots are described below

6.3. Results

Near the solar system the calculated emissivities for interactions with a) starlight and b) the 2.7K blackbody are

a) q^{IC} (>100 MeV) $= 2.75\ 10^{-27}$ γ's $cm^{-3}\ s^{-1}$

b) q^{IC} (>100 MeV) $= 8.5\ 10^{-28}$ γ's $cm^{-3}\ s^{-1}$

The integral spectra from these two processes are shown in figure 6 with the upper and lower limits to both spectra calculated using the upper and lower limits on the electron spectra in the relevant energy intervals.

Figure 7 shows the longitude distribution of the gamma-ray intensities from the calculations described above compared with the 100 MeV data of Fichtel et al. (1975). In figure 8 these data are combined to give the predicted galactic centre spectra from both the starlight and 2.7 K for each of the cosmic ray distributions described above. Figure 8 also shows the observed spectra of Fichtel et al.

6.4. Discussion

Comparison of the observed intensity longitude distribution with the predictions of the model (figure 7) indicates that the maximum contribution which results from the IC process for the case in which the cosmic ray density is constant is a few percent. This is

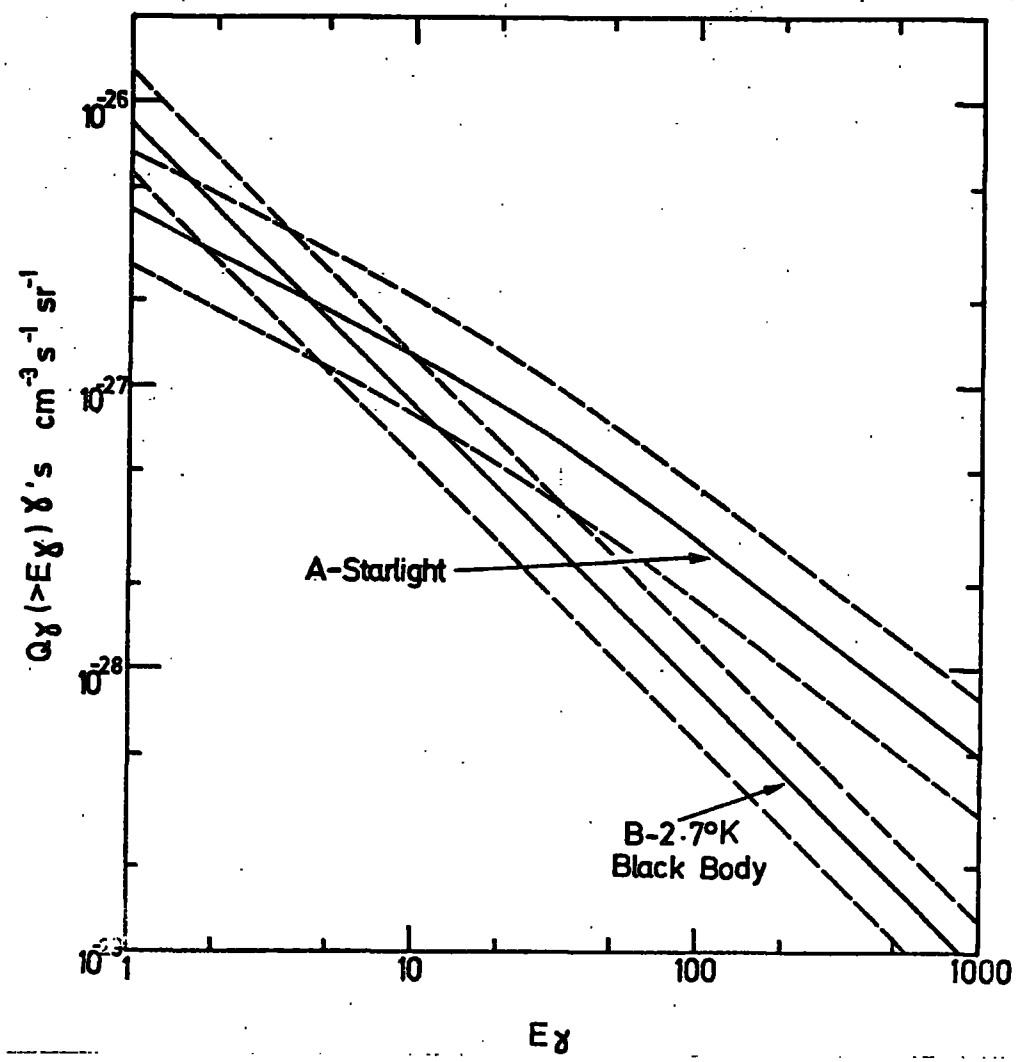

Figure 6. The integral spectra of inverse Compton gamma-rays near the solar system. The dashed lines give the upper and lower limits to the spectra which are obtained using the upper and lower limits to the spectra in figure 3.

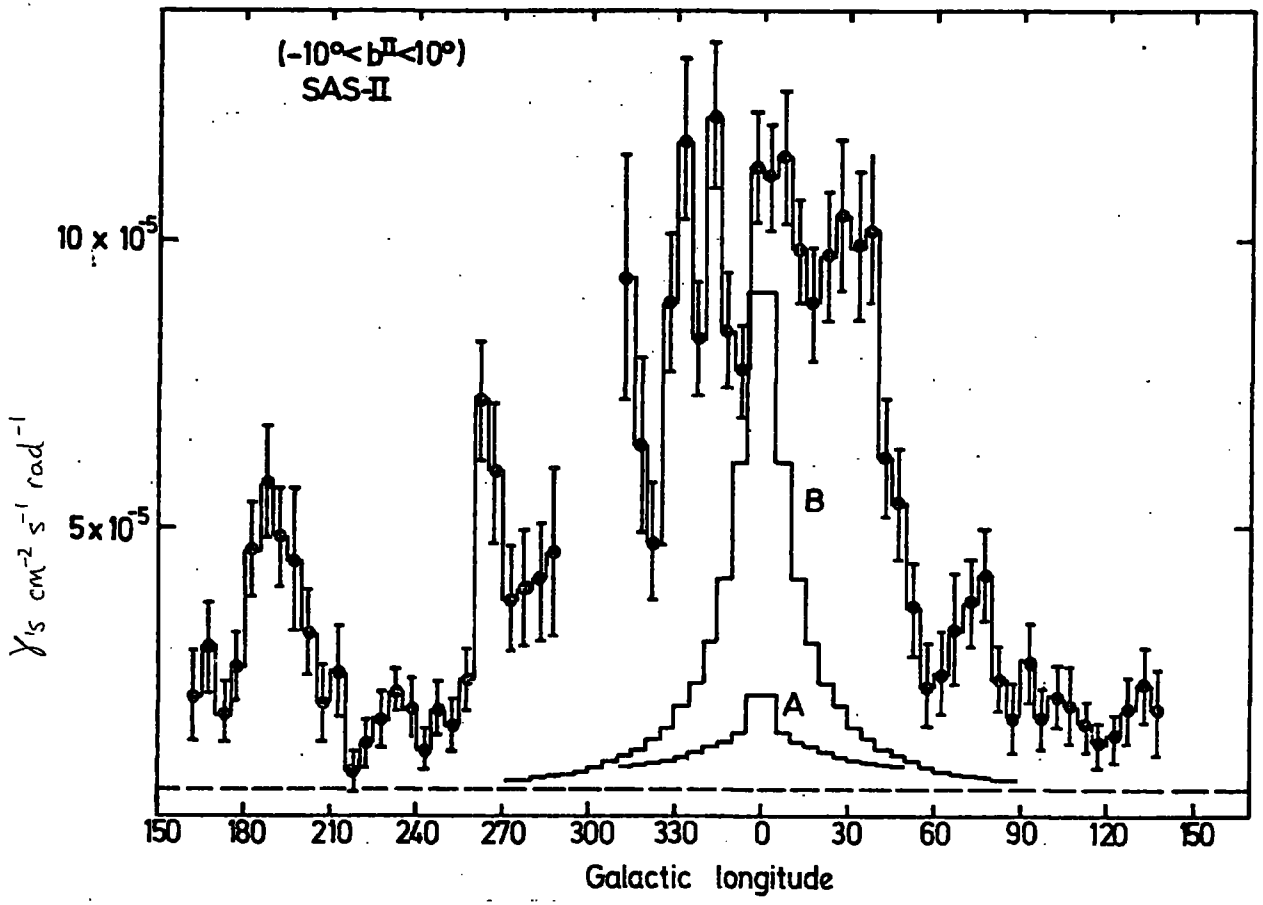

Figure 7. The predicted longitude distribution of gammas from inverse Compton scattering for: A, the density of cosmic rays constant throughout the Galaxy and B, the density of cosmic rays proportional to the density of matter. Also included is the observed distribution from Fichtel et al (1975.

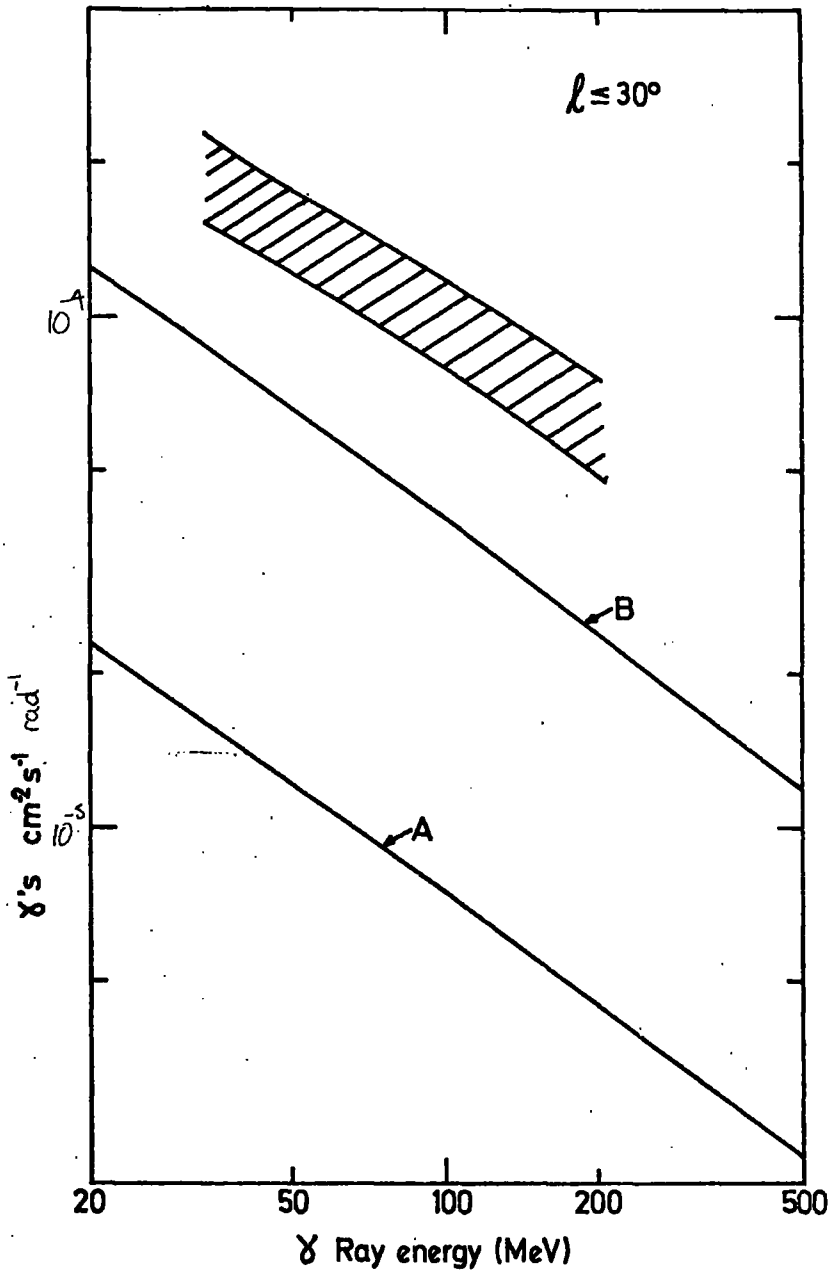

Figure 8. The predicted gamma ray spectrum from the Galactic centre for cases A and B as in figure 7. The hatched region is the Galactic centre spectrum from Fichtel et al (1975).

in clear disagreement with the work of Cowsik and Voges (1974) who predict a 60% contribution. The reasons for the disagreement are threefold.

Firstly, Cowsik and Voges have used a starlight spectrum with a temperature of 10^4K and a mean photon density near the sun of 0.8 photons cm^{-3}. Together, these assumptions imply an energy density which is 1.86 eV/cm^3 or approximately 4X the energy density used in the calculations here. The observational evidence is strongly in favour of a smaller value, say, 0.4 - 0.5 eV/cm^3 as quoted by Allen (1973) or perhaps an even lower value (Stecher and Milligan, 1962).

Secondly, these authors have used a thickness of 2 kpc for the electron disk which will give an increase of a factor of two over the intensities calculated above.

Finally, over a large part of the Galaxy ($2 \leq R \leq 8$) the stellar mass distribution used by Cowsik and Voges is 4X the density given by the model of Innanen (1973) which probably represents the best available work on the distribution of mass in the Galaxy.

One method of checking the above calculations is to compare the results with the Compton gamma ray flux calculated from the observed radio intensities (see for example Felten and Morrison 1966). This method used the fact that the same electrons which produce inverse Compton gamma rays will also produce radio frequency synchrotron radiation with the same spectral slope.

Using the 150 MHz data from Landecker and Wielebinski

(1970) and assuming a uniform magnetic field of $3\ 10^{-6}$ gauss, this method predicts a flux of 1.0×10^{-8} photons $cm^{-2}\ s^{-1}\ ster^{-1}\ MeV^{-1}$ from the Galactic pole. The above model gives a value of 8.6×10^{-9} photons $cm^{-2}\ s^{-1}\ ster^{-1}\ MeV^{-1}$. This excellent agreement supports the choice of parameters above and suggests that the results of Cowsik and Voges represents an overestimate of the contribution from this process.

It is noticeable from figure 7 that the most important features of the observed intensity vs longitude plot, viz the broad flat central maximum, cannot be reproduced by having a cosmic ray distribution in which the density is proportional to the density of sources. The models considered here clearly predicts that the greatest contribution to the Galactic flux will occur in narrow region around the Galactic centre. The magnitude of the observed peak at the Galactic Centre may be used to set limits on the Galactic centre cosmic ray flux (Wolfendale and Worrall, 1976).

Finally, it must be remarked that in these calculations it has been assumed that the ratio of primary to secondary electrons is constant over the whole disk. The effect of this varying will be small since the ratio is 10 to 1 in the Solar System. It will however be considered in the calculations of the next Chapter.

REFERENCES

Allen, C.W., 1973. Astrophysical Quantities. Athlone Press, London.

Baldwin, J.E., 1976. GSFC Symposium on Gamma-Ray Astronomy, to be published.

Beuermann, K.P., 1974. Proc. Ninth ESLAB Symposium, ESRO SP-106, p. 259.

Cowsik, R. & Hutcheon I.D., 1971. Proc. 12th Int. Conf. on Cosmic Rays, 1, 102.

Cowsik, R. & Voges, W., 1974. Proc. Ninth ESLAB Symposium, ESRO SP-106, p. 229.

Cummings, A.C., Stone, E.C. & Vogt, R.E., 1973. Proc. 13th Int. Conf. on Cosmic Rays., Denver, 1, 355.

Dodds, D., Strong, A.W., Wolfendale, A.W., Wdowczyk, J., 1974. Proc. Ninth ESLAB Symposium, ESRO SP-106, p.221.

Fichtel, C.E., Hartman, R.C., Kniffen, D.A., Thompson, D.J., Bignami, G.F., Ogelman, H., Ozel, M.F., & Tumer, T., 1975. Astrophys. J., 198, 163.

Freeman, K.C., 1970. Astrophys. J., 160, 811.

French, D.K. & Osborne, J.L., 1976. Mon. Not.R.astr. Soc., to be published.

Gondhalekar, P.M. & Wilson, R., 1975. Astr.Astrophys., 38, 329.

Habing, H.J., 1968. Bull.astr. Inst. Netherlands, 19, 421.

Holmes, J.A., 1979. Mon. Not. R. astr. Soc., 166, 155.

Ilovaisky, S.A. & Lequeux, J., 1972. Astr. Astrophys., 20, 347.

Innanen, K.A., 1973. Astrophys. Sp. Sci., 22, 393.

Jura, M., 1975. Astrophys. J., 191, 375.

Landecker, T.L. & Weiiebinski, R., 1970. Aust. J. Phys. Astrophys. Suppl., 16, 1.

Meyer, P., 1975. In 'Origin of Cosmic Rays", Eds. J.L. Osborne & A.W.Wolfendale, D.Reidel, Dordrecht.

Mihalas, D., 1968. Galactic Astronomy, Freeman & Co., San Francisco.

Shakla, P.G. & Paul, J., 1975. Preprint.

Simkin, S.M., 1975. Astr. J., 80, 415.

Stecher, T.P. & Milligan, J.E., 1962. Ann.d'Astrophys., 25, 268.

Stephens, S.A., 1969. Ph.D. Thesis, University of Bombay.

Vancouleurs, G.de., 1959., Hdb. d. Phys., 53, 311.

Webber, W.R., 1973. Proc. 13th Int. Conf. on Cosmic Rays, Denver. 5, 3568.

Witt, A.N. & Johnson, 1973. M.W., Astrophys. J., 181, 363.

Wolfendale, A.W. & Worrall, D.M., 1976. Nature, to be published.

Zimmermann, H., 1964. Ast. Nachr., 288, 99.

CHAPTER SEVEN

THE GALACTIC DISTRIBUTION OF GAMMA RAY EMISSION FROM COSMIC RAY-MATTER INTERACTIONS

7.1 Emissivity near the Solar System due to π^o Production

The details of this mechnism were discussed in Chapter 2. In this section the aim is to determine the emissivity of gamma radiation in nearby interstellar space using the observed spectrum of cosmic rays.

The threshold for π^o production in p-H, p-He reactions is a few hundred MeV. Unfortunately the cosmic ray spectrum above this energy and up to a few GeV is not accurately known, the measured energy spectrum at the top of the atmosphere varies over the solar cycle due to the time dependent modulation of the solar wind. Thus the local interstellar spectrum near 1 GeV has to be deduced from the observed modulated spectrum using a theory for the interaction of the solar wind and cosmic rays.

Comstock et al. (1972) have performed a demodulation of the energy spectra measured at solar minimum in 1965. These authors find that the best fit to the data is obtained for an interstellar spectrum which is a power law in total energy, W, with a constant exponent $\Gamma = 2.6$. Their spectra of protons and α particles are shown in figure 1. The actual form of these spectra are for protons $J(T_p) = 5.9\ 10^8\ (T + E_o)^{-2.6}\ m^{-2}\ sr^{-1}\ s^{-1}$ (MeV/nucleon)$^{-1}$ and for α-particles $J(T_\alpha) = 6.5\ 10^7\ (T + E_o)^{-2.6}$ $m^{-2}\ sr^{-1}\ s^{-1}$ (MeV/nucleon)$^{-1}$ where T is the kinetic energy

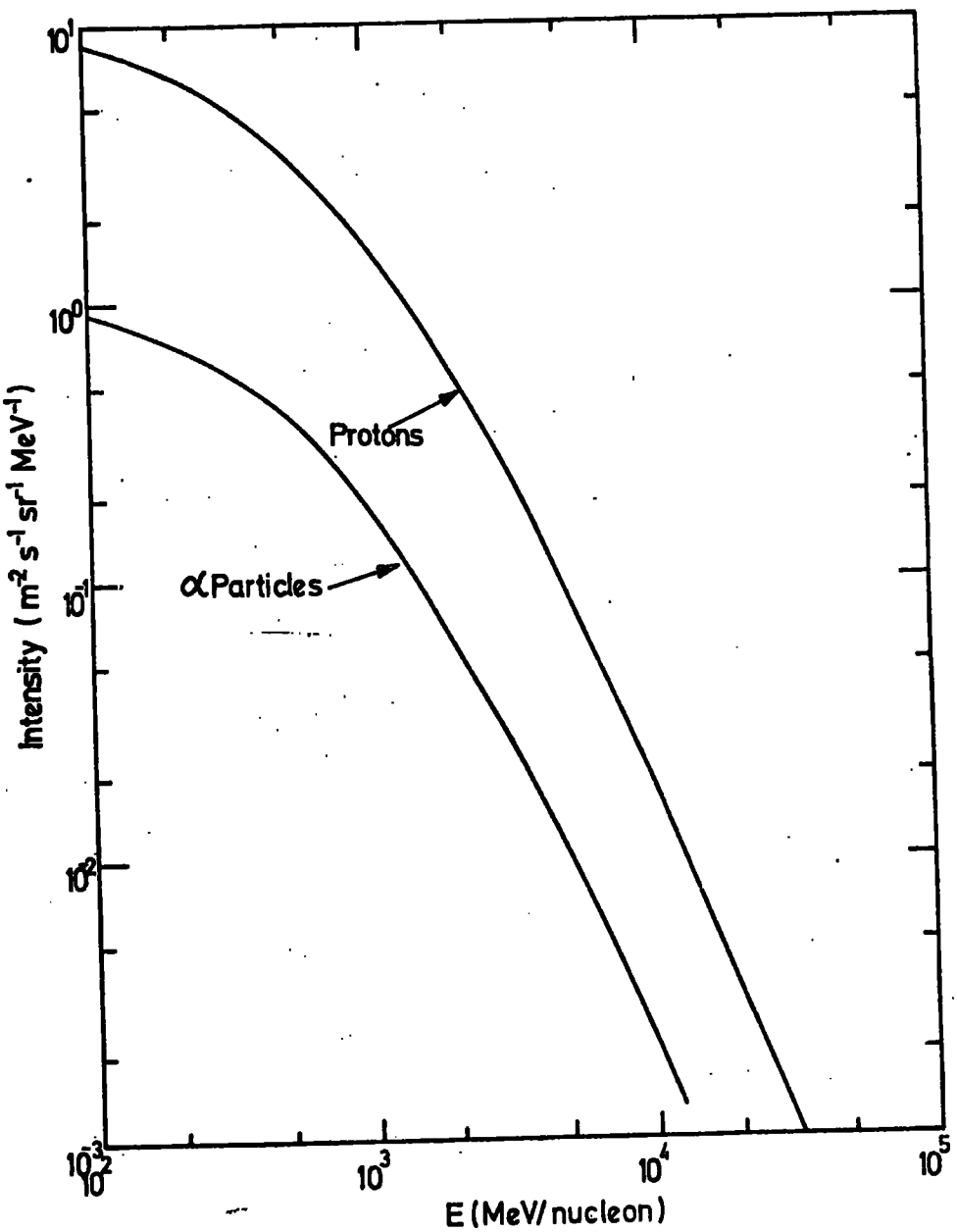

Figure 1. The interstellar spectra of protons and alpha particles according to Comstock et al (1972.

and E_o is the rest energy per nucleon.

Figure 2 shows the product of $J_{CR}(T)$ and $\sigma_{\pi^\circ}(T)\ m_{\pi^\circ}(T)$ for both p - H and α - H collisions. The total yield of gamma rays from π^o decay is given by the equation

$$Q_{\pi^\circ} = \sum_{l}\sum_{k} 8\pi \int_{o}^{\infty} J_k(T)\sigma_{\pi^\circ kl}(T)\ m_{\pi^\circ kl}(T)\ dT$$

where the summations extend over the gas nuclei, l; and the cosmic ray nuclei, k.

Considering p - H collisions only, the yield is given by integration under the distribution in figure 2. Figure 3 is a plot of the cumulative distribution given by

$$\frac{Q_{\pi^\circ}(<T)}{Q_{\pi^\circ}} = \frac{\int_o^T J_p(T)\,\sigma_{\pi^\circ pH}(T)\,m_{\pi^\circ pH}(T)\,dT}{\int_o J_p(T)\,\sigma_{\pi^\circ pH}(T)\,m_{\pi^\circ pH}(T)\,dT} \qquad 1.$$

From an examination of figure 3 the median energy for gamma ray production can be determined. For protons on hydrogen this is 2.7 GeV. In addition, it can be seen from figure 3 that 80% of the emission arises from protons between 900 MeV and 15 GeV. Table I lists the median energies for the three most important processes viz. p - H, p - He and α - H collisions.

Now, although the dominant contribution to π^o production will arise from the collision processes already described and listed in Table I, it is important to consider the possible contribution from cosmic ray nuclei with $Z>2$, which in practice involves mainly the nuclei C, O, Ne, Mg and Si. The observational results on the relative abundances of these elements in cosmic ray has recently been reviewed by Waddington (1974). This author gives the ratio of the number of the nuclei to the total C + O nuclei as 25:1, with approximately equal fluxes of each nucleus.

Unfortunately, there are no measurements of the cross-

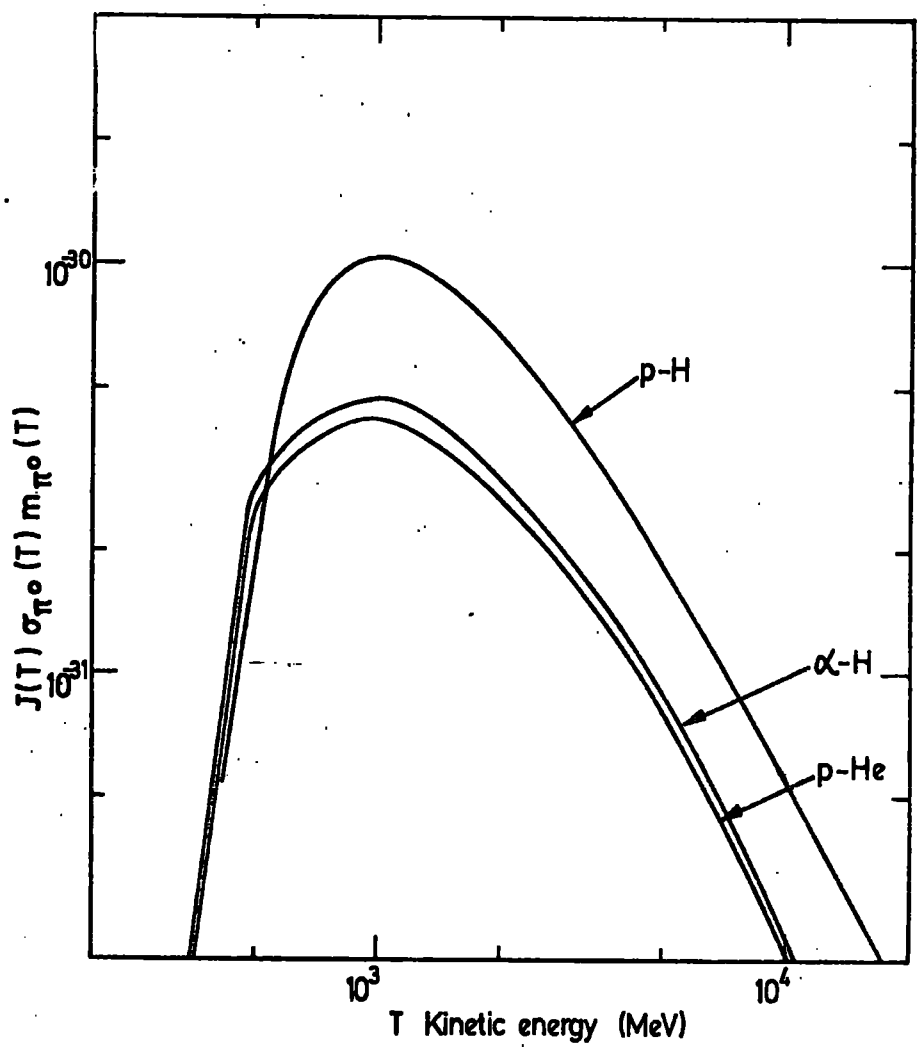

Figure 2. The product of $J_p(T)$ with $\sigma_{\pi^0}(T)\ m_{\pi^0}(T)$ for collisions between: protons and hydrogen (p-H), protons and helium, (p-He); alpha particles and hydrogen, (α - H). The spectra of protons and alpha's in figure 1 was used.

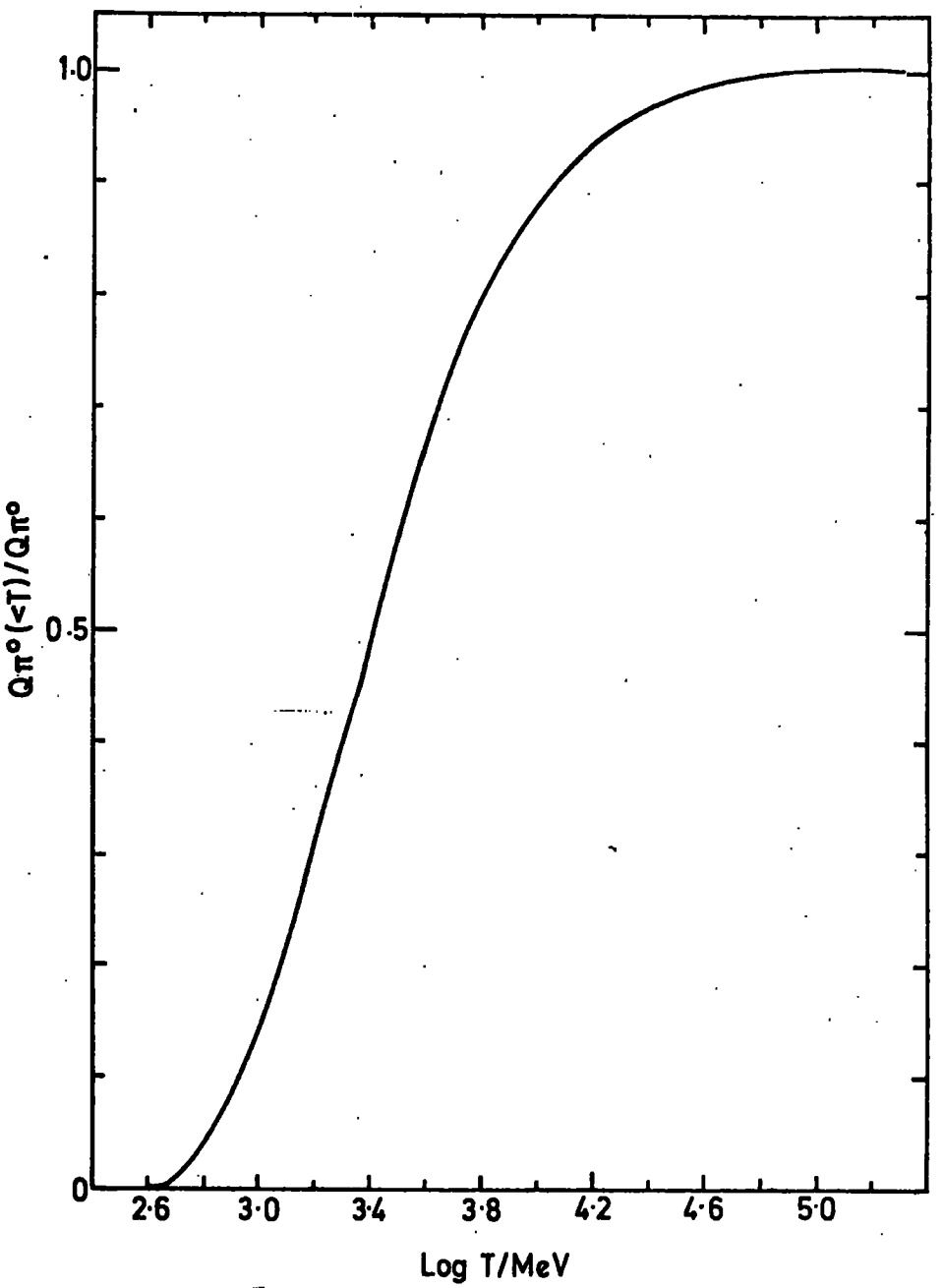

Figure 3. The cumulative distribution of the gamma-ray emissivity in p-H collisions.

sections $\sigma_{\pi^\circ p-c}$, $\sigma_{\pi^\circ p-o}$ etc. Following Pollack and Fazio (1963) the ratio of the cross-sections $\sigma_{\pi^\circ p-N} : \sigma_{\pi^\circ p-\alpha}$ are assumed to be in the ratio of their atomic numbers. Using this assumption the total contribution was estimated from the data on the abundance relative to Helium and this comes to 25% of the contribution from cosmic ray alpha particle-hydrogen collisions.

Table II summarises the results of these calculations and gives both the total yield and the integral flux at 100 MeV (see Chapter 2).

TABLE I

Contributing Collision Process	Median Energy (GeV)
proton - hydrogen	2.7
alpha - hydrogen	2.6
proton - helium	2.5

TABLE II

	Contributing Collision Processes	Emissivity in gamma's (hydrogen atom)$^{-1}$ s^{-1}
Total Yield	protons on hydrogen	0.84 10^{-25}
	alphas on hydrogen	0.38 10^{-25}
	Z > 2 nuclei on hydrogen	0.09 10^{-25}
	All CR on hydrogen	1.31 10^{-25}
	All CR on ISM	1.84 10^{-25}
Above 100 MeV	All CR on ISM	1.25 10^{-25}

The final input parameter for this calculation is the hydrogen density in nearly interstellar space. This was discussed in chapter 4. Here, it is important to stress that there is apparent disagreement between the local hydrogen density from the UV absorption measurements and the results of the radio astronomical observations. Thus, Jenkins (1976) gives a total density of 1.1 atoms cm^{-3}, comprising 0.9 atoms cm^{-3} of atomic hydrogen and 0.2 atoms cm^{-3} of molecular hydrogen, whereas Gordon and Burton (1976) give a total density of 0.8 atoms cm^{-3} made up equally of atomic and molecular hydrogen. However, the disagreement may not be real because the UV observations are restricted to space within 1 kpc of the sun whereas the Gordon and Burton result refers to the average density in an annulus of 10 kpc radius and hence the two values may not be directly comparable.

The gamma rate production rate for a hydrogen density of 0.8 atoms cm^{-3} is 1 10^{-25} photons $cm^{-3}s^{-1}$. Thus the IC contribution calculated in the last chapter is only 3% of the π^{o} contribution. Clearly the majority of the Galactic emission will arise from the π^{o} mechanism. In the later part of this chapter these calculations will be used in conjunction with the observations of Gordon and Burton and the calculations of the next section, to determine the distribution of cosmic rays.

7.2 Gamma Rays from Electron Bremsstrahlung

As described in chapter 2 cosmic ray electron of energy E_e involved in a collision with a nucleus of

the interstellar gas radiate a spectrum of gamma rays with energy between 0 and E_e, the total kinetic energy of the electron. Thus, in order to determine the integral spectrum of gamma rays $I_\gamma(>E_\gamma)$ produced by Bremsstrahlung of a cosmic ray electron spectrum $I_e(E_e)dE_e$ it is necessary to know the form of the electron spectrum down to the electron energy $E_{e_{min}} = E_\gamma$. As a consequence the important energy region of the cosmic ray spectrum for producing bremsstrahlung gamma rays of 100 MeV is poorly known because of the effects of the solar modulation. Figure 4 shows the differential electron spectrum of Cummings et al. (1973) which was used in the last chapter for the calculation of the inverse Compton gamma ray production rate and which extends down to 70 MeV. It is this electron spectrum which is adopted in the following calculation.

The emissivity of bremsstrahlung gamma rays is given by

$$Q_B(E_\gamma) = \sum_j 4\pi n_j \int_{E_\gamma}^{\infty} dE_\gamma' \int_{E_\gamma'}^{\infty} dE_e I_e(E_e)\, \sigma_{B,j}(E_\gamma', E_e) \qquad 2$$

where n_j is the volume density of atoms of type j, $I_e(E_e)$ dE_e is the local interstellar electron spectrum and $\sigma_{B,j}(E_\gamma', E_e)$ is the cross-section.

In this calculation the uncertainty in the electron spectrum at 100 MeV justifies the adoption of the extreme relativistic, screened, cross-section even at 50-100 MeV. Thus the cross-section used was that given by equation 17 Chapter 2.

Figure 5 shows the integral energy spectrum (expressed as the yield per hydrogen atom) for the above assumptions

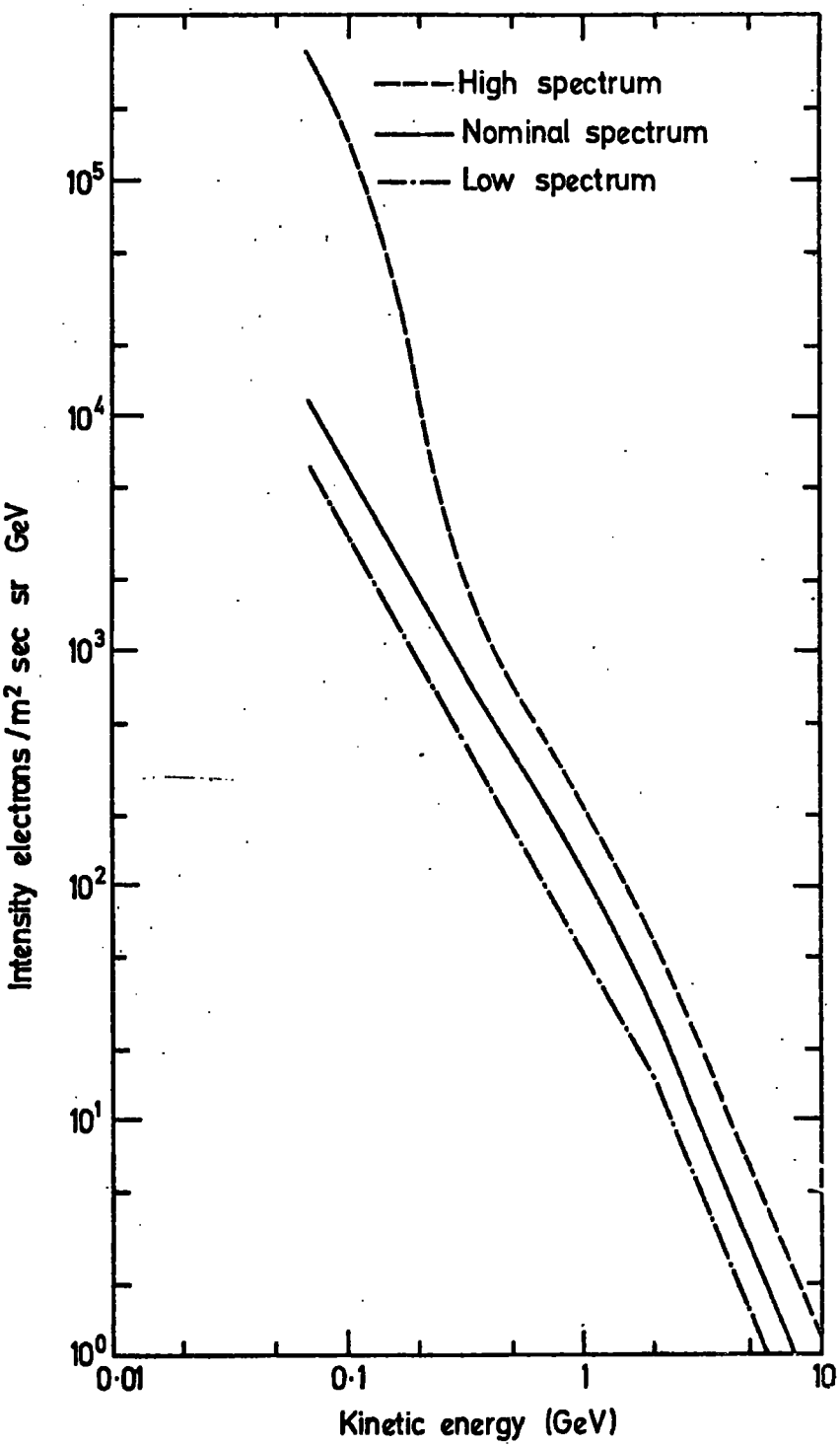

Figure 4. The differential electron spectra of Cummings et al (1973).

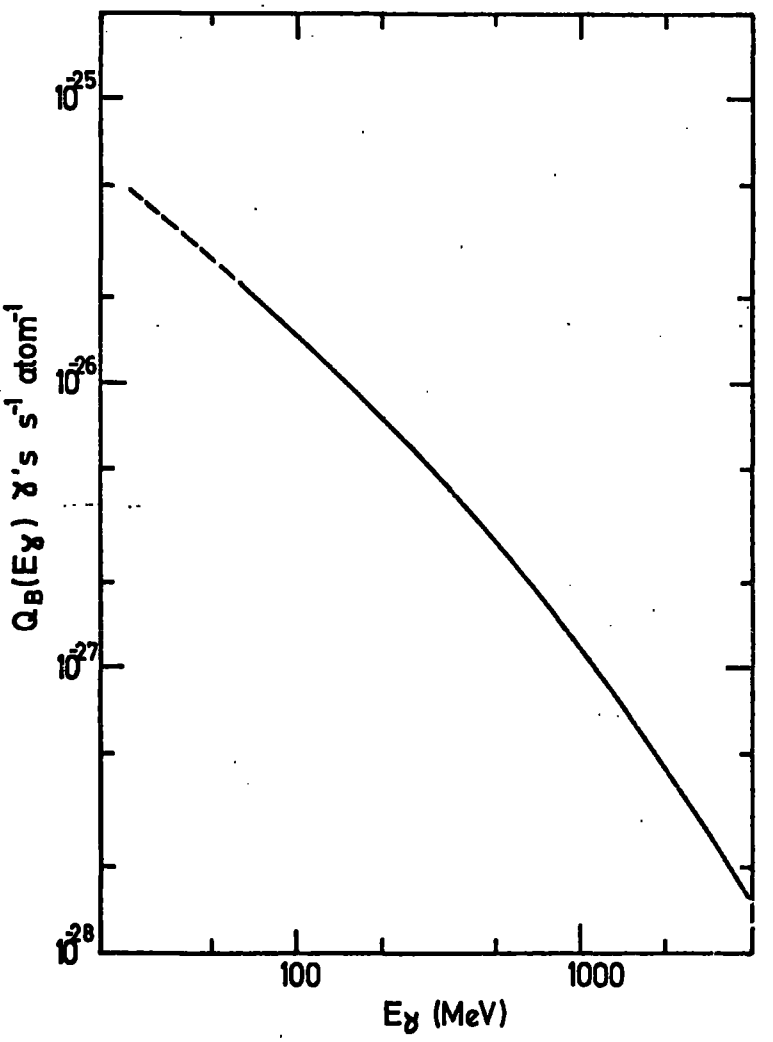

Figure 5. The integral energy spectrum of gamma rays from electron bremsstrahlung near the solar system. The dashed portion represents an estimate of the contribution at low energies.

and an interstellar medium with $\bar{M} = 1.4$ (see chapter 4). The emissivity at 100 MeV is $1.5\ 10^{-26}$ γ's (H atom. s)$^{-1}$ and is 12% of the yield from π^0 production. The upper limit to the bremsstrahlung rate was obtained using the Cummings et al. upper limit to the electron spectrum and corresponds to 20% of the π^0 yield. The result is in very good agreement with the calculations of Kniffen et al. (1975) who use a similar electron spectrum. These authors also quote an emissivity between 10 and 30 MeV of $1.17\ 10^{-25}$ γ's atom^{-1} s^{-1}. Strictly there is no evidence for a spectrum which continues with the same exponent down to these low energies (Cummings et al. 1973). However, if the integral spectrum of figure 3 is extrapolated to 10 MeV a production rate for 10 - 30 MeV gamma rays can be estimated and this is found to give $q_B(10\text{-}30\text{MeV}) = 7.9\ 10^{-26}$ γ's atom^{-1} s^{-1}.

7.3 The Distribution of Gamma Ray Emission in the Galaxy

The radial distribution of gamma-ray emissivity in Galaxy has been derived by Strong and Worrall (1976) from the intensity vs longitude results of Fichtel et al. (1975). Their results are plotted in figure 6 as the relative emissivity, W(R) as a function of Galactic radius where the emissivity at 10 kpc is taken as the datum.

Figure 6 clearly shows that the broad region of high gamma ray intensity seen within 30° of the Galactic centre originates in a ring of enhanced emissivity lying within 5 and 6.5 kpc of the centre. The observations

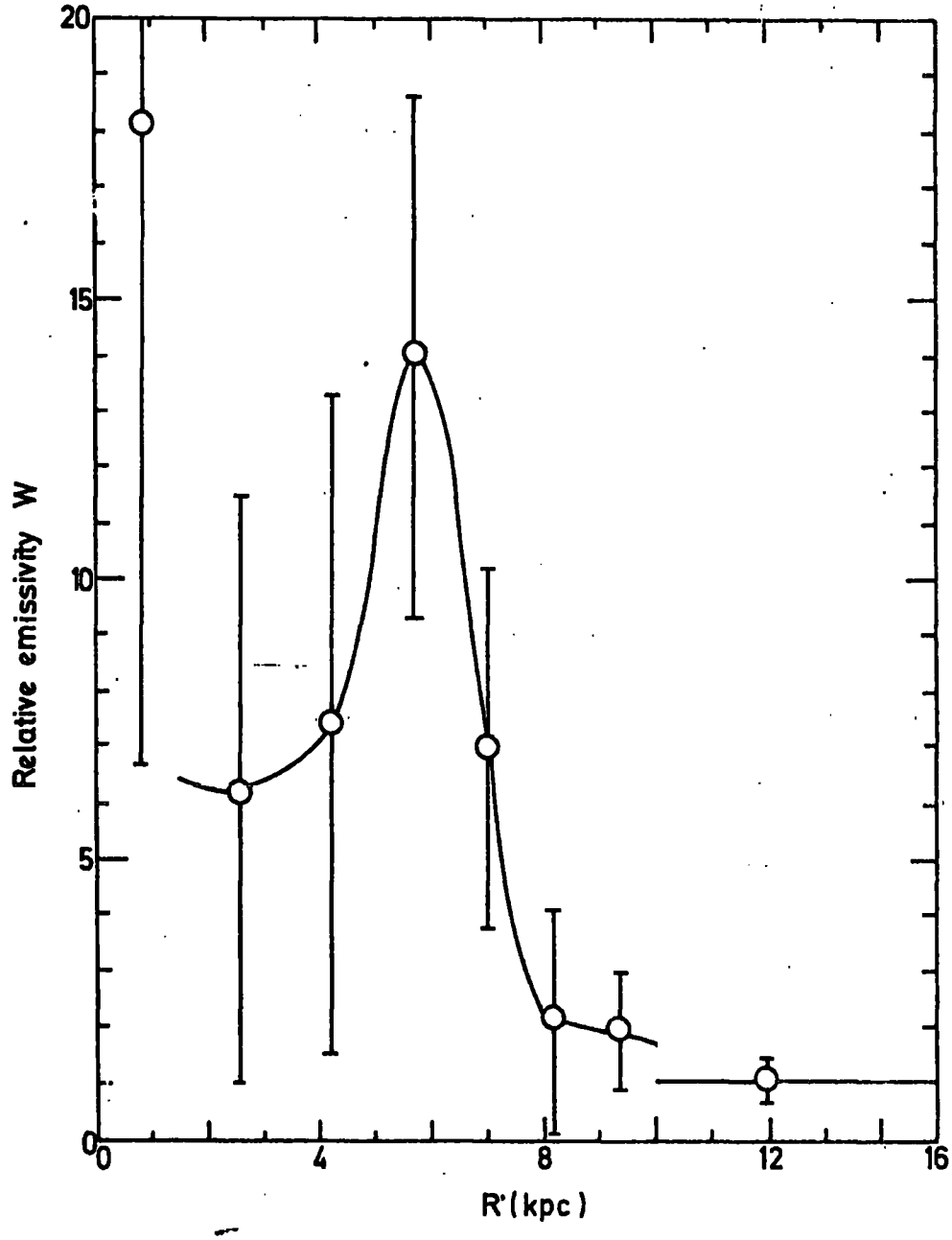

Figure 6. The radial distribution of the relative emissivity of gamma-rays as derived from the SAS II observations.

presented in this way are in a particularly convenient form for comparison with the surface density of gas in order to determine the radial distribution of cosmic ray density.

7.4 The Distribution of Cosmic Rays

The results displayed in figure 6 are actually the distribution of surface emissivity, $\Sigma_\gamma(R)$, as a function of Galactic radius. Thus if $Q_\gamma(R,z)$ is the volume emissivity in gamma rays cm^{-3} s^{-1} at distance R from the Galactic centre and height z from the Galactic plane, then $\Sigma_\gamma(R)$ is given by

$$\Sigma_\gamma(R) = \int_{-\infty}^{\infty} Q_\gamma(R,z)dz$$

Near the solar system the surface emissivity is 6.67 ($\pm$ 2.3) x 10^{-5} gamma rays cm^{-2} s^{-1}.

The best evidence regarding the z distribution of Q_γ suggests that it is dominated by the spread of the gas in z. Firstly the observed shape of the galactic centre intensity vs latitude results of Fichtel et al. (1975) is dominated by a very narrow component only 1 - 2^o in width. This is the same angular width as the gas layer at 5 - 6 kpc from the sun and strongly suggests that the width of this feature is determined by the thickness of the gas layer and not by the cosmic ray layer. Secondly, the observed distribution in latitude of the non thermal radio radiation is very wide implying that cosmic ray electrons and the Galactic magnetic field extend to large distances from the Galactic plane. It seems almost certain that

the cosmic ray electrons which produce the radio emission ($E_e \simeq 1$ GeV) and the protons responsible for gamma ray emission ($E_p \simeq 3$ GeV) will have the same z distribution. If so, then the cosmic ray nucleons will have a constant density in the region occupied by the gas, and the z -dependence of the emission function $Q_\gamma(R, z)$ for Bremsstrahlung and pion production will be determined by the z - dependence of the gas.

Considering pion production alone, then, the surface emissivity $\sum_\gamma^\pi(R)$ becomes

$$\sum_\gamma^\pi(R) = \int_{-\infty}^{+\infty} q_\gamma^\pi(R)\, n_H\,(R, z)\, dz \qquad 4$$

If the simplifying assumption of a position independent proton spectrum is made then $q_\gamma^\pi(R)$ made be expressed as

$$q_\gamma^\pi(R) = \frac{w(R)}{w_\odot} \quad q_\odot^\pi$$

Where $w(R)/w_\odot$ is a function describing the density of cosmic rays at distance R from the Galactic centre relative to the solar value, and $q_\odot^\pi$ is the local gamma ray production rate per hydrogen atom which was calculated above.

In this case then the surface emissivity may be expressed as

$$\sum_\gamma^\pi(R) = q_\odot^\pi \frac{w(R)}{w_\odot} \sigma_H(R) \qquad 5$$

Where $\sigma_H(R)$ is the surface density of hydrogen. A similar expression may be written for the surface emissivity due to bremsstrahlung

$$\sum_\gamma^B(R) = q_\odot^B \cdot \frac{w_e(R)}{w_{e\odot}} \cdot \sigma_H(R) \qquad 6$$

Where now $\frac{w_e(R)}{w_{e\odot}}$ describes the variation of the cosmic ray electron density across the Galaxy, and as in the previous chapter the electron spectrum is assumed to have the same form throughout the Galaxy.

If now it is assumed that

$$\frac{w_e(R)}{w_{e\odot}} = \frac{w(R)}{w_\odot}$$

then $w(R)/w_\odot$ will be given by

$$\frac{w(R)}{w_\odot} = 3.47 \frac{W(R)}{\sigma_H(R)(q_\odot^{\pi^0} + q_\odot^{\bar{n}})}$$

where $\sigma_H(R)$ is in $M_\odot/pc^2$.

However, in writing down an expression for $w(R)/w_\odot$ in 8 two contributions have been neglected. Firstly the contribution from the inverse Compton effect has to be added. This gives a contribution

$$\sum_\gamma^{IC}(R) = q_\odot^{IC}\, t\, \frac{w_e(R)}{w_{eo}} \frac{\sigma_{st}(R)}{\sigma_{st\odot}} \qquad 9$$

Where t is the thickness of the electron disk which is taken as 1 kpc, and q^{IC} is the emissivity of IC gamma rays near the sun expressed as photons cm^{-3} s^{-1}.

A second contribution which must be included covers the variation of the ratio of primary electrons to seondary electrons across the Galaxy. In Chapter 2 it was pointed out that the same process which produces gamma rays through π^0 decay also produces secondary electrons and positrons through $\pi^\pm$ decay. As a result the secondary electron production $Q(\bar{r}, t, E)$ of equation 3.1 has the same spatial dependence as the gamma ray emissivity. It is clear that the secondary part of the electron source function will have the same general structure as the gamma ray emission function in figure 4 i.e. a maximum between 5.0 and 6.5 kpc.

The distribution of secondary electrons is given by

$$\frac{w_e'(R)}{w_{e\odot}'} = \frac{\sigma_H(R)}{\sigma_{Ho}} \frac{w(R)}{w_\odot} \qquad 10$$

here the double prime will be used to denote the secondary electron part of the electron flux and the single prime will denote the primary part. In obtaining 10 a constant value of T_e, the escape lifetime, was assumed over the whole galaxy. Equations 6 and 8 may now be rewritten as

$$\sum_{\gamma}^{B}(R) = q_{\odot}^{B}\left\{\alpha\frac{w_e(R)}{w_{e\odot}}\sigma_H(R) + \beta\frac{w_e(R)}{w_{e\odot}}\sigma_H(R)\right\} \qquad 11$$

$$\sum_{\gamma}^{IC}(R) = q_{\odot}^{IC}\left\{\mu\frac{w_e(R)}{w_{e\odot}} + \nu\frac{w_e(R)}{w_{e\odot}}\right\}\frac{\sigma_{st}(R)}{\sigma_{st\odot}} \qquad 12$$

where

α = fraction of bremsstrahlung gamma rays produced by primary electrons near the solar system

β = ditto . . by secondary electrons

μ = fraction of inverse Compton gamma ray produced by primary electrons near the solar system

ν = ditto ... by secondary electrons.

In order to determine α, β, μ and ν the energy spectra of the primary and secondary electrons are required. These may be determined from the observations of flux of positrons relative to the total flux of electrons and from the physics of the $\pi^{\pm}$ production process. Figure 7 shows the experimental results (Meyer 1975) on the fraction $N_{e^+}/(N_{e^+} + N_{e^-})$ as a function of energy. It can be seen from figure 7 that the secondary electrons have an energy spectrum between 100 MeV and 1 GeV which is steeper than that of the primaries. As a result α has a value < 0.3 the fraction of the electron flux at 100 MeV which is of secondary origin. The values of α

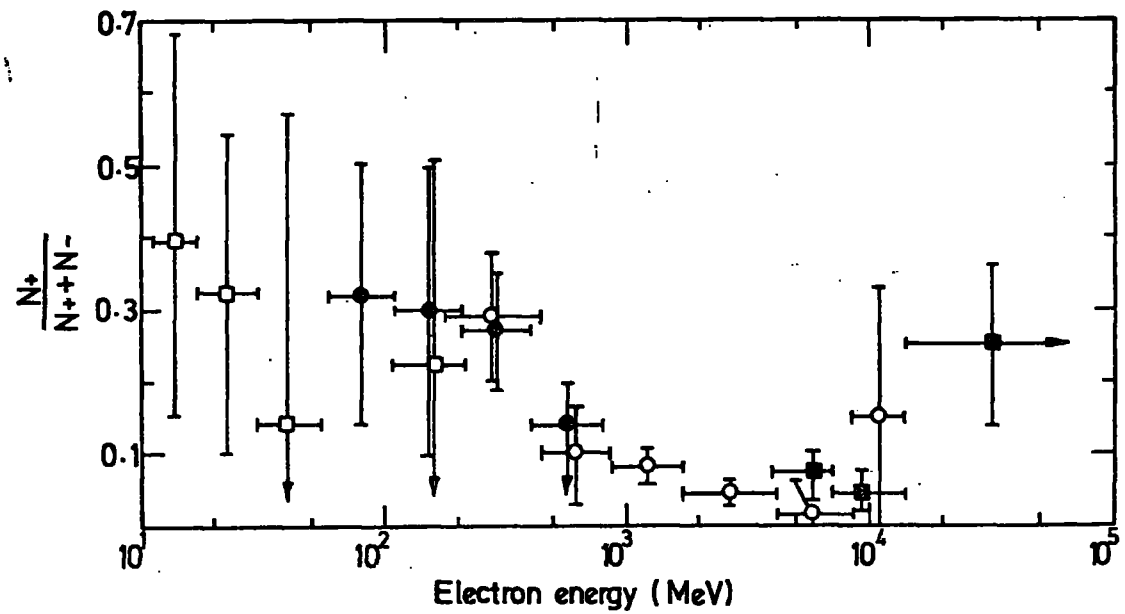

Figure 7. The variation with electron energy of the fraction of positrons in the electron flux.

and β were found to be 0.84 and 0.16 respectively.

The problem of the IC contribution is much simpler since the secondary spectrum has approximately the same slope as the primary spectrum above 1 GeV. The values of μ and ν are therefore 0.9 and 0.1.

Combining together the various terms for the surface emissivity given in equations 5, 10, 11 and 12, the values of α, β, μ & ν calculated above and the assumption $w'_e(R)/w'_{e\odot} = w(R)/w_\odot$ together gives $w(R)/w_\odot$. This is shown in figure 8. The error bars represent the errors in the unfolding alone and do not include the uncertainty in the gas density.

The cosmic ray distribution of figure 8 is very similar to both the pulsar and supernova remnant distributions and in the region $5 < R < 10$ kpc is consistent with the cosmic ray density being proportional to the stellar mass density.

The ratio of the energy densities in primaries and secondaries $w'_e(R)/w''_e(R)$ is determined by the density of hydrogen. Thus

$$\frac{w'_e(R)}{w''_e(R)} = \frac{w'_{e\odot}}{w''_{e\odot}} \frac{\sigma_H(R)}{\sigma_{H\odot}}$$

Since at 5 - 6 kpc $\sigma_H(R)/\sigma_{H\odot}$ is $\simeq 2$, the primary electrons dominate at 1 GeV and the spectrum of radio emission will be the same as the local spectrum, in agreement with the results of Stephens (1969).

7.5 The Sensitivity of the Conclusions to the cloud penetration probability

In the above calculations it was assumed, though

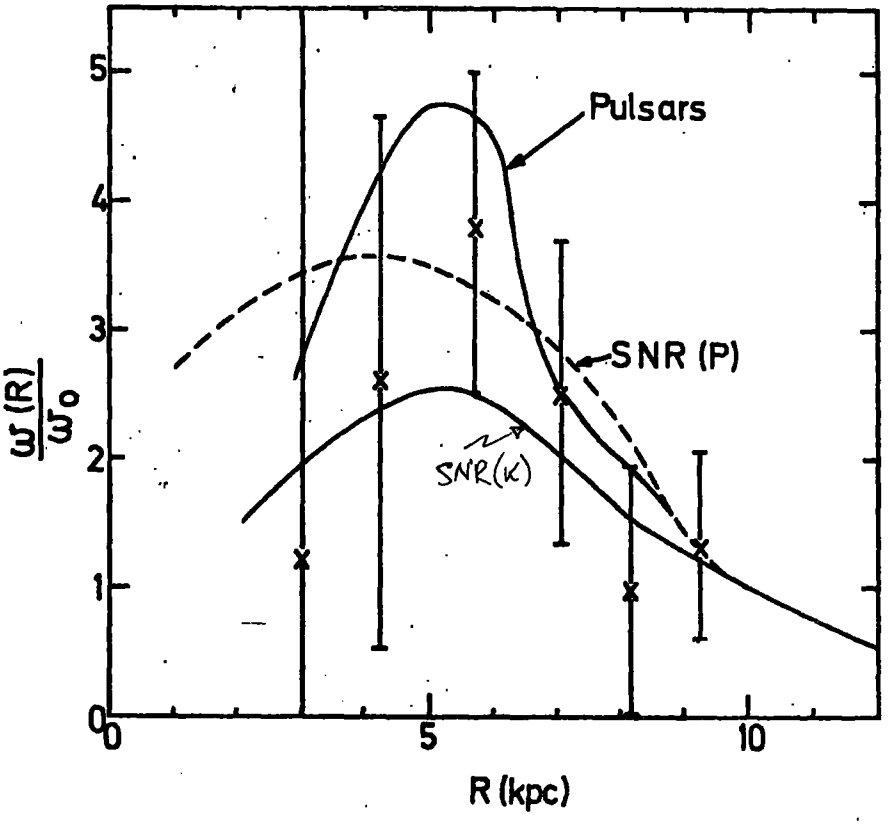

Figure 8. The radial distribution of cosmic ray intensity, $w(R)/w_{\odot}$ as deduced from the gamma-ray observations. Also included for comparison are the radial distributions of pulsars and supernova remnants.

not explicitly stated, that the atoms of the hydrogen were distributed uniformly over the interstellar medium. However, this is not the case, since the molecular hydrogen is concentrated in clouds with typical diameters of 5 - 10 pc and densities of $\sim$ 3000 atoms cm^{-3}. The question which naturally arises is whether or not the cosmic rays are free to penetrate deep into the clouds. This problem will be discussed in this section.

The typical column density of a molecular hydrogen cloud is $\sim 10^{22}$ atoms cm^{-2}. This makes the cloud optically thin to cosmic rays and implies that unless some other mechanism screens the cloud centre then the density of cosmic rays at the cloud centre, n^c, and the density in the space outside the cloud, n^o are approximately equal. However, the small anisotropy in the cosmic ray flux at the cloud surface can produce Alfven waves which may, in the manner described in Chapter 3, scatter the cosmic rays, producing a cosmic ray mirror at the edge of the cloud. It is possible that this may screen the centre from the cosmic rays outside the cloud.

Consider the cylindrical cloud of figure 9. At the surface A the fluxes of coasmic rays in and out of the cloud are $\frac{n^o c}{4}$ and $\frac{n^o(1-\tau)}{4}$ c respectively. where c is the cosmic ray velocity, n^o the cosmic ray density outside the cloud and τ is the average optical depth for cosmic rays. Since the average velocity of the cosmic rays in the direction BA is $c/2$, τ is given by

$$\tau = 2R\,\sigma_{Inelastic}\,n_H$$

At the cloud surface A, cosmic rays stream into

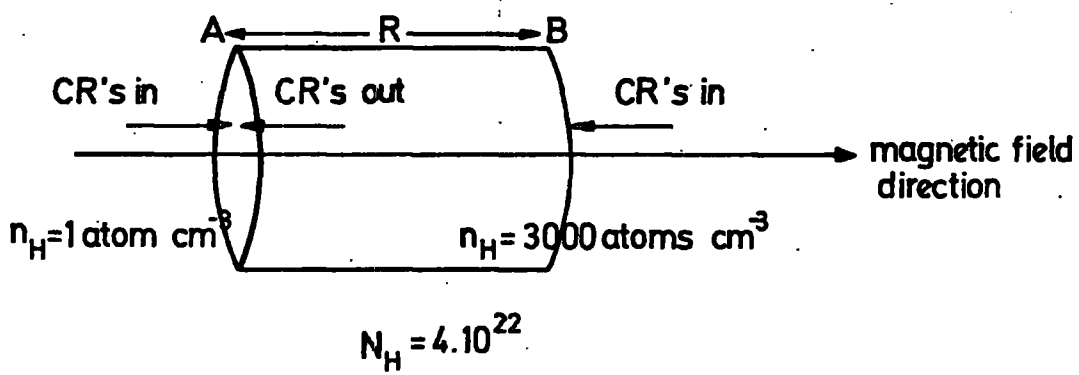

Figure 9. The idealized interstellar molecular cloud considered in Section 7.5.

the cloud with velocity v_{st} where,

$$v_{st} = \frac{\tau n^o c}{4n^o} = \frac{\tau c}{4}$$

At A, Alfven waves will be created and the energy density in the waves will grow if the growth rate due to the cosmic ray streaming exceeds the damping rate due to ion-neutral collisions. Following Dickinson (1975) the growth rate Γ_G and damping rate Γ_D are given by

$$\Gamma_G = \frac{1.69\ 10^{-10}}{(E/GeV)^{1.5}} \left(\frac{V_{st}}{V_A} - 1 \right)$$

$$\Gamma_D = 1.12\ 10^{-9} \left(\frac{n_H}{1cm^{-3}} \right) \left(\frac{T}{1000\ K} \right)^{-1/2}$$

where v_A = Alfven velocity

Inside the cloud the situation is such that n_H = 3000, T = 10K and waves are rapidly damped. On the other hand outside the cloud n_H = 1, T = 100K and the condition for $\Gamma_G > \Gamma_D$ becomes $v_{st} > v_A$. In other words this requires the optical depth of the cloud to be a few times v_A/c. In the general ISM the value of v_A is 30 km s^{-1}, thus $v_A/c = 10^{-4}$, whereas the parameters of the cloud in figure 7 give $\tau = 2\ 10^{-3}$. Thus the conditions at A (and B) are such that the Alfven waves grow, and the streaming velocity becomes v_A.

As a result of this process the density of cosmic ray nuclei inside the cloud drops to a value n^c, where n^c is governed by the equilibrium between the rate at which cosmic rays are carried in through the surface and the rate at which they disappear inside the cloud due to inelastic collisions with the gas atoms. Thus

Rate of cosmic ray replacement = $n^o\ v_A \times$ Area

= Death rate = $n^c\ n_H\ \sigma_{In}\ c \times$ Volume

$$\frac{n^c}{n^o} = \frac{v_A}{n_H \sigma c R} = \frac{2v_A}{\tau c}$$

for the parameters given above

$$\frac{n^c}{n^o} \simeq \frac{1}{10}$$

Such a reduction means a large reduction in the gamma ray yield from π^o decay.

A more detailed analysis (Skilling and Strong 1976) has shown that this process is very efficient below 1 GeV but that at higher energies the reduction is small. At 10 MeV the reduction is a factor of 80. These authors obtain significant gamma ray depletions when the column density of the cloud and/or the cosmic ray density are a factor of 10 larger. Thus this process works for protons for only the most massive clouds.

In their analysis, Skilling and Strong did not include the electron contribution to the gamma ray flux. At first sight the problem is a simple one. The electrons will be resonantly scattered by waves set up by the non-relativistic protons. For example a 100 MeV electron and a 4 MeV proton have the same Larmor radius. As a result the depletion of cosmic ray electrons inside the cloud is expected to be large. However, the analysis assumed no sources of cosmic rays within the cloud. In practice the cosmic ray nuclei with kinetic energies $>$ 1 GeV/nucleon are not excluded very efficiently and secondary electrons are produced inside the cloud. These are prevented from escape by the waves set up by the low energy protons and consequently the secondaries build up inside. The equilibrium level is governed by a balance between

losses due to bremsstrahlung or ionization and creation in nucleon-nucleon collisions.

Thus equibrium implies:

creation rate = destruction rate

$$\frac{n_1}{n_2} Q = \frac{n^c}{T_d}$$

Where Q is the secondary electron production rate outside the cloud; n_1 and n_2 are the gas densities in the cloud and outside the cloud respectively; n^c is now the density of secondaries inside the cloud and T_d is the lifetime of secondaries on the inside due mainly to ionization and bremsstrahlung losses.

The equilibrium level outside the cloud is

$$n^o = Q\, T_e$$

where T_e is the escape lifetime.

Therefore

$$\frac{n^c}{n^o} = \frac{n_1}{n_2} \frac{T_d}{T_e}$$

If the typical paramters quoted above are substituted the ratio is found to have the value $n^c/n^o \simeq 4$.

Clearly this is an important problem since it implies that a large part of the gamma ray emission may be due to bremsstrahlung by the secondary electrons. A more detailed calculation Strong (Private Communication) gives a depletion in the density of cosmic ray electrons inside the cloud relative to the total density (primaries and secondaries) outside. In the calculation by Kniffen et al. (1975) the electrons were assumed to have free access to the hydrogen. A more complete calculation of the gamma ray yield requires more information on the distribution of cloud masses.

7.6 Conclusions

The available evidence is in favour of a cosmic ray density gradient between 5 and 10 kpc with approximately the same distribution as that of the main cosmic ray source candidates. From this it may be concluded that the lifetime of cosmic rays in the galaxy is not a strong function of R and that the cosmic rays do not diffuse far from their sources. It is necessary, however, to examine again the possibility that the CR density is uniform (in Extragalactic origin or Galactic plus long diffusion paths) and to see under what conditions this situation would pertain.

In order to reproduce the gamma ray observations using a uniform cosmic ray density distribution it is required that the hydrogen surface density at 6 kpc is $51 \pm 17\ M_\odot/pc^2$. Gordon and Burton (1976) give a density at 6 kpc of $13\ M_\odot/pc^2$ and Scoville and Solomon (1975) give a density of $21\ M_\odot/pc^2$. There is a large uncertainty attached to the quoted figures of the hydrogen density. This arises because of the difficulties in converting from the CO emission data to the column density of molecular hydrogen and also because the layer thickness is not known; both the Gordon and Burton and the Scoville and Solomon results are based on only a very limited number of observations of the layer thickness. As a consequence of these problems the uncertainty in the quoted figures for σ_{H2} may be as large as a factor of 2.

This fact suggests that the possibility of a uniform cosmic ray density cannot be ruled out completely.

However, it will be seen in the next chapter that the observations of the Galactic anticentre do not imply such a uniform distribution.

REFERENCES

Comstock, G.M., Hseih, K.C. and Simpson, J.A., 1972. Astrophys. J., 173, 691.

Cummings, A.C., Stone, E.C. and Vogt, R.E., 1973. Proc. 13th Int. Conf. on Cosmic Rays, Denver, 1, 335.

Dickinson, G.J., 1975. Ph. D. Thesis, University of Durham.

Fichtel, C.E., Hartman, R.C., Kniffen, D.A., Thompson, D.J., Bignami, G.F., Ogelman, H., Ozel, M.F., and Turner, T., 1975. Astrophys. J., 198, 163.

Gordon, M.A. and Burton, W.B., 1976. Astrophys. J. to be published.

Jenkins, E.B., 1976. GSFC Sympoisium on Gamma-Ray Astronomy, to be published.

Kniffen, D.A., Bignami, G.F. Fichtel, C.E. and Thompson, D.J., 1975. Proc. 14th Int. Conf. on Cosmic Rays, 1, 40.

Meyer, P., 1975. In 'Origin of Cosmic Rays', Eds. J.L.Osborne and A.W. Wolfendale, D.Reidel, Dordrecht.

Pollack, J.B. and Fazio, G.G., 1963. Phys. Rev., 131, 2684.

Scoville, N.Z. and Solomon, P.M., 1975. Astrophys. J., 199,L105.

Skilling, J. and Strong, A.W., 1976. Ast. Astrophys. to be published.

Stephens, S A., 1969. Ph.D. Thesis, University of Bombay.

Strong, A.W. and Worrall, D.M., 1976. J.Phys. A., 9, 823.

Waddington, C.J., 1974. The Nuclear Particles of the Cosmic Radiation, University of Minnesota.

CHAPTER EIGHT

GAMMA RAY EMISSION FROM THE GALACTIC ANTICENTRE.

8.1 Introduction

In the last chapter it was shown that the evidence from gamma ray emission and gas distributions indicated that there was a gradient in the cosmic ray density between 5 and 10 kpc from the Galactic centre. However, no strong conclusion was possible because of many problems associated with molecular hydrogen. In this chapter attention is switched to a broad region centred on the Galactic anticentre extending from 90° to 270° in longitude.

In the anticentre direction the line of sight crosses regions more distant from the Galactic centre than the sun itself. Since the results of the CO emission surveys of Gordon and Burton (1976) and Scoville and Solomon (1975) showed that the dense molecular clouds were concentrated to the region within 8 kpc of the Galactic centre, their contribution to the hydrogen column densities will generally be small. Hence the atomic hydrogen column density may be used to give a lower limit to the flux of gamma-rays to be expected as a result of interactions between the cosmic rays and gas and will allow comparison between predictions of Galactic and Extragalactic models for cosmic ray origin.

In a sense the method proposed here is somewhat similar to that put forward by Ginzburg (1972) for the Magellanic Clouds. Ginzburg suggested using these objects to test for the existence of extragalactic cosmic rays by searching for the gamma rays which would

be produced by cosmic rays interacting with the hydrogen in the Clouds.

If no gamma rays are observed, then this would be definite proof of the Galactic origin of cosmic rays. Unfortunately, this proposal suffers from the disadvantage that the observation of gamma rays does not in fact rule out a Galactic origin. The present method is in principle much more sensitive than Ginzburg's because the difference in intensities between the Galactic and Extragalactic models should be greater than for the small signal to be expected from Magellanic Clouds. In addition this method should afford more possibilities for analysis through the l and b distribution of the gamma ray intensities. The method is also unambiguous, unlike Ginzburg's.

In the sections which follow two models for the distribution of cosmic rays are used to predict the latitude and longitude distribution of gamma rays around the anticentre direction. The available measurements are then used to attempt to identify the better model.

8.2 The Cosmic Ray Distribution

8.2.1 Galactic Sources

The radial dependence of the density of the cosmic ray source candidates was discussed in Chapter 3, and it was shown how the radial dependence of the cosmic ray density might be related to the source distribution. Here it is assumed that the escape lifetime for cosmic

rays is R independent and hence that on a Galactic model for cosmic ray origin that the density of cosmic rays is proportional to the density of sources.

In the outer regions of the Galaxy (i.e. R>10 kpc) the distribution of sources is close to the distribution of the surface mass density. This is represented in the calculations by an exponenial function $W(R) = \exp((10-R)/2.44)$ which approximately represents the surface mass distribution given by Innanen (1973) for the ou.er regions of the Galaxy.

In this calculation it is assumed that the z distribution of the cosmic ray is rather wide so that the cosmic ray intensity can be considered to be constant over the region occupied by the hydrogen (a few hundred pc). Thus, the surface density of the sources is taken to give the relative cosmic ray intensity. Justification for this assumption may be derived from the distribution of synchrotron radiation with Galactic latitude. Figure 1 shows the average b distribution at 150 MHz towards the anticentre taken from the compilation by Landecker & Wielebinski (1970). Its width indicates a wide z distribution for both the magnetic field and the cosmic electrons. It is reasonable to assume that the z distributions of the GeV electrons which produce the radio and the GeV protons which produce the gamma rays are similar.

8.2.2 Extragalatic Sources

The model adopted here is of the Galaxy bathed in a uniform flux of cosmic rays. Some propagation

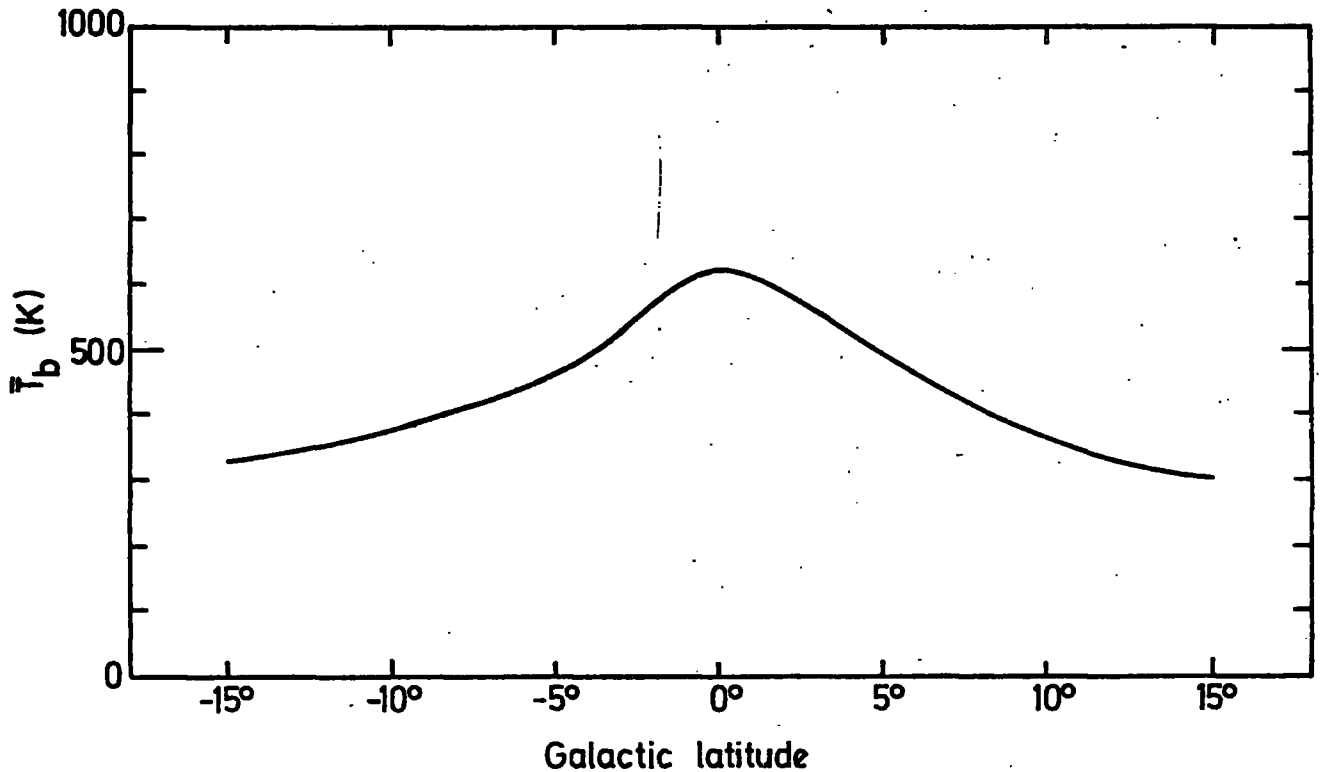

Figure 1. The Latitude distribution of radio brightness temperature (T_b) at 150 MHz, using the data of Landecker and Wielebinski (1970). The distribution is averaged over the same longitude intervals as the gamma ray observations in figure 5.

models e.g. Dickinson 1975 predict a uniform cosmic ray density distribution even for Galactic origin (see Chapter 5). Thus, even if agreement between the predictions of the 'extragalactic' model and the gamma-ray observations is found, a Galactic origin will still not be ruled out.

8.3 The Distribution of Atomic Hydrogen

A convenient survey of the atomic hydrogen distribution in this region is given by Lindblad (1966), in the form of contour maps of the 21-cm optical depth in velocity-latitude planes at 5^{o} intervals of longitude. The optical depth maps were constructed from the brightness temperature maps (after correction for the various instrumental effects such as antenna efficiency) by assuming a spin temperature, T_{spin} of 125 K.

The optical depth-velocity profiles at various latitudes were read from the contour maps given by Lindblad. Figure 2 shows a typical optical depth-velocity profile for l = 117.3 and b = 0.0. The column density of atomic hydrogen is obtained from the optical depth-velocity profile, thus

$$N_H = 1.823 \times 10^{18} T_{spin} \int \tau(v)dv \qquad 1$$

where v is in km s^{-1}.

Using the Galactic rotation velocity-radius relation, and simple geometry the density of hydrogen as a function of position may be derived from the optical depth.

$$n_H = 1.823\ 10^{18} T_{spin} \quad \tau(v)\frac{dv}{dr} \qquad 2$$

atoms cm^{-3}

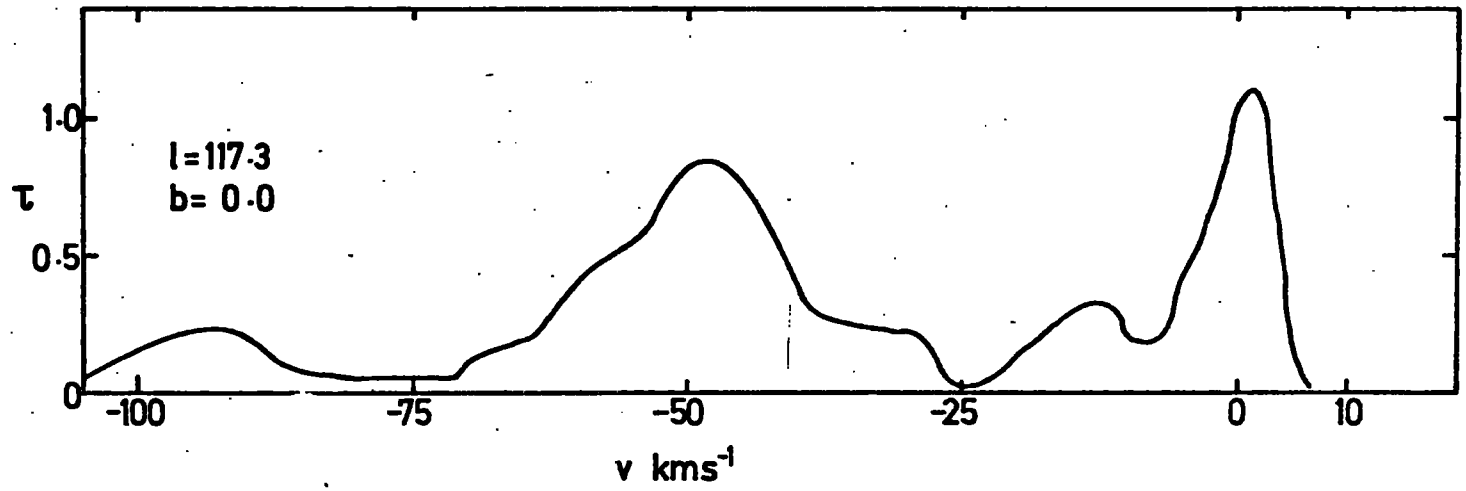

Figure 2. A typical optical depth (τ), velocity profile from Lindblad (1966).

The rotation curve used was that of Contopoulos and Stromgren (1965) and for computation this was represented by the interpolation formula given by Minalas and Routly (1968):

$$(R) = 67.76 + 50.06R - 4.0448R^2 + 0.0861\ R^3$$

Θ kms^{-1} R in kpc

Comparison of the column densities obtained by integration under the profiles of $T(v)$ with those given in the compilation of column densities by Daltabuit and Meyer (1972) shows that the Lindblad data gives lower values at b = 0.0. There are a number of observational difficulties which could have lead to this disagreement. In particular, when comparing two surveys made by different instruments it is not always certain that a common zero level and temperature scale have been used. This last problem has recently been tackled by Harten et al. (1975) who have compared the temperature scales of the main 21 cm survey instruments and give conversion factors for some surveys. For the early Leiden Survey used here the agreement of the temperature scale with that of the most modern instruments is to within 1%.

In this case the Lindblad data presumably represents a lower limit to the amount of hydrogen and this will be shown later to be adequate for the conclusions reached.

The z distribution of the hydrogen has been determined from 21 cm brightness temperature - velocity profiles by Jackson and Kellman (1974). These authors find that the thickness $z_{\frac{1}{2}}$ (defined as the distance

between half density points) generally increases with increasing R in the longitude interval $200 \leq l \leq 300$ but that for $110 \leq l \leq 160$ the thickness remains fairly constant. These results are shown in figure 3. This departure from axial symmetry is the reason for employing an empirical hydrogen distribution rather than the averaged hydrogen density given by Gordon and Burton (1976).

8.4 The Distribution of Gamma-ray Intensity around the Galactic Anticentre

Using the atomic hydrogen distribution derived from the 21 cm data as described in section 3, the values of the gamma-ray intensity $j(l,b)$ can be calculated for those regions where experimental data exist. The SAS II data relates to the regions $90 \leq l \leq 150$, $160 \leq l \leq 170$ and $200 \leq l \leq 260$, and the events above 100 MeV have been summed to give the overall b distribution (Fichtel et al. 1975).

The gamma ray intensity is given by

$$j(l,b) = \frac{1}{4\pi} \int_0^\infty q_\gamma(r,l,b)\, dr \qquad 4$$

gammas cm^{-2} s^{-1} $ster^{-1}$

Where $Q_\gamma(r, l, b)$ is the emissivity of gamma rays with $E > 100$ MeV in the direction (l, b) as a function of r. This is given by

$$Q(r,l,b) = q_\gamma^{\pi+B}\, w(R) n_H(r,l,b) \qquad 5$$

Where $q_\gamma^{\pi+B}$ is the local gamma ray emissivity for both bremsstrahlung and pion production combined, which was

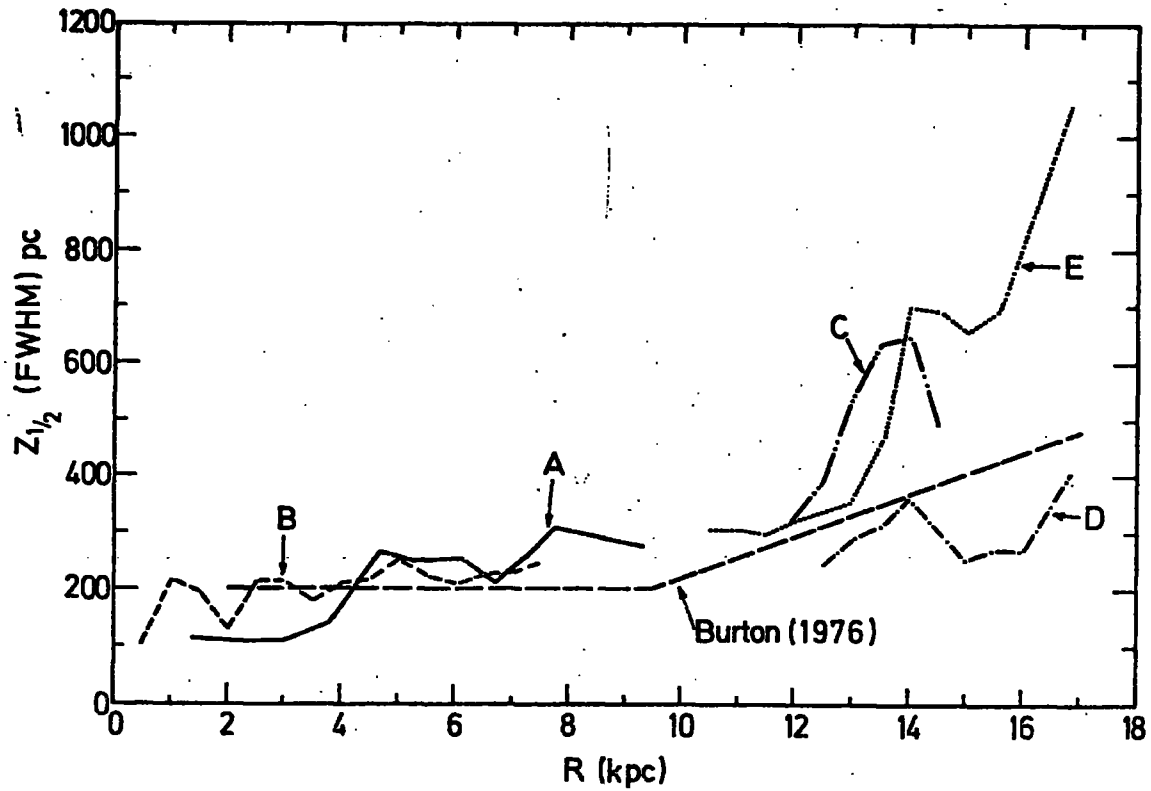

Figure 3. The variation of $Z_{\frac{1}{2}}$ with Galactocentric radius R. Curves A-E are from Jackson and Kellman (1974) and refer to the longitude intervals; A, $0 \leq l \leq 90$; B, $270 \leq l \leq 360$; C, $160 \leq l \leq 205$; D, $110 \leq l \leq 160$; E, $200 \leq l \leq 300$. For comparison the results of Burton (1976) are also shown.

calculated in the last chapter, n_H (r, l, b) is the hydrogen density distribution and W(R) represents the relative intensity of the CR flux at distance R from the Galactic centre with respect to the intensity near to the Earth.

$$W(R) = \frac{I_{cr}(R)}{I_{cr}(10)} \qquad 6$$

In the calculations two forms of W(R) are used, representing Galactic and Extragalactic origin respectively.

For Galactic origin

$$W(R) = \exp \frac{10 - R}{2.44} \qquad 7$$

and for Extragalactic origin

$$W(R) = 1.0 \qquad 8$$

Figure 4 shows the predicted mean latitude distributions for $90 < l < 180$ and $180 < l < 270$. It is interesting to note the asymmetry with respect to b = 0, in opposite senses for the two directions. This effect should be detectable when eventually the gamma ray observations are presented in this form. Figure 5 shows the latitude distribution for the Extragalactic and Galactic models, the predicted intensities in 5 being averaged over the same longitude intervals as the data. In 5 the detector response function was assumed to be a gaussian of width 3°. Figure 6 compares the longitude distribution of the gamma ray line flux predicted by the models with the observations.

In figures 4, 5 and 6 the effect of the Galactic model is to reduce the fluxes below the predictions of the Extragalactic model by a factor which in figures

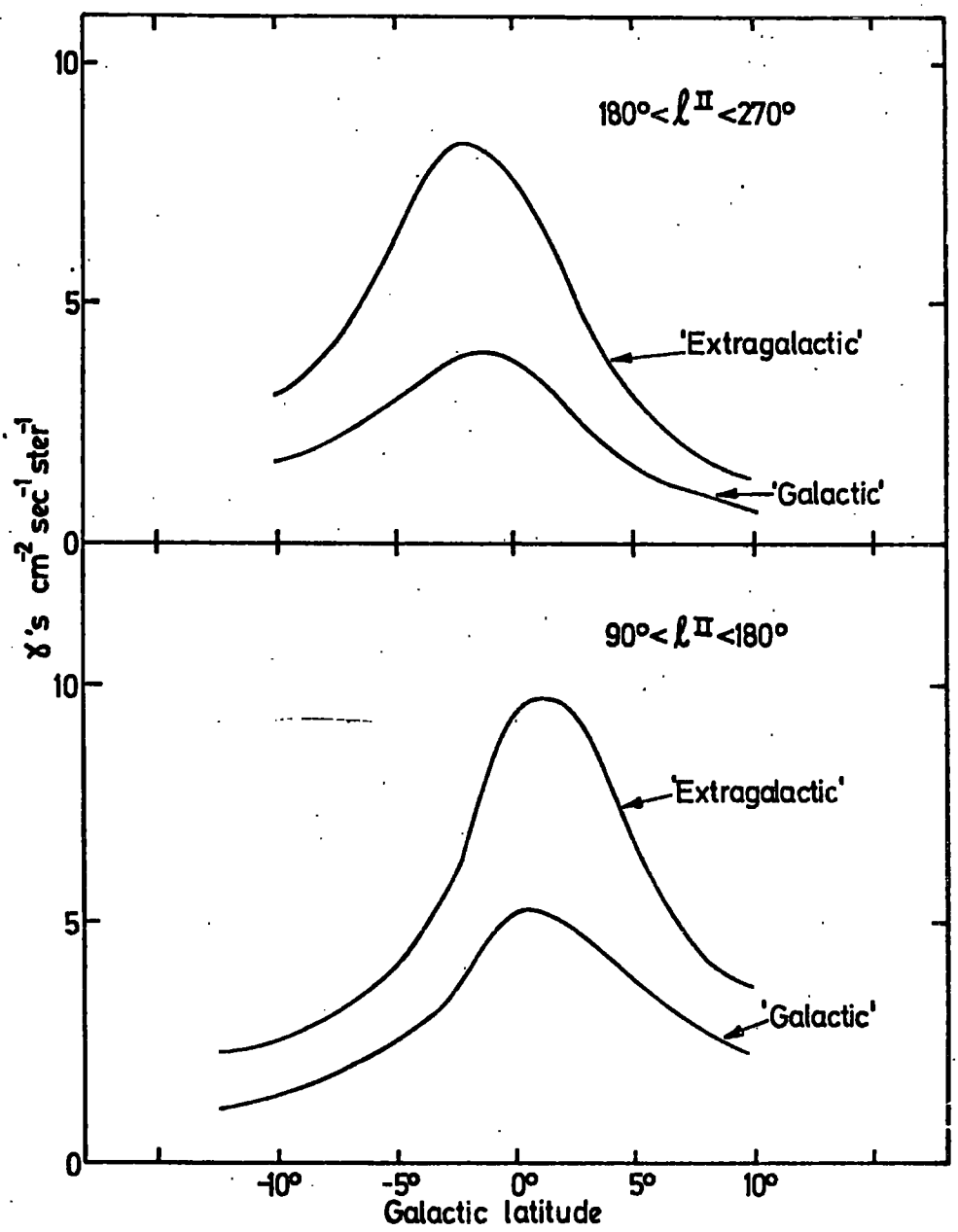

Figure 4. The latitude distributions of the predicted gamma ray intensities averaged over a) l = 90°- 180° and b) l = 180°-270°, for Galactic and Extragalactic models.

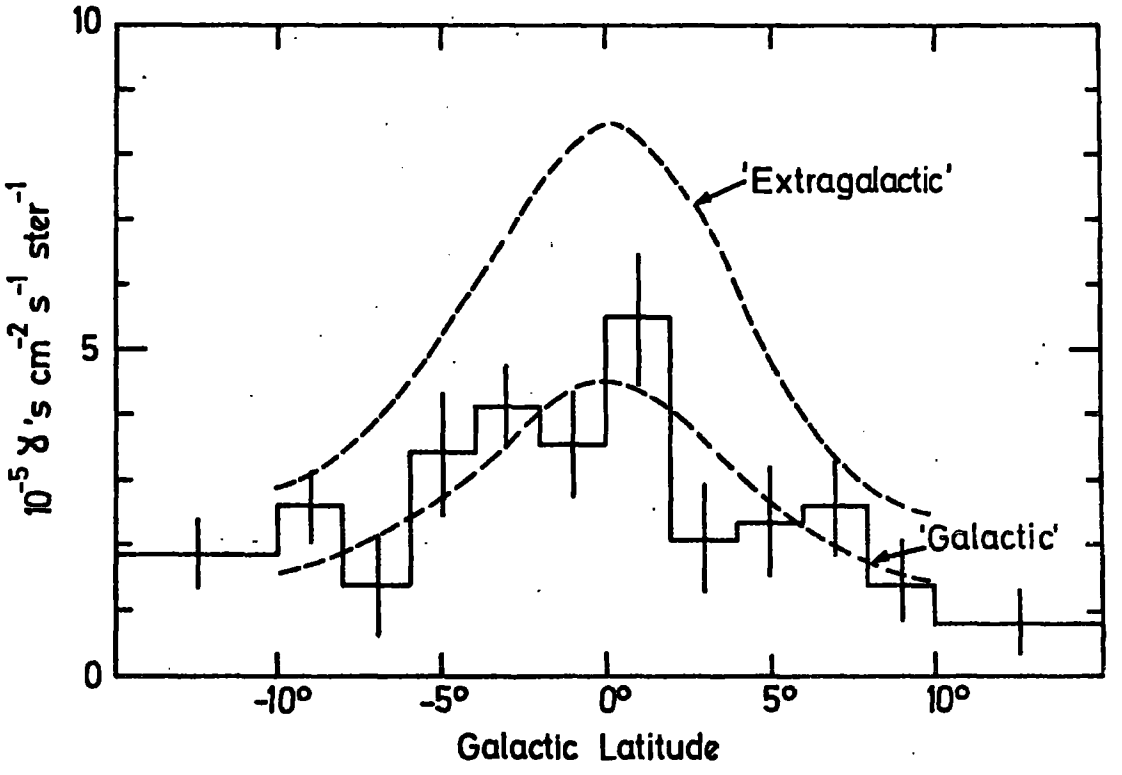

Figure 5. Comparison of latitude distribution of gamma-ray intensity on 'Galactic' and 'Extragalactic' models with the SAS II data. The predictions are averaged over the same longitude regions as the data.

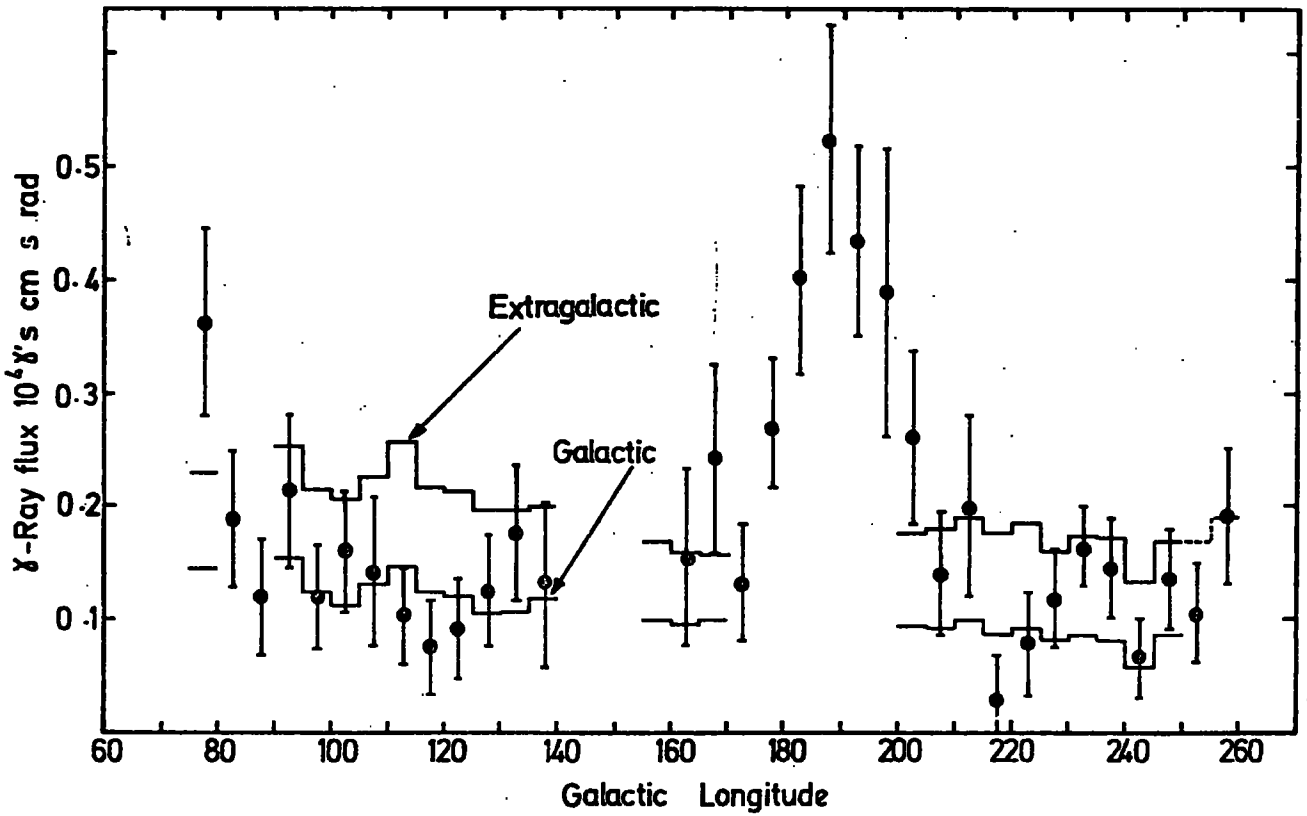

Figure 6. Comparison of predicted longitude distributions of gamma-ray line fluxes for - $10^{\circ} < b < 10^{\circ}$ around the anticentre direction, on the Galactic and Extra-galactic models, with the SAS II data.

4 and 5 is virtually latitude independent; it does not flatten the latitude distribution, as would be anticipated for a Galaxy which is a flat slab. The rapid increase in the width of the Galactic gas shown in figure 3 is responsible for this effect, which means that even at b = 10 gamma rays are reaching us from distances of a few kpc.

8.5 Discussion on the CR and gas distribution in the Anticentre

The most striking feature arising from the comparison of the observations with the two models is that the Extra-Galactic hypothesis predicts a flux about a factor of two in excess of what is observed, while the Galactic model does seem to give a good representation of the observed distribution in latitude and also agreement in the absolute flux levels.

It is important to examine the sources of errors in these calculations. For the hydrogen distribution there are two main areas of uncertainty (excluding the instrumental problems).

Firstly, the spin temperature of the gas has been taken to be 125 K. The evidence of 21 cm absorption studies by Hughes et al. (1971) and Radhakrishnan et al (1972) is for a temperature which is $<$125 K. Hughes et al. quote a mean value of 71 K and for 90% of the clouds observed find temperatures $<$130 K. The effect of choosing 125 K as the temperature is to consistently underestimate the optical depth of optically thick

features and hence to underestimate their column densities.

Secondly, no allowance has been made for the presence of molecular hydrogen in the interstellar medium. The evidence from the UV absorption measurements (Spitzer 1973) is for considerable quantities of molecular hydrogen in the denser clouds. Jenkins (1976) suggests a local density of hydrogen of 1.1 atoms cm^{-3} of which 0.2 atoms cm^{-3} is molecular.

Both these factors act to increase the column density. Thus the above calculations have tended to underestimate the hydrogen density implying greater disagreement between the observations and the predictions of the Extragalactic model.

The remaining uncertainty is in the Cosmic ray flux near the Earth. It is unlikely that the error in the experimentally measured flux at 3 GeV can be as large as a factor of two, since the effects of solar modulation at these energies are small. Another explanation is that the local cosmic ray flux is not representative of the average flux at this distance from the Galactic centre; the average flux being at least a factor of two lower to reach agreement with the gamma-ray observations. This is also unlikely since the very high isotropy at 10^{11} eV makes the probability of being in a small local excess very small (Dickinson and Osborne 1974). Such a local excess would in any case imply a Galactic origin for cosmic rays.

All these factors weigh heavily against the Extra-

galactic model especially since the Galactic model adopted here agrees with the observations to within the experimental errors. This is consistent with cosmic ray origin in supernovae, supernova remnants, pulsars or any other source whose density falls off like the distribution of mass in the outer Galaxy; alternatively, this may be considered as indicating the existence of a cosmic ray disk which is of smaller radial extent than the hydrogen disk.

REFERENCES

Contopoulas, G.& Stromgren, B., 1965. In Tables of plane galactic orbits', NASA Institute for Space Studies.

Daltabuit, E. & Meyer, S., 1972. Astr.Astrophys., 20, 415.

Dickinson, G.J. & Osborne, J.L., 1974. J.Phys. A., 7, 728.

Dickinson, G.J., 1975. Ph.D. Thesis University of Durham.

Fichtel, C.E., Hartman, R.C., Kniffen, D.A., Thompson, D.J., Bignami, G.F., Ogelman, H., Ozel, M.F. & Tumer, T. 1975. Astrophys. J. 198, 163.

Ginzburg, V.L., 1972. Nature Phys. Sci., 239, 8.

Gordon, M.A. & Burton, W.B., 1976. Astrophys. J. to be published.

Harten, R.H., Westerhout, G. & Kerr, F.J., 1975. Astr. J. 80, 307.

Hughes, M.P., Thompson, A.R. & Colvin, R.S., 1971. Astrophys. J. Suppl. No. 200, 23, 323.

Innanen, K.A., 1973. Astrophys. and Sp. Sci., 22, 393.

Jackson, P.D. & Kellman, S.A., 1974. Astrophys. J., 190, 53.

Jenkins, E.B., 1976. Goddard Space Flight Centre Syposium on Gamma Ray Stronomy, to be published.

Landecker, T.L. & Wielebinski, R., 1970, Aust. J. Phys. Astrophys. Suppl., 16, 1.

Lindblad, P.O., 1966. Bull. Astr. Inst. Netherl., Suppl., 1, 77.

Mihalas, D. & Routly, P.M., 1968. Galactic Astronomy, Freeman & Co., San Francisco.

Radhakrishnan, V., Murray, J.D., Lockhart, P. & Whittle, R.P.J., 1972. Astrophys. J. Suppl. No. 203, 24, 15.

Scoville, N.Z., & Solomon, P.M., 1975., Astrophys. J., 199, L105.

Spitzer, L., Drake, J.F., Jenkins, E.B., Morton, D.C., Rogerson, J.B. & York, D.G., 1973. Astrophys. J., 181, L116.

CHAPTER NINE

ON THE EVIDENCE FOR A GALACTIC ORIGIN FOR THE COSMIC RAY NUCLEI BETWEEN 1 - 10 GeV

The observations of 100 MeV gamma rays from the Galaxy give us a useful way of studying the Galactic distribution of the 1 to 10 GeV cosmic ray nuclear component. This is because the gamma rays appear to predominantly originate in collisions between the cosmic ray nuclei and the interstellar gas. Comparison of the measured spectrum of gamma-rays between 10 - 1000 MeV from the Galactic centre (figure 3 Chapter 3) and the theoretical spectrum for this process (figure Chapter 2) indicates that this is indeed the case and enables one to rule out a large contribution from electron Bremsstrahlung at, say, 100 MeV. Furthermore, in Chapters 6 and 7 it was shown that the contribution from the cosmic ray electrons in Bremsstrahlung and inverse Compton scattering was considerably smaller than that from the cosmic ray nuclei. The fact that the π^0 production and decay process apparently dominates is of great importance in simplifying the interpretation, especially since the electrons are already known to be of Galactic origin.

Assuming this fact, the Galactic distribution of the intensity of the cosmic ray nuclei may be deduced from the gamma ray observations using a map of the Galactic gas distribution. This was carried out in Chapter 7 where it was shown that the flux of gamma rays from the broad region of enhancement around the Galactic Centre implied an increase in the cosmic ray intensity near the Galactic centre. A comparison between the deduced cosmic ray and the source candidate distribution was made and some tentative conclusions were drawn about cosmic ray propagation. Thus it was found

that the distribution of the cosmic rays and the source candidates were very similar supporting the hypothesis of cosmic ray origin in supernovae, their remnants or pulsars and suggesting that cosmic rays diffuse no more than 1 - 2 kpc before escaping.

However, there are some difficulties with this interpretation of the Galactic centre observations. Basically, there are two major problems which introduce considerable uncertainty into the interpretation.

Firstly, as discussed in Chapter 7, the absolute densities of molecular hydrogen are not known with any confidence. In Chapter 7 it was shown that to achieve agreement with the observations using the atomic and molecular hydrogen distributions of Gordon and Burton (1976) the cosmic ray intensities at 5 - 6 kpc must be a factor of 4 greater than the solar system values. The form of Scoville & Solomon (1975) molecular hydrogen distribution is basically in agreement with that of Gordon & Burton; yet using these authors' normalization, it is found that the cosmic ray intensity required to explain the observed gamma ray flux is only a factor of 2 up on the solar system value. Since it is generally agreed that the uncertainty in converting from the carbon monoxide observations to the molecular hydrogen density is the order of a factor of 2 this leaves open the possibility of explaining the observations by a constant cosmic ray intensity.

The second problem is that of the contribution from pulsars.

The simplest procedure to estimate the pulsar contribution, given the Crab and Vela pulsars as examples

of gamma ray sources is to assume that the rate of gamma ray production is proportional to the rate of total energy loss, (obtained from the spin down rate), and use the Crab or Vela pulsars as normalization. This method was used by Dahanayake et al (1976) using the pulsar catalogue of Taylor and Manchester (1975). The contribution was found to be negligible except for the Crab and Vela pulsars. Higdon and Lingenfelter (1976), however, have used much the same method but concentrate on the contribution from as yet unobserved young pulsars and their results suggest that the gamma ray observations may be explainable by a uniform cosmic ray intensity over the whole Galaxy plus a contribution from 40 or 50 or so young pulsars.

Clearly, it is not possible to decide between the Galactic and Extragalactic origins for cosmic rays by using the Galactic centre observations, simply because of the uncertainties in the interpretation. Fortunately, these problems do not complicate the interpretation of the Galactic anticentre to the same degree. Thus, in chapter 8 where the gamma ray flux from the Galactic anticentre was examined in some detail, it was possible to rule out, with some confidence, a uniform cosmic ray flux and hence reject an Extragalactic origin for the majority of the cosmic ray nuclei with energies around 1 - 10 GeV. At the same time a plausible model for the cosmic ray distribution based on the distribution of population I objects in outer part of the Galaxy was found to give good agreement with the observations. Furthermore, it is important to note that the existence of a significant quantity of

molecular hydrogen or a contribution from pulsars merely requires that the cosmic ray gradient be steeper and strengthens the conclusions.

There remain a number of questions to be resolved. For example, in Chapter 7 it was shown that the intensity of cosmic rays within dense molecular bearing clouds may not necessarily be uniform across the cloud. The screening process proposed may be very important for the gamma ray yield from the Galactic centre but to include it in the calculations requires more theoretical work on the process and additionally an improved knowledge of the spectrum of cloud sizes. Further, the problem of the thickness of the molecular hydrogen layer requires more observations since the present observations of the layer thickness are restricted to very few directions. It is possible that the layer thickness may vary across the Galaxy and hence the present estimated molecular hydrogen content may be greatly in error.

Finally, it is to be hoped that future observations of the fluxes of the gamma rays from the Galactic plane may help to resolve the question of the point source contributions and enable the controversy of Galactic or Extragalactic origin for cosmic ray nuclei to be quite definitely resolved.

REFERENCES

Dahanayake, C., Dodds, D. & Wolfendale, A.W., 1976. Reprint.

Gordon, M.A., & Burton, W.B., 1976. Reprint.

Higdon, J.C., & Lingenfelter, R.E., 1976. Astrophys. J., 208, L107.

Scoville, N.Z., & Solomon, P.M., 1975. Astrophys. J., 199, L105.

Taylor, J.H., & Manchester, R.N., 1975. Astron. J., 80, 794.

ACKNOWLEDGEMENTS

This work was carried out while the author was a research student at the University of Durham. The financial support of the Science Research Council and the use of the facilities of the University of Durham are gratefully acknowledged.

I am very grateful to my supervisor, Professor A.W. Wolfendale, for his help and encouragement during the period of my research. I would like to thank Dr. A.W. Strong for his advice and many useful discussions. The advice and criticism of my colleagues at the University of Durham is also acknowledged.

I must thank Mrs J. McGough for the work she has done in typing this thesis and Mrs A.Gregory for drawing the diagrams so well.

Finally I must acknowledge the support and encouragement of my wife, without whom this work might never have been completed.